UNIVERSIDADE FEDERAL DO RIO GRANDE DO SUL
INSTITUTO DE CIÊNCIAS BÁSICAS DA SAÚDE
PROGRAMA DE PÓS-GRADUAÇÃO EM CIÊNCIAS BIOLÓGICAS:
BIOQUÍMICA

Ângela Beatris Zemniaçak

MECANISMOS MOLECULARES DE NEUROTOXICIDADE DO ÁCIDO α-CETOISOCAPROICO EM MODELOS EXPERIMENTAIS DA DOENÇA DO XAROPE DO BORDO

Porto Alegre
2026

Ângela Beatris Zemniaçak

MECANISMOS MOLECULARES DE NEUROTOXICIDADE DO ÁCIDO α-CETOISOCAPROICO EM MODELOS EXPERIMENTAIS DA DOENÇA DO XAROPE DO BORDO

Tese apresentada ao Programa de Pós-Graduação em Ciências Biológicas: Bioquímica do Instituto de Ciências Básicas da Saúde da Universidade Federal do Rio Grande do Sul como requisito parcial para a obtenção do título de doutora em Bioquímica.

Orientador: Prof. Dr. Alexandre Umpierrez Amaral
Coorientador: Prof. Dr. Moacir Wajner

Porto Alegre

2026

“É muito melhor lançar-se em busca de conquistas grandiosas, mesmo expondo-se ao fracasso, do que alinhar-se com os pobres de espírito, que nem gozam muito nem sofrem muito, porque vivem numa penumbra cinzenta, onde não conhecem nem vitória, nem derrota.”

(Theodore Roosevelt)

AGRADECIMENTOS

Ao Departamento de Bioquímica, por fornecer todo o suporte necessário para o desenvolvimento desse trabalho e aos funcionários e professores por todo o profissionalismo e competência.

Ao meu orientador professor Alexandre, por todos os ensinamentos, incentivo, carinho e respeito que venho recebendo ao longo dos últimos anos.

Ao meu coorientador professor Moacir, por ter me aceitado em seu laboratório, acreditado em mim e me ensinado ao logo desses anos.

Aos meus colegas de laboratório, Rafael, Ediandra, Ange, Tailine que estão sempre dispostos a me ajudar, a aqueles que não estão mais no laboratório, mas também trilharam esse caminho comigo. Aos novos colegas que mesmo com pouco tempo de convívio, me ensinaram muito. Ao pessoal do 27, principalmente a Manu e a Camila, que foram parceiras em muitos momentos da minha jornada.

A Vitória, minha mãe de Porto Alegre, pela companhia com seu chimarrão, pela ajuda que me deu em vários momentos da minha vida aqui em porto alegre, por ser a "cuidadora" oficial da Roxy quando eu precisava.

Aos meus tios e primos, pela ajuda em Porto Alegre e aos convites de final de semana.

A Roxy, minha cachorrinha, que foi minha companheira nesses últimos anos, sempre me arrancando risadas.

E aos meus pais, por todo o amor e incentivo que me deram para trilhar esse caminho. Quando outros duvidavam de mim, eles sempre estavam lá para me incentivar. Amo muito vocês.

RESUMO

A doença do xarope do bordo (DXB) é um distúrbio neurometabólico hereditário causado pela deficiência da atividade do complexo da desidrogenase dos α-cetoácidos de cadeia ramificada. Os pacientes afetados apresentam sintomas neurológicos severos, tais como coma e convulsões, bem como edema, atrofia e outras anormalidades cerebrais, e sofrem risco de vida alto. Os compostos que mais se acumulam na DXB são os aminoácidos de cadeia ramificada leucina, isoleucina e valina e os α-cetoácidos de cadeia ramificada α-cetoisocaproico (CIC), α-cetoisovalérico (CIV) e α-ceto-β-metilvalérico (CMV), particularmente a leucina e o CIC que podem atingir até 5 mM no plasma. Considerando que os mecanismos neurotóxicos na DXB não estão completamente esclarecidos no período perinatal, o objetivo do presente projeto foi investigar os efeitos *in vivo* (administração intracerebroventricular aguda) ou *in vitro* de CIC em ratos neonatos (1 a 7 dias de vida) sobre a homeostase redox e mitocondrial, bem como sobre a resposta inflamatória e mitofagia, a imunohistopatologia cerebral e o desenvolvimento neuromotor. Investigamos também o papel dos antioxidantes/anti-inflamatórios N-acetilcisteína, melatonina e L-carnitina sobre algumas das alterações observadas. Verificamos que o CIC *in vivo* altera a homeostase redox, pelo aumento da peroxidação lipídica e da oxidação proteica, além da diminuição da defesa antioxidante glutationa reduzida e alterações nas atividades de enzimas antioxidantes no córtex cerebral e estriado dos animais. Também foi verificado que 15 dias após a injeção intracerebroventricular do CIC ocorreu perda neuronal (redução da imunorreatividade do NeuN) e ativação astrocitária (aumento do marcador astrocitário GFAP) no córtex cerebral e estriado, bem como um distúrbio na mielinização (diminuição dos níveis de MBP e CNPase). Finalmente, observamos que os antioxidantes N-acetilcisteína e melatonina previnem a maioria das alterações da homeostase redox induzidas por esse metabólito. Outros achados revelaram que o CIC, mas não os outros cetoácidos de cadeia ramificada CMV e CIV, diminuiu *in vitro* a respiração mitocondrial estimulada por ADP e desacoplada (induzida por CCCP) em homogeneizado de córtex cerebral de ratos neonatos, indicando uma inibição metabólica seletiva para o CIC, além de inibir a atividade da α-cetoglutarato desidrogenase no cérebro de forma não-competitiva, interagindo preferencialmente com as subunidades E2 e E3 no sítio de ligação da diidrolipoamida, e a síntese de ATP. Finalmente, demonstramos que a administração combinada aguda intracerebroventricular de CIC e intraperitoneal de lipopolissacarídeo (LPS) causam uma resposta neuroinflamatória aumentada no córtex cerebral de ratos neonatos, ao elevar significativamente a expressão dos mediadores pró-inflamatórios TNF-α, IL-6, COX-2 e iNOS. O tratamento combinado de CIC e LPS também causou aumento da mitofagia no cérebro por aumentar a expressão dos marcadores PINK1, Parkin e FUNDC1, que pode estar relacionada com a disfunção mitocondrial. Nossos resultados também mostraram que a administração de L-carnitina preveniu significativamente a expressão dos marcadores inflamatórios e dos genes relacionados à mitofagia. Por outro lado, a administração intracerebroventicular de CIC no período neonatal não foi capaz de afetar o desenvolvimento neuromotor dos animais. Esperamos que a elucidação dos mecanismos neurotóxicos do CIC aqui demonstrados em modelos *in vivo* e *in vitro* de DXB em cérebro de ratos neonatos possa contribuir de forma significativa para uma melhor compreensão da disfunção neurológica encontrada em portadores da DXB, especialmente durante períodos de crise de descompensação metabólica nas fases iniciais do desenvolvimento em que os níveis cerebrais dos metabólitos acumulados aumentam significativamente. Além disso, a ação neuroprotetora dos agentes antioxidantes/anti-inflamatórios sugerem que tais compostos possam ser utilizados em pacientes após validação por ensaios clínicos.

ABSTRACT

Maple syrup urine disease (MSUD) is a hereditary neurometabolic disorder caused by a deficiency in the activity of the branched-chain α-keto acid dehydrogenase complex. Affected patients exhibit severe neurological symptoms such as coma and seizures, as well as edema, atrophy, and other brain abnormalities, and are at high risk of death. The compounds that most accumulate in MSUD are the branched-chain amino acids leucine, isoleucine, and valine, and the branched-chain α-keto acids α- ketoisocaproic (KIC), α-ketoisovaleric, and α-keto-β-methylisoseleric, particularly leucine and KIC, which can reach up to 5 mM in plasma. Considering that the neurotoxic mechanisms in MSUD are not fully understood in the perinatal period, the aim of this project was to investigate the *in vivo* (acute intracerebroventricular administration) or *in vitro* effects of KIC in neonatal rats (1 to 7 day-old) on redox and mitochondrial homeostasis, as well as the inflammatory response, cerebral immunohistopathology, and neuromotor development. We also investigated the role of the antioxidants/anti-inflammatories N-acetylcysteine, melatonin, and L-carnitine on some of the observed alterations. We found that KIC *in vivo* alters redox homeostasis by increasing the lipid and protein oxidation, as well as decreasing the antioxidant defense of reduced glutathione and altering the activities of antioxidant enzymes in the cerebral cortex and striatum of the animals. It was also verified that 15 days after intracerebroventricular injection of KIC, neuronal loss (reduction in NeuN immunoreactivity), astrocytic activation (increase in the astrocytic marker GFAP) in the cerebral cortex and striatum were observed, as well as a disturbance in myelination (decrease in MBP and CNPase levels). Finally, we observed that the antioxidant N-acetylcysteine and melatonin prevent most of the redox homeostasis alterations induced by this metabolite. Other findings revealed that KIC, but not the other branched-chain ketoacids KMV and KIV, decreased *in vitro* ADP-stimulated and uncoupled (CCCP-induced) mitochondrial respiration in neonatal rat cerebral cortex homogenates, indicating a selective metabolic inhibition for KIC, in addition to inhibit the α-ketoglutarate dehydrogenase activity in a non-competitive fashion, preferentially interacting with the E2 and E3 subunits at the dihydrolipoamide binding site, and the ATP synthesis. Finally, we demonstrated that acute intracerebroventricular administration of KIC combined with intraperitoneal lipopolysaccharide (LPS) causes an increased neuroinflammatory response in the cerebral cortex of neonatal rats, significantly elevating the expression of the pro-inflammatory mediators TNF-α and IL-6, COX-2, and iNOS. Combined treatment with KIC and LPS also caused increased mitophagy in the brain by increasing the expression of the markers PINK1, Parkin, and FUNDC1, which may be related to mitochondrial dysfunction. Our results also showed that L-carnitine administration significantly prevented the expression of inflammatory markers and genes related to mitophagy. On the other hand, intracerebroventricular CIC administration was not capable to affect the neuromotor development of the animals. We hope that the elucidation of the neurotoxic mechanisms of KIC demonstrated here in *in vivo* and *in vitro* models of MSUD in neonatal rat brain can significantly contribute to a better understanding of the neurological dysfunction found in MSUD patients, especially during periods of metabolic decompensation crisis in the early stages of development, when brain levels of accumulated metabolites increase significantly. Furthermore, the neuroprotective action of antioxidant/anti-inflammatory agents suggests that such compounds could be used in patients after validation by clinical trials.

LISTA DE ILUSTRAÇÕES

Figura 1. Rotas catabólicas dos aminoácidos de cadeia ramificada leucina, isoleucina e valina..... 2

Figura 2. Efeito neurotóxico do CIC em cérebro de ratos neonatos: Prevenção com NAC, MEL e L-Carnitina.....96

LISTA DE ABREVIATURAS E SIGLAS

ACR - aminoácidos de cadeia ramificada

ADP - adenosina difosfato

ALC – acetil-L-carnitina

ATP - adenosina trifosfato

CAT – catalase

CCCP - carbonil cianeto m-clorofenil hidrazona

CCR - α-cetoácidos de cadeia ramificada

CDCCR - complexo desidrogenase dos α-cetoacidos de cadeia ramificada

CIC – ácido α-cetoisocaproico

CIV - ácido α-cetoisovalérico

CMV - ácido α-ceto-β-metilvalérico

CNPase - 2′,3′-nucleotídeo cíclico 3′-fosfodiesterase

CRM - cadeia respiratória mitocondrial

CoA - coenzima A

COX-2 – ciclo-oxigenase-2

DCFH - 2',7'-diclorodihidrofluoresceína

DNA - ácido desoxirribonucleico

DXB – Doença do Xarope de Bordo

ERN - espécies reativas de nitrogênio

ERO - espécies reativas de oxigênio

FADH2 – flavina adenina dinucleotídeo reduzido

FUNDC1 - proteína contendo domínio FUN14 1

GFAP – proteína glial fibrilar ácida

GPx - glutationa peroxidase

GR - glutationa redutase

GSH – glutationa reduzida

H_2S - sulfeto de hidrogênio

IBA1 - molécula adaptadora ligante de cálcio ionizado 1

IFN-γ - interferon gama

IL-1 - interleucina 1

IL-1β - interleucina 1 beta

IL-6 - interleucina 6

IL-10 – interleucina 10

iNOS - óxido nítrico sintase induzível

KGDH - α-cetoglutarato desidrogenase

LPS – lipopolissacarídeo

MAPK - proteína quinase ativada por mitógeno

MBP – proteína básica da mielina

MDA – malondialdeído

MEL - melatonina

NAC - N-acetilcisteína

NADH - nicotinamida adenina dinucleotídeo reduzido

NeuN – proteína nuclear neuronal

NF-κB – fator nuclear kappa B

NO• – óxido nítrico

O2•- – ânion superóxido

OH• – radical hidroxila

ONOO- – peroxinitrito

Parkin - proteína Parkin (E3 ubiquitina ligase)

PGE2 - prostaglandina E2

PINK1 - quinase 1 induzida por PTEN

QI - quociente de inteligência

S100B – proteína ligante de cálcio S100B

SNC - sistema nervoso central

SOD – enzima superóxido dismutase

TAR - resposta antioxidante total

TNF-α - fator de necrose tumoral alfa

SUMÁRIO

PARTE I: INTODUÇÃO E OBJETIVOS

1.INTRODUÇÃO.....1

1.1.Doença do Xarope do Bordo.....1
1.2. Diagnóstico.....3
1.3. Fenótipos clínicos.....3
1.4. Neuropatologia.....5
1.5. Tratamento.....6
1.6. Fisiopatogenia do dano neurológico.....7
1.7. Funções mitocondriais: Bioenergética, Ciclo do ácido cítrico, fosforilação oxidativa, cadeia transportadora de elétrons e parâmetros respiratórios.....9
1.8. Homeostase redox e estresse oxidativo 10

1.9. Melatonina.....12
1.10.N-acetilcisteína.....13
1.11.L-Carnitina.....13
1.12.Neuroinflamação 15
1.13.Lipopolissacarídeo (LPS).....17
1.14.Justificativa.....18
2. OBJETIVO GERAL 19
2.1. OBJETIVOS ESPECÍFICOS 19

PARTE II: ARTIGOS CIENTÍFICOS

3.CAPÍTULO I.....21
4.CAPÍTULO II.....40
5.CAPÍTULO III.....56

PARTE III: DISCUSSÕES E CONCLUSÕES

6.DISCUSSÃO.....78

7.CONCLUSÕES 97

8.PERSPECTIVAS.....99

REFERÊNCIAS.....100

ANEXOS.....116

CARTA DE APROVAÇÃO COMISSÃO DE ÉTICA NO USO DE ANIMAIS.....116

PARTE I: Introdução e Objetivos

1. INTRODUÇÃO

1.1. Doença do Xarope do Bordo

Erros inatos do metabolismo são distúrbios hereditários, majoritariamente de herança autossômica recessiva, cuja característica bioquímica principal é a deficiência ou ausência da atividade de uma enzima específica de uma rota metabólica. Além das enzimas, outras proteínas com função alterada como proteínas de transporte e proteínas estruturais, imunoglobulinas, hormônios, entre outras, podem estar afetadas nos erros inatos do metabolismo. O resultado deste bloqueio pode levar ao acúmulo de substâncias tóxicas nos tecidos e fluidos corporais ou à falta de substâncias essenciais, muitas vezes, acarretando prejuízo no desenvolvimento mental e/ou físico dos indivíduos afetados [1]. Além disso, rotas alternativas também poderão originar outras substâncias possivelmente tóxicas.

Em 1954, Menkes e colaboradores [2] descreveram uma doença degenerativa cerebral em quatro membros de uma mesma família. A manifestação do quadro clínico se dava na primeira semana de vida com prognóstico fatal nos três meses subsequentes. O achado mais proeminente foi um odor forte de açúcar queimado na urina dos pacientes, o que deu origem ao nome "Doença do Xarope do Bordo" (DXB). Em 1957, Westall e colaboradores [3] observaram outro paciente e encontraram concentrações muito altas dos aminoácidos de cadeia ramificada (ACR), leucina, isoleucina e valina. Em 1959, Menkes [4] isolou na urina dos pacientes os α-cetoácidos de cadeia ramificada (CCR) ácido α-cetoisocaproico (CIC), ácido α-ceto-β-metilvalérico (CMV) e ácido α-cetoisovalérico (CIV), que derivam dos aminoácidos leucina, isoleucina e valina, respectivamente.

A DXB é um distúrbio metabólico de herança autossômica recessiva causada pela deficiência na atividade do complexo desidrogenase dos α-cetoácidos de cadeia ramificada (CDCCR) [5, 6]. Esta deficiência enzimática resulta no acúmulo dos ACR, bem como de seus respectivos CCR. Da mesma forma são encontrados em concentrações elevadas os hidroxiácidos derivativos correspondentes ácido α-hidroxi-isocaproico, ácido α-hidroxi-isovalérico e ácido α-hidroxi-β-metilvalérico (Figura 1). Por outro lado, os compostos que mais se acumulam nessa doença são a leucina e o CIC, que podem atingir uma concentração plasmática de 5 mM no plasma dos pacientes durante as crises de descompensação metabólica [5].

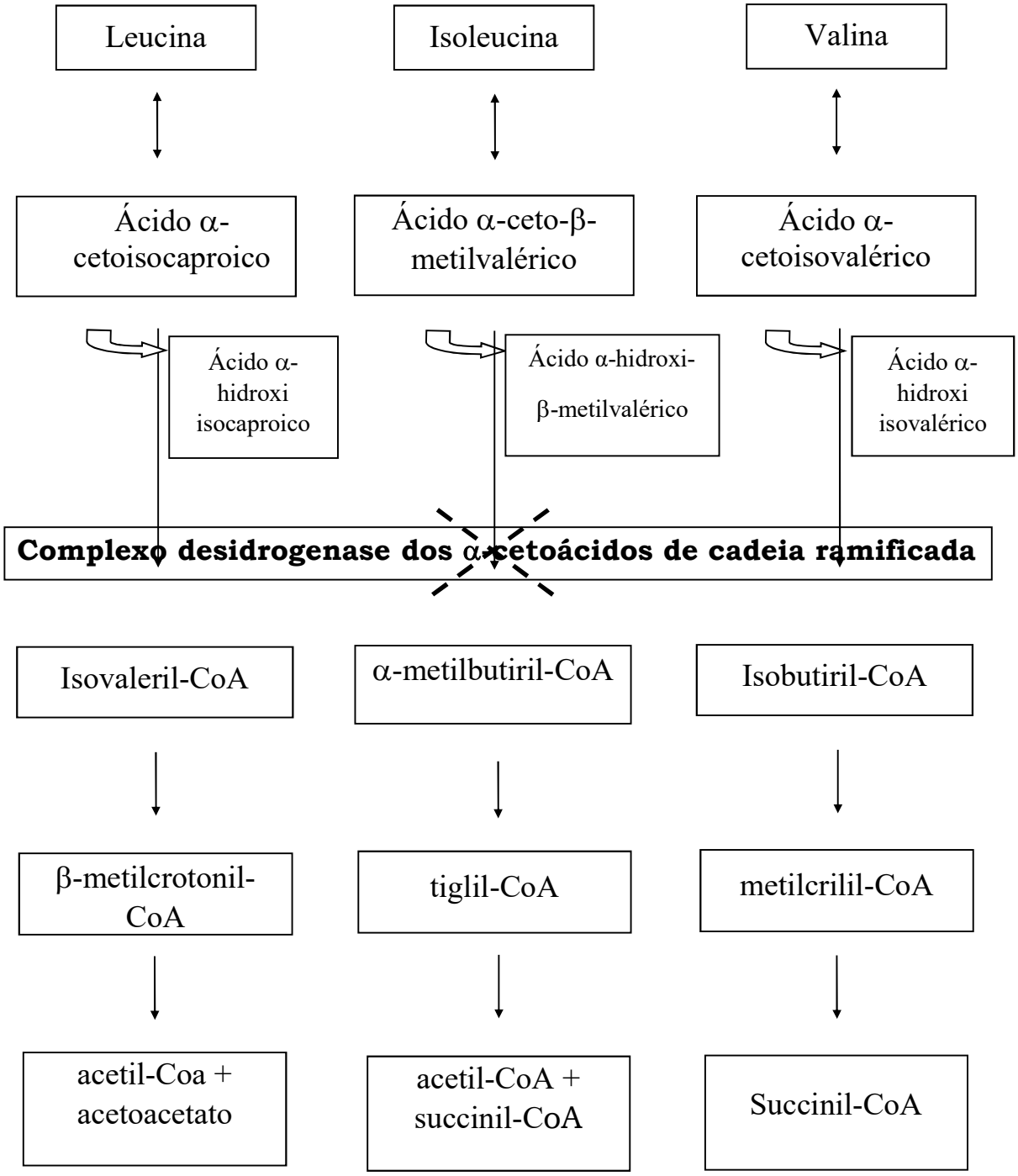


Figura 1 - Rotas catabólicas dos aminoácidos de cadeia ramificada leucina, isoleucina e valina. As duas primeiras reações comuns são catalisadas pelas seguintes enzimas: transaminação reversível pela aminotransferase dos aminoácidos de cadeia ramificada, descarboxilação oxidativa dos cetoácidos de cadeia ramificada e esterificação da coenzima A pelo complexo α-cetoácido desidrogenase. Em destaque é mostrada a etapa em que a enzima é deficiente nos pacientes com DXB e os metabólitos que se acumulam nessa doença.

1.2. Diagnóstico

O diagnóstico da DXB é fundamentalmente laboratorial através da identificação de concentrações plasmáticas e urinárias elevadas de leucina, isoleucina e valina ou de seus respectivos CCR através de cromatografia de aminoácidos e ácidos orgânicos, respectivamente. Como mencionado anteriormente, são encontradas concentrações muito elevadas dos metabólitos leucina e CIC (5 mM) no plasma de pacientes não tratados, enquanto os demais metabólitos também possuem concentrações plasmáticas significativamente elevadas [5, 6]. Neste particular, foi observado que as concentrações desses metabólitos são próximas a 1 mM em líquido cefalorraquidiano [7]. A quase totalidade dos estados norte-americanos, bem como muitos outros países possuem programa de triagem neonatal em massa para identificar essa doença nos recém-nascidos através da detecção de níveis plasmáticos de leucina, usualmente acima de 2 mg/dL (153 μM) [8].

Importante salientar que a presença de quantidades mensuráveis de L-aloisoleucina, outro metabólito acumulado no plasma nessa doença, um produto da racemização da isoleucina, tem sido considerada um achado patognomônico para a DXB. Na análise de rotina dos aminoácidos, a L-aloisoleucina é indetectável no plasma de indivíduos saudáveis devido à sua baixa concentração e à presença de compostos interferentes [9].

Embora não seja regularmente feita, a ausência ou severa deficiência na atividade do CDCCR em cultura de leucócitos periféricos dos pacientes é um achado confirmatório da DXB [10].

O diagnóstico pré-natal da DXB pode ser realizado em cultura de células do fluido amniótico retiradas por amniocentese entre a 14ª e a 18ª semana de gestação, ou por análise direta do tecido em vilosidades coriônicas e cultura de células de vilosidades coriônicas [5].

1.3. Fenótipos clínicos

A DXB possui 5 diferentes fenótipos clínicos: clássico, intermediário, intermitente, tiamina-responsivo e E3 deficiente. A forma clássica da DXB corresponde a 80% dos casos e apresenta um quadro neonatal de encefalopatia e representa o fenótipo mais grave e comum da doença. Os níveis dos ACR e CCR, particularmente de leucina

e CIC, estão muito aumentados no sangue, chegando a 5 mM, bem como no líquido cefalorraquidiano e na urina dos pacientes afetados. A atividade do CDCCR em fibroblastos ou cultura de linfócitos encontra-se usualmente menor que 2% quando comparada à atividade normal da enzima. Os pacientes afetados apresentam-se normais ao nascimento e os sintomas, que se desenvolvem geralmente entre o 4º e o 7º dia de vida, incluem letargia, recusa alimentar, alterações neurológicas progressivas como hypotonia e hipertonia, cetose, odor de açúcar queimado na urina, hipoglicemia, convulsões e coma. A maioria dos pacientes, quando não tratados, morre nos primeiros meses de vida em decorrência de crises metabólicas recorrentes e de deterioração neurológica, frequentemente precipitada por infecções ou outros eventos relacionados ao catabolismo, tais como vacinações ou cirurgias. Aqueles que sobrevivem apresentam atraso no desenvolvimento neuromotor e déficit cognitivo observados posteriormente [5, 11–13].

Pacientes com a forma intermediária apresentam elevações persistentes dos ACR, porém menores do que as verificadas na forma clássica (acompanhadas por comprometimento neurológico associado à déficit cognitivo), mas não apresentam sintomas severos no período neonatal. Muitos casos não apresentam episódios de descompensação metabólica aguda. A atividade residual da enzima é geralmente maior do que a apresentada no fenótipo clássico e varia entre 3 a 30% da normal, embora existam relatos de níveis menores [14–16]. O diagnóstico geralmente ocorre entre 5 meses a 7 anos de idade em decorrência de atraso no desenvolvimento e/ou convulsões e cetoacidose, embora encefalopatia aguda raramente ocorra.

No que se refere aos pacientes que apresentam o fenótipo intermitente da doença, caracterizam-se por um desenvolvimento inicial normal. No entanto, eles apresentam risco de sofrerem descompensação metabólica durante situações de estresse metabólico. No período assintomático da doença os níveis dos ACR são normais, sendo que a atividade enzimática situa-se entre 5 a 20% da normal. Os sintomas iniciais normalmente surgem entre os 5 meses e 2 anos de vida em associação com otite média ou outras infecções. Os episódios de mudanças agudas no comportamento e dificuldade de caminhar podem evoluir para crises de descompensação com choque e coma. Os perfis de ACR e CCR nestes casos equiparam-se ao do fenótipo clássico da DXB durante as crises [5].

Os pacientes tiamina-responsivos não apresentam doença neonatal aguda e suas manifestações clínicas são semelhantes às da forma intermediária. A concentração de ACR no plasma é cerca de 5 vezes maior que o normal. Estes níveis (2-5 mM) são reduzidos abruptamente para níveis normais com doses de 10 a 1000 mg/dia de tiamina e com dieta restrita em proteínas. A atividade enzimática situa-se entre 2 a 40% da normal. As manifestações clínicas e laboratoriais mais frequentes são descompensação metabólica e acidose, acompanhada de desenvolvimento físico normal [5].

Já a deficiência de E3 é um distúrbio raro. Apresenta sinais clínicos semelhantes aos da forma intermediária, mas é acompanhada de acidose lática grave. O perfil de ácidos orgânicos na urina exibe anormalidades encontradas tanto na acidose lática como na DXB. O lactato, o piruvato, o α-cetoglutarato, o α-hidroxi-β-isovalerato e o α-hidroxiglutarato estão aumentados neste fenótipo. A hiperalaninemia secundária ao acúmulo de piruvato é também frequente. Os ACR estão leve ou moderadamente aumentados no plasma, quando comparados aos níveis encontrados na forma clássica. Estes pacientes têm deficiência das três enzimas desidrogenases em que E3 é um componente, a α-cetoglutarato desidrogenase (KGDH), a piruvato desidrogenase e o CDCCR. Os pacientes que apresentam este fenótipo normalmente não apresentam sintomatologia nos primeiros meses de vida. Quando surge acidose lática persistente, entre 8 semanas e 6 meses de idade, ocorre a deterioração neurológica progressiva caracterizada por hipotonia, atraso no desenvolvimento e encefalopatia similar a de Leigh e déficit cognitivo [5]. Os resultados dos tratamentos com doses farmacológicas de tiamina, biotina, e ácido lipoico, combinados com restrição na dieta de gorduras e ACR não têm se revelado satisfatórios, pois, apesar de diminuir a mortalidade, os pacientes frequentemente apresentam complicações neurológicas.

1.4. Neuropatologia

Em relação às alterações neuropatológicas de pacientes com a DXB, imagens de ressonância magnética cerebral demonstraram hipomielinização e edema de bainha intramielínica citotóxica nos gânglios da base, córtex cerebral, cerebelo, substância branca periventricular e tronco encefálico [17–19]. Edema vasogênico-intersticial em áreas não-mielinizadas dos lobos frontal e temporal também foram descritos [20]. Atrofia cerebral é comumente observada em pacientes que apresentaram longos períodos de descontrole metabólico na infância e durante a progressão da doença [11, 21].

Estudos *post-mortem* confirmaram os achados da ressonância magnética cerebral observada nos pacientes vivos, revelando edema cerebral extenso e aparência esponjosa generalizada da substância branca associada a mielinização defeituosa, mais pronunciada em áreas subcorticais, gânglios da base, cápsula interna, núcleos dentários, cerebelo e tronco cerebral [22–24]. Anormalidades neuronais no córtex cerebral [22], edema de astrócitos na coroa radiada dos hemisférios cerebrais [2], astrogliose e diminuição do número de oligodendrócitos na substância branca cerebral e cerebelar também foram observados [24–26].

Evidências experimentais indicam toxicidade cerebral induzida pelos ACR e CCR acumulados na DXB que podem explicar a neuropatologia da doença. Nesse particular, as crises de descompensação metabólica caracterizadas por altos níveis circulantes de leucina e CIC, geralmente estão associadas à piora dos sintomas neurológicos, sugerindo que o acúmulo cerebral desses metabólitos desempenha um papel central na neuropatologia da DXB [5].

1.5. Tratamento

O tratamento dos pacientes com DXB consiste basicamente em restrição dos ACR da dieta para minimizar o acúmulo dos metabólitos e seus efeitos tóxicos, principalmente sobre o sistema nervoso central (SNC). O objetivo do tratamento é normalizar as concentrações dos ACR sem prejudicar o crescimento e desenvolvimento dos pacientes e, para tanto, deve ser iniciado o mais cedo possível e ainda no período neonatal. Administra-se um leite especial com concentrações reduzidas de leucina, valina e isoleucine [27]. Outras preparações dietéticas específicas para pacientes com DXB também foram desenvolvidas. A terapia com tiamina (50 a 300 mg/dia) por 3 semanas é empregada no início do tratamento para a detecção de pacientes responsivos à tiamina [5]. Em casos mais graves tem sido utilizado o transplante de fígado, substituindo o órgão com gene alterado por um órgão com gene normal [11, 12, 28, 29]. Desta forma, os ACR podem ser metabolizados normalmente.

Na fase aguda, emprega-se um tratamento mais agressivo, pois o aumento na concentração dos ACR e CCR, geralmente precipitado por infecções ou outras situações que promovem descompensação metabólica, leva à deterioração das funções cerebrais. Três medidas devem ser tomadas para o controle das crises metabólicas: remoção dos

metabólitos tóxicos; promoção de suporte nutricional adequado e minimização do catabolismo e/ou promoção do anabolismo. Supõe-se que promover o anabolismo pode ser um dos mais importantes fatores no controle da descompensação metabólica [5]. A diálise peritoneal e a transfusão sanguínea são utilizadas para a remoção dos metabólitos com melhora significativa e rápida do quadro neurológico. No entanto, a hemodiálise é mais eficaz na depuração dos ACR e dos CCR do plasma do que a diálise peritoneal. A diálise peritoneal é um procedimento relativamente simples, enquanto a hemodiálise requer um equipamento sofisticado e treinamento especializado. Desenvolveu-se, para os pacientes com DXB, uma terapia com nutrição parenteral que inclui uma mistura de ACR em combinação com glicose, lipídios, eletrólitos e vitaminas a fim de proporcionar uma nutrição balanceada. Esta preparação é utilizada nos casos de descompensação metabólica moderada ou em combinação com outras terapias na descompensação metabólica severa. Uma terapia alternativa consiste em evitar o estado catabólico com administração de insulina e glicose [30, 31]. Para os pacientes pouco responsivos ao tratamento dietético, tem sido realizado transplante de fígado que tem diminuído sobremaneira a mortalidade dos pacientes, mas não impede, na maioria deles, as complicações neurológicas, provavelmente porque o catabolismo dos ACR também ocorre no SNC [12, 28, 29, 32]. Deve-se, no entanto, enfatizar que um grau variável de comprometimento da cognição é observado na maioria dos pacientes com DXB, os quais foram submetidos a um tratamento aparentemente adequado, sugerindo que o tratamento para esta doença deva ser melhorado.

1.6. Fisiopatogenia do dano cerebral

A fisiopatogenia do dano cerebral na DXB é um processo multifatorial, no qual o acúmulo dos ACR e de seus α-cetoácidos, especialmente a leucina e o CIC, desencadeia alterações neuroquímicas, energéticas, oxidativas e inflamatórias que culminam em disfunção e morte celular neuronal.

Deve-se ainda enfatizar o desequilíbrio de aminoácidos cerebrais, pois a elevada concentração plasmática de leucina satura o transportador LAT1 (SLC7A5) [33] na barreira hematoencefálica, reduzindo a entrada de outros aminoácidos neutros de grande porte, como fenilalanina, tirosina, triptofano e metionina [22, 34–37]. Como esses aminoácidos são precursores de neurotransmissores importantes, sua deficiência cerebral

leva à redução da síntese de dopamina, serotonina, noradrenalina e histamina, além de comprometer a síntese proteica neuronal.

Paralelamente, o CIC acumulado no cérebro promove alterações profundas no metabolismo do glutamato. Por meio de reações de transaminação reversa, ocorre consumo de glutamato e aumento de α-cetoglutarato, resultando em diminuição dos níveis de glutamato, glutamina e GABA [11, 38–40]. Como consequência, há comprometimento simultâneo da neurotransmissão excitatória glutamatérgica e da neurotransmissão inibitória GABAérgica, além de alterações no ciclo glutamato-glutamina. Estudos em pacientes e modelos animais demonstraram reduções significativas dessas moléculas, associadas a déficits cognitivos, alterações psiquiátricas e distúrbios motores [11, 38–40].

Também foi demonstrado que a leucina e o CIC induzem apoptose neuronal, ativação de caspases, alterações morfológicas em astrócitos e oligodendrócitos e redução da viabilidade celular. Essas alterações podem ajudar a explicar os achados neuropatológicos observados em pacientes, incluindo edema cerebral, hipomielinização, perda de oligodendrócitos, astrogliosis e degeneração da substância branca [41].

Outro componente central da fisiopatologia é a disfunção bioenergética mitocondrial. O acúmulo de ACR e CCR inibe enzimas importantes do metabolismo energético, incluindo as do ciclo do ácido cítrico e da cadeia respiratória mitocondrial. Como consequência, ocorre redução da produção de adenosina trifosfato (ATP), diminuição da oxidação de nicotinamida adenina dinucleotídeo reduzido (NADH) e aumento da formação de lactato. A deficiência energética cerebral resultante compromete a função neuronal e favorece a progressão do dano neurológico [40, 42].

A desregulação do metabolismo energético está intimamente associada ao estresse oxidativo. Estudos *in vitro* demonstraram que os metabólitos acumulados na doença aumentam a produção de espécies reativas de oxigênio e nitrogênio (ERO e ERN), promovendo peroxidação lipídica, oxidação de proteínas e danos ao ácido desoxirribonucleico (DNA). Simultaneamente, ocorre redução das defesas antioxidantes, incluindo diminuição da atividade de enzimas como glutationa peroxidase (GPx), catalase (CAT) e superóxido dismutase (SOD). Considerando a elevada demanda energética e a vulnerabilidade oxidativa do tecido nervoso, esses processos contribuem significativamente para a lesão neuronal progressiva observada na doença [43].

Mais recentemente, a neuroinflamação passou a ser reconhecida como um importante mecanismo complementar [41]. O aumento das concentrações cerebrais de ACR e CCR estimula a produção de citocinas pró-inflamatórias, incluindo fator de necrose tumoral alfa (TNF-α), interleucina 1 beta (IL-1β), interleucina 6 (IL-6) e interferon gama (IFN-γ), favorecendo a ativação glial e amplificando os processos de dano neuronal [44].

1.7. Funções mitocondriais: Bioenergética, ciclo do ácido cítrico, fosforilação oxidativa, cadeia transportadora de elétrons e parâmetros respiratórios

As mitocôndrias são organelas recobertas por uma membrana externa, altamente permeável a pequenas moléculas e íons, e que possuem uma membrana interna impermeável à maioria das moléculas e íons [45]. Estas complexas estruturas subcelulares desempenham papel central no metabolismo energético por meio da fosforilação oxidativa, respostas adaptativas ao estresse e de processos de biossíntese. Também desempenham papeis fundamentais em processos celulares, incluindo inflamação, homeostase redox e do cálcio, e morte celular [46–51].

O acetil-CoA proveniente da oxidação de carboidratos, aminoácidos, ácidos graxos e corpos cetônicos pode ser completamente oxidado no ciclo do ácido cítrico a CO2, fornecendo as coenzimas reduzidas NADH e $FADH_2$ (flavina adenina dinucleotídeo reduzido), que são transportadores de elétrons para os complexos I e II, respectivamente, da cadeia respiratória mitocondrial. O fluxo de elétrons através dos complexos I, II, III e IV da cadeia respiratória, tendo o O_2 como aceptor final dos elétrons provenientes do complexo IV, é acompanhado pelo bombeamento de H^+ da matriz mitocondrial para o espaço intermembrana, através dos complexos I, III e IV, gerando um acúmulo desse íon e, por consequência, formando um gradiente eletroquímico. Em sequência, a ATP sintase (complexo V) abre um canal na porção Fo capaz de dissipar os H^+ de volta para a matriz mitocondrial, utilizando então a energia liberada para realizar a fosforilação da adenosina difosfato (ADP) em ATP [52, 53].

A respiração mitocondrial pode ser estimada através da medida do consumo de O_2, sendo um excelente sensor da atividade da cadeia respiratória mitocondrial e da oxidação de substratos no ciclo do ácido cítrico, uma vez que os processos de transferência de elétrons, bombeamento de H^+, formação do gradiente eletroquímico e

síntese de ATP, são acoplados e estão interligados ao consumo de O_2. Experimentalmente, pode-se dividir a respiração mitocondrial em estados respiratórios, sendo que o estado 3 representa o consumo de O_2 quando as mitocôndrias, em um meio contendo substrato oxidável capaz de estimular o fornecimento de elétrons para a cadeia respiratória, são expostas ao ADP, estimulando o consumo de O_2 e produzindo ATP (estado fosforilante). O estado 4 geralmente é estimulado por oligomicina, um inibidor da ATP sintase, refletindo o consumo de O_2 necessário para a formação e manutenção do gradiente eletroquímico, reduzindo a taxa da respiração (estado não-fosforilante). Ainda, é possível utilizar compostos desacopladores da fosforilação oxidativa, os quais provocam um vazamento de H^+ do espaço intermembrana para a matriz mitocondrial, acelerando a atividade da cadeia respiratória mitocondrial e o consumo de O_2 sem produção de ATP (estado desacoplado) [52, 54].

1.8. Homeostase redox e estresse oxidativo

As espécies reativas são moléculas ou átomos que frequentemente apresentam elétrons desemparelhados em seus orbitais, característica que lhes confere elevada instabilidade eletrônica e, consequentemente, grande capacidade de reagir com outras moléculas ou átomos, promovendo sua oxidação [55, 56]. Em condições fisiológicas, o O_2 é reduzido no complexo IV da cadeia respiratória mitocondrial (CRM), resultando na formação de água (H_2O). Entretanto, centros redox presentes em complexos da CRM, especialmente nos complexos I e III, podem transferir diretamente um elétron ao O_2, originando o ânion superóxido ($O_2^{\bullet -}$).

O ânion superóxido pode ser convertido em peróxido de hidrogênio (H_2O_2) pela ação da SOD. Embora o H_2O_2 não possua elétrons desemparelhados, ele pode reagir com íons ferroso (Fe^{2+}) por meio da reação de Fenton, gerando o radical hidroxila (•OH), uma das espécies reativas mais agressivas biologicamente. O superóxido, o peróxido de hidrogênio e o radical hidroxila compõem o grupo dos ERO. Além destas, destacam-se as ERNs, representadas principalmente pelo óxido nítrico (NO•) e pelo peroxinitrito ($ONOO^-$) [55].

As espécies reativas desempenham funções fisiológicas importantes como moléculas sinalizadoras, participando de diversos processos celulares essenciais. Entre eles destacam-se a sinalização da insulina, as adaptações induzidas pelo exercício físico

e os mecanismos de defesa imunológica, nos quais neutrófilos produzem espécies reativas para combater agentes infecciosos [57–62]. Dessa forma, a produção controlada de EROs e ERNs é fundamental para a manutenção da função celular normal.

Em condições fisiológicas, a geração de espécies reativas é continuamente equilibrada por sistemas antioxidantes endógenos. No entanto, quando sua produção excede a capacidade de neutralização celular, podem ocorrer danos oxidativos a biomoléculas, incluindo proteínas, lipídios, carboidratos e ácidos nucleicos [55].

Para prevenir esses danos, as células dispõem de um complexo sistema de defesa antioxidante, composto por mecanismos enzimáticos e não enzimáticos distribuídos estrategicamente entre diferentes compartimentos celulares e tecidos. Entre os principais componentes desse sistema encontram-se a SOD, CAT e GPx, responsáveis pela remoção catalítica de espécies reativas. Além disso, proteínas quelantes, como as transferrinas, reduzem a disponibilidade de metais pró-oxidantes, enquanto moléculas antioxidantes, como a glutationa reduzida (GSH), atuam diretamente na neutralização de radicais livres e servem como substratos para enzimas antioxidantes. Outros mecanismos incluem proteínas capazes de proteger biomoléculas por diferentes vias de defesa celular [55, 63, 64].

Quando o aumento na produção de espécies reativas é discreto, os sistemas antioxidantes geralmente conseguem restabelecer o equilíbrio redox. Entretanto, em diversas condições patológicas, a produção de oxidantes pode superar a capacidade antioxidante celular, comprometendo a manutenção da homeostase redox [55]. Esse desequilíbrio entre fatores pró-oxidantes e mecanismos antioxidantes caracteriza o estresse oxidativo, considerado um importante mecanismo envolvido na fisiopatologia de inúmeras doenças humanas [65].

O estresse oxidativo pode resultar tanto do aumento na geração de oxidantes quanto da redução das defesas antioxidantes. Adicionalmente, a liberação de metais de transição ou a combinação desses fatores também pode contribuir para sua instalação[55]. Em níveis moderados, o estresse oxidativo pode ser tolerado pelas células e, frequentemente, induz mecanismos adaptativos que incluem o aumento da expressão de enzimas antioxidantes. Contudo, quando os danos oxidativos se tornam excessivos, ocorre comprometimento da integridade celular, podendo culminar em morte celular por apoptose ou necrose [55].

1.9. Melatonina

A melatonina (MEL) é um hormônio neuroendócrino derivado do aminoácido triptofano, sintetizado e secretado predominantemente pela glândula pineal em resposta à redução da luminosidade ambiental. Esse hormônio desempenha papel fundamental na regulação de diversos processos biológicos, incluindo o ciclo sono-vigília, os ritmos circadianos, a função imunológica e a reprodução [66].

Além de suas funções fisiológicas clássicas, a MEL tem despertado crescente interesse devido às suas propriedades antioxidantes, evidenciadas em diferentes condições fisiológicas e patológicas. Sua ação antioxidante ocorre por múltiplos mecanismos, incluindo a neutralização direta de EROs e ERNs, atuando como sequestradora de radicais livres (scavenger), bem como pela modulação indireta das defesas antioxidantes celulares por meio da indução da expressão e atividade de enzimas antioxidantes [67, 68].

Adicionalmente, a MEL apresenta capacidade de quelar metais de transição, como ferro e cobre, reduzindo sua participação nas reações de Fenton e Haber-Weiss. Como consequência, ocorre diminuição da formação do radical hidroxila, considerado uma das espécies reativas mais agressivas e potencialmente danosas às estruturas celulares [69].

A ampla distribuição intracelular da melatonina, embora heterogênea, contribui significativamente para suas propriedades citoprotetoras. Destaca-se sua elevada concentração nas mitocôndrias, organelas que representam importantes fontes de geração de espécies reativas. Essa característica favorece sua atuação na preservação da homeostase redox, na proteção contra danos oxidativos e na prevenção da apoptose celular [68, 70].

Além disso, diversos estudos têm demonstrado os efeitos neuroprotetores da MEL, especialmente no SNC. Em modelos experimentais *in vivo* e *in vitro* de distúrbios hereditários do metabolismo, a administração desse hormônio foi capaz de atenuar o estresse oxidativo induzido pelo acúmulo de metabólitos tóxicos, contribuindo para a proteção celular e para a redução dos danos neurológicos associados a essas doenças [71–73].

1.10. N-Acetilcisteína

A N-acetilcisteína (NAC) é um derivado acetilado do aminoácido L-cisteína e tem sido utilizada na prática clínica há mais de 60 anos [74]. Inicialmente, seu uso esteve relacionado à ação mucolítica, devido à capacidade de romper pontes dissulfeto presentes nas glicoproteínas do muco, reduzindo sua viscosidade e facilitando a eliminação das secreções respiratórias. Posteriormente, a NAC passou a ser amplamente utilizada como antídoto na intoxicação por paracetamol [75]

Durante muitos anos, a NAC foi considerada principalmente um antioxidante. Entretanto, estudos mais recentes demonstram que seus mecanismos de ação são mais complexos do que simplesmente neutralizar EROs [76]. Embora apresente alguma capacidade antioxidante direta, sua principal ação ocorre de forma indireta, por meio do fornecimento de cisteína para a síntese de GSH, um dos mais importantes sistemas antioxidantes intracelulares. Como a disponibilidade de cisteína é um fator limitante para a produção de GSH, a administração de NAC contribui para a restauração dos estoques celulares desse tripeptídeo, favorecendo a manutenção do equilíbrio redox e a proteção contra danos oxidativos [76].

Além de atuar como precursora da GSH, a NAC possui capacidade de reduzir ligações dissulfeto em proteínas e outras moléculas biológicas. Essa propriedade explica não apenas seu efeito mucolítico, mas também sua participação na manutenção da funcionalidade de proteínas sensíveis ao estado redox celular [62]

Evidências recentes sugerem ainda que parte dos efeitos citoprotetores da NAC pode estar relacionada à sua conversão metabólica em sulfeto de hidrogênio (H_2S) e espécies de enxofre sulfurado [62, 76]. Essas moléculas participam de vias de sinalização celular associadas à proteção contra o estresse oxidativo, inflamação e morte celular, ampliando a compreensão dos benefícios observados com o uso da NAC em diferentes condições experimentais e clínicas.

1.11. L-Carnitina

A L-carnitina é uma amina quaternária hidrossolúvel derivada dos aminoácidos lisina e metionina, desempenhando papel essencial no metabolismo energético celular. Embora parte da carnitina seja sintetizada endogenamente, principalmente no fígado e nos rins, a maior parte é obtida por meio da alimentação, especialmente a partir de carnes

vermelhas e produtos lácteos. No organismo, a carnitina está presente tanto na forma livre quanto esterificada, destacando-se a acetil-L-carnitina (ALC) e outras acilcarnitinas. Mais de 99% da carnitina corporal encontra-se no meio intracelular, com elevadas concentrações no fígado e no músculo esquelético [77].

A principal função fisiológica da L-carnitina está relacionada ao transporte de ácidos graxos de cadeia longa para o interior das mitocôndrias, onde são submetidos à β-oxidação para geração de energia. Esse processo é fundamental para a produção de ATP, especialmente em condições de jejum prolongado, exercício físico intenso ou redução da disponibilidade de carboidratos [77]. Dessa forma, a disponibilidade adequada de carnitina é indispensável para a manutenção do metabolismo energético celular, sendo que sua deficiência pode comprometer a utilização de ácidos graxos como fonte de energia.

Além de participar diretamente do metabolismo lipídico, a L-carnitina desempenha papel importante na regulação do equilíbrio metabólico intracelular. A molécula atua no transporte de grupos acila entre compartimentos celulares, favorecendo a regeneração da coenzima A livre (CoA) no interior das mitocôndrias. Esse mecanismo auxilia na manutenção das funções metabólicas mitocondriais e influencia processos como glicólise, gliconeogênese, catabolismo de aminoácidos e produção de corpos cetônicos. Adicionalmente, a formação de acilcarnitinas permite a remoção de metabólitos potencialmente tóxicos da matriz mitocondrial, contribuindo para a proteção celular contra o acúmulo de compostos prejudiciais [78].

Nos últimos anos, evidências experimentais têm demonstrado que a L-carnitina exerce funções que vão além do metabolismo energético. Estudos indicam propriedades neuroprotetoras, neuromoduladoras e citoprotetoras associadas a essa molécula. No SNC, a L-carnitina atravessa a barreira hematoencefálica por meio do transportador OCTN2, acumulando-se principalmente na forma de ALC [77, 78]. Essa forma participa do fornecimento de grupos acetila para a síntese de acetilcolina, neurotransmissor fundamental para processos cognitivos, além de atuar na modulação da expressão gênica, da sinalização celular e da regeneração neuronal.

Outro aspecto relevante refere-se ao potencial antioxidante da L-carnitina. Diversos estudos sugerem que essa molécula contribui para a redução dos danos associados ao estresse oxidativo, especialmente em situações caracterizadas por disfunção mitocondrial. Em doenças neurodegenerativas, como as doenças de Parkinson

e Alzheimer, bem como em erros inatos do metabolismo, o aumento da produção de espécies reativas de oxigênio está associado à progressão do dano celular. Nesses contextos, a L-carnitina parece atuar preservando a função mitocondrial, reduzindo a formação de espécies reativas e minimizando os danos oxidativos[79–81].

1.12. Neuroinflamação

O sistema imunológico desencadeia respostas agudas e crônicas com o objetivo de preservar a integridade estrutural e funcional dos tecidos e órgãos, garantindo o equilíbrio entre processos lesivos e mecanismos de defesa. No SNC, a resposta inflamatória é denominada neuroinflamação e caracteriza-se principalmente pela ativação de células gliais, especialmente micróglia e astrócitos. Esse processo representa um importante mecanismo de defesa frente a estímulos capazes de provocar danos ao tecido nervoso [82].

A microglia é composta por células imunes inatas de origem mieloide que colonizam o SNC durante o desenvolvimento embrionário. Essas células desempenham papel fundamental na vigilância imunológica do tecido nervoso, sendo capazes de iniciar e modular respostas imunes inatas e adaptativas [83, 84]. Em geral, a neuroinflamação é iniciada pelo recrutamento e ativação da micróglia em resposta a sinais liberados por neurônios lesionados ou submetidos a condições de estresse [85, 86].

A ativação microglial é acompanhada por profundas alterações morfológicas e funcionais, incluindo mudanças no tamanho celular, na expressão de proteínas de superfície e no perfil de produção de citocinas e fatores de crescimento [87]. Entre os principais marcadores desse processo destaca-se a molécula adaptadora ligante de cálcio ionizado 1 (IBA1), cuja expressão aumenta significativamente durante a ativação microglial, tornando-a um importante indicador desse fenômeno [88]. Uma vez ativadas, as células microgliais adquirem elevada capacidade fagocítica, participando da remoção de detritos celulares, corpos apoptóticos, microrganismos e outras partículas exógenas por meio de mecanismos especializados de fagocitose [89].

Os astrócitos, por sua vez, constituem a população glial mais abundante do cérebro e exercem funções que vão muito além do suporte estrutural aos neurônios. Essas células desempenham papel essencial na manutenção da homeostase cerebral, regulando o fluxo sanguíneo cerebral, a integridade da barreira hematoencefálica, o fornecimento de

substratos energéticos aos neurônios, a atividade sináptica, a secreção de neurotrofinas e o equilíbrio extracelular de íons, líquidos e neurotransmissores [90, 91].

Além de suas funções homeostáticas, os astrócitos atuam como importantes moduladores das respostas imunes no SNC. Dependendo do contexto fisiopatológico, essas células podem contribuir tanto para a amplificação quanto para a resolução da resposta inflamatória. A ativação excessiva dos astrócitos pode exacerbar a neuroinflamação e favorecer o dano tecidual, enquanto, em outras situações, pode promover imunossupressão e reparo celular [92].

A reatividade astrocitária é caracterizada por alterações morfológicas e moleculares, sendo frequentemente avaliada pela expressão da proteína glial fibrilar ácida (GFAP). O aumento da expressão dessa proteína é considerado um marcador clássico de astrogliose reativa e está associado a diversas patologias do SNC. Além da GFAP, outras moléculas, como a proteína ligante de cálcio S100B (S100B), a glicoproteína semelhante à cartilagem YKL-40 e a D-serina, têm sido utilizadas como biomarcadores de ativação astrocitária. Na doença de Alzheimer, por exemplo, GFAP, S100B, YKL-40 e D-serina podem ser detectadas no líquido cefalorraquidiano, enquanto GFAP e S100B também são utilizadas como biomarcadores séricos [93]

Diversos estudos demonstram que uma intensa reatividade astrocitária durante as fases iniciais de doenças neurológicas, como lesão medular e encefalomielite autoimune experimental, está associada ao agravamento dos desfechos clínicos, ao aumento da neuroinflamação, à disfunção da barreira hematoencefálica e à morte neuronal [92].

A neuroinflamação constitui um componente importante da fisiopatologia de diversas doenças neurodegenerativas, incluindo as doenças de Parkinson e Alzheimer, bem como a esclerose lateral amiotrófica. Nessas condições, observa-se aumento na produção de citocinas pró-inflamatórias e de espécies reativas, contribuindo para a disfunção celular e, em determinadas circunstâncias, para a morte neuronal [94].

Além das doenças neurodegenerativas clássicas, evidências crescentes indicam que processos neuroinflamatórios também estão envolvidos na fisiopatologia de diversos distúrbios hereditários do metabolismo. Tanto em pacientes quanto em modelos experimentais dessas doenças, tem sido descrita a ativação de vias inflamatórias associadas ao aumento da expressão de citocinas pró-inflamatórias, ativação glial e comprometimento da homeostase cerebral, sugerindo que a neuroinflamação desempenha

papel relevante na progressão das alterações neurológicas observadas nesses distúrbios [95–100].

1.13. Lipopolissacarídeo (LPS)

O lipopolissacarídeo (LPS) é uma molécula que constitui a bicamada lipídica de bactérias gram-negativas, como por exemplo a Escherichia coli, sendo crítico na estabilidade da membrana. Sua molécula é composta por três distintos domínios: uma cadeia lateral de polissacarídeo (Antígeno O) ligada à região do "core", um oligossacarídeo (2-ceto-3-ácido deoxioctônico), este por sua vez está ligado a uma molécula lipídica (Lipídeo A). O antígeno O varia entre as espécies de bactérias gram negativas tanto em composição como em comprimento, enquanto do core e do lipídeo A são mais conservados entre as diferentes espécies destas bactérias. O domínio lipídeo A é o componente bioativo e tóxico da endotoxina reconhecido durante a infecção humana [101]. O LPS é uma molécula alvo, uma vez que sua presença é crítica na estabilidade de membrana bacteriana e tem um papel proeminente na intensificação da resposta imunológica [102]; ele tem sido implicado como a molécula responsável por uma variedade de patologias que vão de leves, como febre, a letais, como choque séptico e morte. Esta molécula desencadeia a liberação de muitas citocinas, incluindo IL-1β, IL-6 e TNFα, e é provavelmente o estímulo mais frequentemente usado para desencadear vias de sinalização envolvidas na resposta imunológica [103].

A via de sinalização desencadeada por LPS inicia com a ligação deste ao receptor TLR4, este receptor faz parte de uma família de receptores "Toll-like" (TLRs) descritos como um receptor transmembrana tipo I que controla o desenvolvimento do eixo dorsal-ventral da Drosophila melanogaster [104], tendo um papel na resposta imunológica à infecção por fungo nesta espécie. Os receptores TLRs são uma grande família de receptores evolutivamente conservados no sistema imune de vertebrados, que reconhecem modelos moleculares associados a patógenos, produzidos por diversos organismos, incluindo bactérias, vírus, fungos e parasitas, e compreendem 10 genes funcionais em mamíferos [105]. Eles são expressos por célula gliais no SNC sinalizando para dano e autoimunidade neste sistema. A microglia expressa uma ampla variedade destes receptores (TLRs1-9), assim como os astrócitos [106]. A ativação de TLR4 por

LPS inicia uma sequência de sinalização intracelular similar a observada com a ativação do receptor para interleucina 1 (IL-1).

Por essas características e sua alta imunoatividade, o LPS é muito usado por pesquisadores para desenvolver modelos de neuroinflamação *in vivo* e *in vitro*. Estudos *in vitro* mostram que culturas de astrócitos neonatais de diferentes regiões cerebrais exibem diferenças na expressão de fatores pro-inflamatórios sob estímulo com LPS [107], assim como em outro estudo usando o mesmo modelo *in vitro* mostrou que o LPS induz uma regulação positiva de enzimas responsáveis pela síntese de prostaglandina E2 (PGE2) e uma regulação negativa de enzimas que catalisam a sua degradação [108]. Um estudo *in vivo* usando injeções de LPS intracerebroventricular para mimetizar um quadro de inflamação cerebral em camundongos, mostrou ocorrer um recrutamento e adesão de leucócitos à microvasculatura cerebral e que este recrutamento é mediado por células que apresentam a via de sinalização ligada ao TLR4 como a microglia, e que a sinalização por TNF-α é crucial para o recrutamento de leucócitos [109]. Estudos também mostram em outro modelo *in vivo* que injeção intraperitoneal de LPS em camundongos velhos promove hiperatividade microglial estando associada com indução exagerada da IL-1ß e da anti-inflamatória interleucina 10 (IL-10) [110].

1.14. Justificativa

A fisiopatogenia do dano neurológico apresentado pelos pacientes com a DXB ainda não está completamente esclarecida, bem como os mescanismos que desencadeiam as crises encefalopáticas associadas a infecções e uma resposta inflamatória aumentada no cérebro imaturo. Enfatize-se que a maioria dos trabalhos experimentais testando os efeitos do ACR e CCR foram realizados usando ratos de 30 dias de vida ou mais. Portanto, investigar o papel desses metabólitos no cérebro neonatal parece justificado, uma vez que os pacientes com DXB manifestam disfunção neurológica nos primeiros dias de vida.

2. OBJETIVO GERAL

Estudar os efeitos do CIC sobre a homeostase redox, a bioenergética, a resposta inflamatória e a imunohistopatologia em cérebro de ratos neonatos, bem como sobre o desenvolvimento neuromotor dos animais. Também se estudará o efeito de antioxidantes/antiinflamatórios sobre algumas alterações bioquímicas, imunohistopatolóticas e o neurodesenvolvimento causadas pelo CIC.

2.1. OBJETIVOS ESPECÍFICOS

a) Avaliar os efeitos *in vivo* da administração intracerebroventricular do CIC sobre parâmetros da homeostase redox (oxidação de 2',7'-diclorodihidrofluoresceína (DCFH), níveis de malondialdeído (MDA), concentrações de GSH e a atividade das enzimas antioxidantes GPx e SOD, marcadores neuroquímicos neuronais (proteína nuclear neuronal - NeuN), astrocitários (GFAP) e de mielinização (proteína básica da mielina - MBP e 2′,3′-nucleotídeo cíclico 3′-fosfodiesterase - CNPase) no córtex cerebral e no estriado de ratos neonatos.

b) Estudar os efeitos antioxidantes da NAC e da MEL sobre os parâmetros da homeostase redox em córtex cerebral e estriado de ratos neonatos injetados com CIC.

c) Avaliar os efeitos *in vitro* de concentrações patológicas de CIC (5 mM), CMV (1 mM) e CIV (1 mM) sobre a respiração mitocondrial, atividade de enzimas do ciclo do ácido cítrico e produção de ATP no córtex cerebral de ratos neonatos.

d) Avaliar os efeitos *in vivo* da administração combinada intracerebroventricular de CIC e intraperitoneal do indutor de resposta infamatória LPS sobre a expressão gênica de parâmetros pró-inflamatórios como as citocinas IL-6 e o TNFα e os fatores de sinalização ciclo-oxigenase-2 (COX-2) e óxido nítrico sintase induzível (iNOS), bem como sobre marcadores de mitofagia Parkin e PTEN- quinase induzida 1 (PINK1).

e) Estudar os efeitos antioxidantes/antiinflamatórios da L-carnitina sobre a resposta inflamatória e a mitofagia em córtex cerebral e estriado de ratos neonatos injetados com CIC e LPS.

f) Estudar os efeitos *in vivo* da administração combinada intracerebroventricular de CIC e LPS em ratos neonatos sobre o desenvolvimento neuromotor

PARTE II: Artigos Científicos

3. Capítulo I

In Vivo Intracerebral Administration of α-Ketoisocaproic Acid to Neonate Rats Disrupts Brain Redox Homeostasis and Promotes Neuronal Death, Glial Reactivity, and Myelination Injury

Ângela Beatris Zemniaçak, Rafael Teixeira Ribeiro, Camila Vieira Pinheiro, Sâmela de Azevedo Cunha, Tailine Quevedo Tavares, Ediandra Tissot Castro, Guilhian Leipnitz, Moacir Wajner, Alexandre Umpierrez Amaral

Artigo científico publicado em

Molecular Neurobiology (2024) 61:2496–2513

Molecular Neurobiology (2024) 61:2496–2513
https://doi.org/10.1007/s12035-023-03718-9

In Vivo Intracerebral Administration of α-Ketoisocaproic Acid to Neonate Rats Disrupts Brain Redox Homeostasis and Promotes Neuronal Death, Glial Reactivity, and Myelination Injury

Ângela Beatris Zemniaçak[1] · Rafael Teixeira Ribeiro[1] · Camila Vieira Pinheiro[1] · Sâmela de Azevedo Cunha[1] · Tailine Quevedo Tavares[1] · Ediandra Tissot Castro[1] · Guilhian Leipnitz[1,2] · Moacir Wajner[1,2,3] · Alexandre Umpierrez Amaral[1,4]

Received: 27 August 2023 / Accepted: 17 October 2023 / Published online: 1 November 2023
© The Author(s), under exclusive licence to Springer Science+Business Media, LLC, part of Springer Nature 2023

Abstract

Maple syrup urine disease (MSUD) is caused by severe deficiency of branched-chain α-keto acid dehydrogenase complex activity, resulting in tissue accumulation of branched-chain α-keto acids and amino acids, particularly α-ketoisocaproic acid (KIC) and leucine. Affected patients regularly manifest with acute episodes of encephalopathy including seizures, coma, and potentially fatal brain edema during the newborn period. The present work investigated the ex vivo effects of a single intracerebroventricular injection of KIC to neonate rats on redox homeostasis and neurochemical markers of neuronal viability (neuronal nuclear protein (NeuN)), astrogliosis (glial fibrillary acidic protein (GFAP)), and myelination (myelin basic protein (MBP) and 2′,3′-cyclic-nucleotide 3′-phosphodiesterase (CNPase)) in the cerebral cortex and striatum. KIC significantly disturbed redox homeostasis in these brain structures 6 h after injection, as observed by increased 2′,7′-dichlorofluorescein oxidation (reactive oxygen species generation), malondialdehyde levels (lipid oxidative damage), and carbonyl formation (protein oxidative damage), besides impairing the antioxidant defenses (diminished levels of reduced glutathione and altered glutathione peroxidase, glutathione reductase, and superoxide dismutase activities) in both cerebral structures. Noteworthy, the antioxidants N-acetylcysteine and melatonin attenuated or normalized most of the KIC-induced effects on redox homeostasis. Furthermore, a reduction of NeuN, MBP, and CNPase, and an increase of GFAP levels were observed at postnatal day 15, suggesting neuronal loss, myelination injury, and astrocyte reactivity, respectively. Our data indicate that disruption of redox homeostasis, associated with neural damage caused by acute intracerebral accumulation of KIC in the neonatal period may contribute to the neuropathology characteristic of MSUD patients.

Keywords Maple syrup urine disease · α-Ketoisocaproic acid · Cerebral cortex · Striatum · Redox homeostasis · Neurochemical markers

Abbreviations

ANOVA	One-way analysis of variance
BCAA	Branched-chain amino acids
BCKA	Branched-chain α-keto acids
BCKDH	Branched-chain α-keto acid dehydrogenase
CNPase	2′,3′-Cyclic-nucleotide 3′-phosphodiesterase
DCFH	2′,7′-Dichlorofluorescein

✉ Alexandre Umpierrez Amaral
alexandreamaral@uricer.edu.br

[1] Programa de Pós-Graduação em Ciências Biológicas: Bioquímica, Instituto de Ciências Básicas da Saúde, Universidade Federal do Rio Grande do Sul, Porto Alegre, RS, Brazil

[2] Departamento de Bioquímica, Instituto de Ciências Básicas da Saúde, Universidade Federal do Rio Grande do Sul, Porto Alegre, RS, Brazil

[3] Serviço de Genética Médica, Hospital de Clínicas de Porto Alegre, Porto Alegre, RS, Brazil

[4] Programa de Pós-Graduação em Atenção Integral à Saúde, Universidade Regional Integrada do Alto Uruguai e das Missões, Avenida Sete de Setembro, 1621, Erechim, RS 99709-910, Brazil

GFAP	Glial fibrillary acidic protein
GPx	Glutathione peroxidase
GR	Glutathione reductase
GSH	Reduced glutathione
GSSG	Oxidized glutathione
HO-1	Heme oxygenase-1
icv	Intracerebroventricular
KIC	α-Ketoisocaproic acid
MDA	Malondialdehyde
MEL	Melatonin
MCT/SLC16A1	Monocarboxylate transporter
MSUD	Maple syrup urine disease
MBP	Myelin basic protein
NAC	N-Acetylcysteine
NeuN	Neuronal nuclear protein
Nrf2	Nuclear factor erythroid 2-related factor 2
PBS	Phosphate-buffered saline
PND	Postnatal day
RNS	Reactive nitrogen species
ROS	Reactive oxygen species
SOD	Superoxide dismutase
TCA	Trichloroacetic acid

Introduction

Maple syrup urine disease (MSUD) (MIM 248600) is an autosomal recessive inherited disorder, with a worldwide incidence of 1:185,000 live births. It is caused by defects of the branched-chain α-ketoacid dehydrogenase (BCKDH, EC 1.2.4.4) complex, leading to accumulation in tissues and biological fluids of the branched-chain α-keto acids (BCKA), α-ketoisocaproic acid (KIC), α-keto-β-methylvaleric acid, and α-ketoisovaleric acid, and the equivalent amino acids leucine, isoleucine, and valine [1, 2]. MSUD is classified into four genetic variants, the classic, the intermediate, the intermittent, and the thiamine-responsive forms [1]. The classical form is the most severe, presenting during the neonatal period, sometimes called neonatal MSUD [3, 4].

Patients with classical neonatal MSUD usually manifest with nonspecific signs of metabolic intoxication, such as irritability, somnolence, anorexia, vomiting, dehydration, and ketoacidosis, which is followed by neurological symptoms, such as lethargy, coma, apnea, opisthotonos, and cytotoxic cerebral edema. Later in infancy or childhood, they develop physical and psychomotor delay with intellectual disability and movements disorders such as dystonia and tremor [1, 2]. Neuropathological findings comprise hypomyelination and cytotoxic edema in various brain areas, including the basal ganglia and cerebral cortex [5–7], and brain atrophy [8, 9]. Noteworthy, MSUD is considered an intoxicating inherited disorder in which KIC and leucine are the main neurotoxic metabolites, once augmented plasma concentrations of these compounds are associated with the appearance or worsening of the neurological symptoms that take place during crises of metabolic decompensation accompanied by excessive proteolysis [1, 2]. Although various mechanisms have been proposed to explain the cerebral damage in MSUD, the exact underlying pathophysiological mechanisms are still poorly known.

Regarding the BCKA, intracerebroventricular (icv) administration of KIC to adult (60-day-old) or young (30-day-old) rats was shown to cause learning deficits and behavioral changes [10]. KIC icv injection was also shown to induce oxidative damage to biomolecules [11], decrease of brain-derived neurotrophic factor and nerve growth factor levels [12], as well as of the activities of the respiratory chain complexes I and II-III [13] in different cerebral regions. KIC was also shown to alter the levels of interferon-γ and tumor necrosis factor-α [14].

Furthermore, in vitro exposition of brain to the BCKA, particularly to KIC, caused lipid oxidative damage and impairment of the antioxidant defenses [15, 16], as well as inhibition of α-ketoglutarate dehydrogenase and pyruvate dehydrogenase activities [17, 18]. KIC also reduced oxygen consumption in state 3 respiration and disrupted mitochondrial membrane potential [19]. Another work showed that the BCKA accumulating in MSUD inhibit CO_2 formation and increase lactate release in the brain of young rats [20].

On the other hand, several studies revealed that in vivo and in vitro exposition of rat brain to the BCAA induce oxidative stress through lipid peroxidation, DNA, and protein damage, and altered activities of antioxidant enzymes [21–24]. BCAA also decreased CO_2 production and the activities of creatine kinase, and respiratory chain complexes II–III, III, and IV [18, 25, 26]. Of note, lipid and protein oxidative damage was found in the plasma of MSUD patients [27–30], corroborating the investigations with the chemical animal models of this disease. Noteworthy, all these previous studies designed to clarify MSUD pathogenesis were performed in the brain of young or adult rats, whereas the onset of the neurological findings in MSUD patients is usually manifested in the first few days of life. Therefore, further studies using neonatal brain are necessary to clarify the pathophysiology of the brain damage in this disease.

Therefore, since to the best of our knowledge, there were no reports on the deleterious effects of KIC on brain functioning in early days of development, the present work evaluated the ex vivo effects of intracerebral administration of KIC to neonate rats on redox homeostasis, as well as on neuropathological landmarks in the cerebral cortex and striatum. The antioxidants N-acetylcysteine (NAC) and melatonin (MEL) were used in some experiments to evaluate their neuroprotective effects on redox homeostasis.

Material and Methods

Animals and Reagents

A total of 84 1-day-old (neonate) Wistar rats from Centro de Reprodução e Experimentação de Animais de Laboratório (CREAL) at the Federal University of Rio Grande do Sul (UFRGS), Porto Alegre, Brazil, were used in this work. The newborn rats were kept with their dam on a 12:12-h light/dark cycle at temperature of 22 ± 1 °C. Free water and commercial chow with 20% (w/w) protein were available to dams.

All reagents were purchased from Merck (St. Louis, MO, USA). On the day of the experiments, KIC, MEL, and NAC solutions were made, and the pH adjusted to 7.4.

icv Injection of KIC

A schematic representation of the experimental design is shown in Fig. 1. Neonate rats were submitted to an icv injection of KIC (1 µmol/g body weight, dissolved in 0.01 M phosphate-buffered saline (PBS), pH 7.4, in a volume of 0.5 µL/g body weight), or an equal volume of 0.01 M PBS, pH 7.4 (control), into the cisterna magna, as previously described [31, 32]. After recovering in a heating pad at 37 °C, neonate animals returned to their dam until euthanasia that was immediately followed by the various analyses. In some experiments, neonatal rats were pre-treated with two intraperitoneal injections (volume of 2 µL/g body weight) of NAC (300 mg/kg and 400 mg/kg, respectively) or MEL (40 mg/kg, each) 24 and 1 h prior to KIC icv administration [32, 33]. The animals were then euthanized at 6 h after KIC icv infusion to evaluate redox homeostasis parameters and heme oxygenase-1 (HO-1) protein immunocontent, at postnatal day (PND) 7 to determine oxidative stress measures, or at PND 15 for the immunofluorescence analyses. It is stressed that the neonates were randomly distributed into the various experimental groups, the researchers that conducted the experimental procedures did not know which solution was administered to the animals (PBS, KIC, NAC, or MEL), and the groups were not identified during the analyses. The sample size and power calculations for the biochemical assays, Western blotting, and immunofluorescence analysis utilized the software Minitab 16, and considered the following parameters: standard deviation of 10%, power of 0.9, difference of 25%, and 2 or 3 levels (experimental groups). These parameters were based on previous reports from our and other research groups [32, 34, 35].

Parameters of Redox Homeostasis

Preparation of Tissue Homogenates

The animals were euthanized by decapitation, the brain removed, and the cerebral cortex and striatum dissected. These cerebral structures were then homogenized (1:10) in 20 mM sodium phosphate buffer, pH 7.4, with 140 mM KCl, centrifuged at 800 *g* and the supernatants used for the determination of redox homeostasis parameters, excepting for the nitrate and nitrite levels that were measured with the forebrain supernatants.

2',7'-Dichlorofluorescein (DCFH) Oxidation

Reactive oxygen species (ROS) production was measured by DCFH oxidation, as described by LeBel et al. [36]. Tissue homogenates were incubated for 30 min at 37 °C with the cell-permeant diacetate form (DCF-DA), which is cleaved to generate DCFH that is oxidized by ROS to form the fluorescent product DCF. Fluorescence was measured in a Spectramax M5 at 480 nm (excitation) and 535 nm (emission). A standard curve was carried out with DCF (0–10 µM) and the data expressed as µmol DCF per milligram protein.

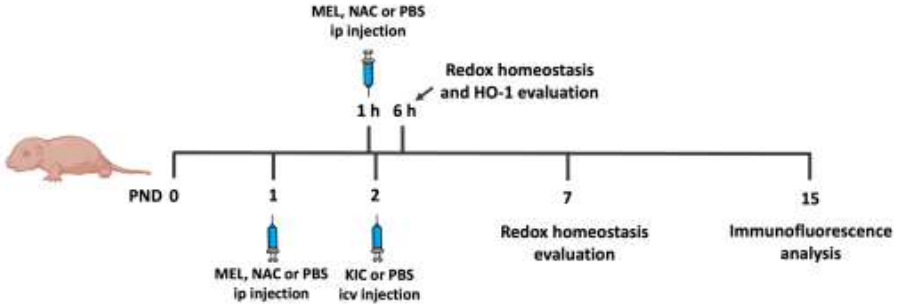


Fig. 1 Schematic representation of the experimental design showing the procedures performed in Wistar rats from postnatal day 1 (PND 1) to postnatal day 15 (PND 15). HO-1, heme oxygenase-1; icv, intracerebroventricular; ip, intraperitoneal; KIC, α-ketoisocaproic acid; MEL, melatonin; NAC, N-acetylcysteine; PND, postnatal day; PBS, phosphate-buffered saline

Nitrate and Nitrite Levels

Reactive nitrogen species (RNS) levels were evaluated by the determination of the nitric oxide derivatives nitrate (NO_3^-) and nitrite (NO_2^-), according to the method described by Navarro-Gonzálvez et al. [37]. Tissue homogenates were deproteinized by a solution of 75 mM $ZnSO_4$, centrifuged, and the supernatant neutralized with a solution of 55 mM NaOH. Then, all nitrates were converted to nitrite by the addition of copper-coated cadmium granules. Next, an aliquot of the samples was treated with the Griess reagent and incubated for 10 min at room temperature in the dark. The absorbance was determined in a Spectramax M5 microplate reader at 505 nm. A standard curve was performed with sodium nitrite (2.5–100 µM). Results were expressed as µmol nitrates and nitrites per milligram protein.

Malondialdehyde (MDA) Levels

MDA levels were determined by measuring thiobarbituric acid reactive substances, according to the method of Yagi [38]. After pre-incubation, tissue homogenates were incubated for 1 h at 100 °C in the presence of 10% trichloroacetic acid (TCA) and 0.67% thiobarbituric acid. The resultant pink color was extracted with butanol and separated by centrifugation. The fluorescence of the organic phase was measured at 515 nm (excitation) and 553 nm (emission). A standard curve was made by using 1,1,3,3-tetramethoxypropane. Results were expressed as nmol MDA per milligram protein.

Carbonyl Content

In order to determine the carbonyl content, tissue homogenates were treated with 2,4-dinitrophenylhydrazine (10 mM) and incubated for 1 h in the dark at room temperature. Proteins were precipitated with 20% TCA, the sediment obtained after centrifugation was washed with a mixture of ethanol:ethyl acetate (1:1, v/v) and resuspended in 6 M guanidine. The carbonyl content was spectrophotometric determined at 365 nm in a Spectramax M5 [39]. Results were expressed as nmol carbonyl content per milligram protein.

Reduced Glutathione (GSH) Levels

Tissue homogenates reacted with o-phthaldialdehyde (1 mg/mL) and were incubated for 15 min at room temperature in the dark. Next, the fluorescence was determined in Spectramax M5 microplates at 350 nm (excitation) and 420 nm (emission) [40]. GSH levels were calculated from a standard curve of GSH (0.001–1 mM) as nmol GSH per milligram protein.

Glutathione Peroxidase (GPx) Activity

GPx activity was determined in tissue homogenates by the method of Wendel [41], using tert-butyl hydroperoxide as substrate. The decrease of NADPH absorbance at 340 nm was monitored in a Spectramax M5. GPx activity was expressed as unit per milligram protein.

Glutathione Reductase (GR) Activity

GR activity was measured in tissue homogenates according to the method described by Carlberg and Mannervik [42], using oxidized glutathione (GSSG) and NADPH as substrates. This enzymatic activity was determined by monitoring the decrease of NADPH absorbance at 340 nm in a Spectramax M5. GR activity was expressed as unit per milligram protein.

Superoxide Dismutase (SOD) Activity

SOD activity was measured in tissue homogenates according to the method of Marklund [43], which is based on the autoxidation of pyrogallol that can be measured by determining the absorbance at 420 nm in a Spectramax M5. A standard curve was made with commercially purified SOD (S8408, Merck) to calculate the SOD activity. The results were expressed as unit per milligram protein.

Western Blotting

For the determination of HO-1 protein immunocontent, animals were euthanized by decapitation; the cerebral cortex was dissected, homogenized, and centrifuged; and the supernatants were prepared for the analyses, as described by Seminotti et al. [33]. The primary antibody anti-HO-1 (1:500, Abcam ab13248) was used and the results expressed as a ratio comparative to β-actin (1:20000, Merck A1978).

Neurochemical Markers

The neurochemical markers were measured by immunofluorescence. A transcardiac perfusion with 0.9% saline containing 0.16% sodium citrate was first carried out in the anesthetized rats and followed by a second perfusion with 4% paraformaldehyde, after which the brain was removed and coronal slices (35 µm) prepared using a Vibratome (VT1000S; Leica, Nussloch, Germany). Three transverse brain slices containing the cerebral cortex and striatum were obtained from each animal and the immunostaining

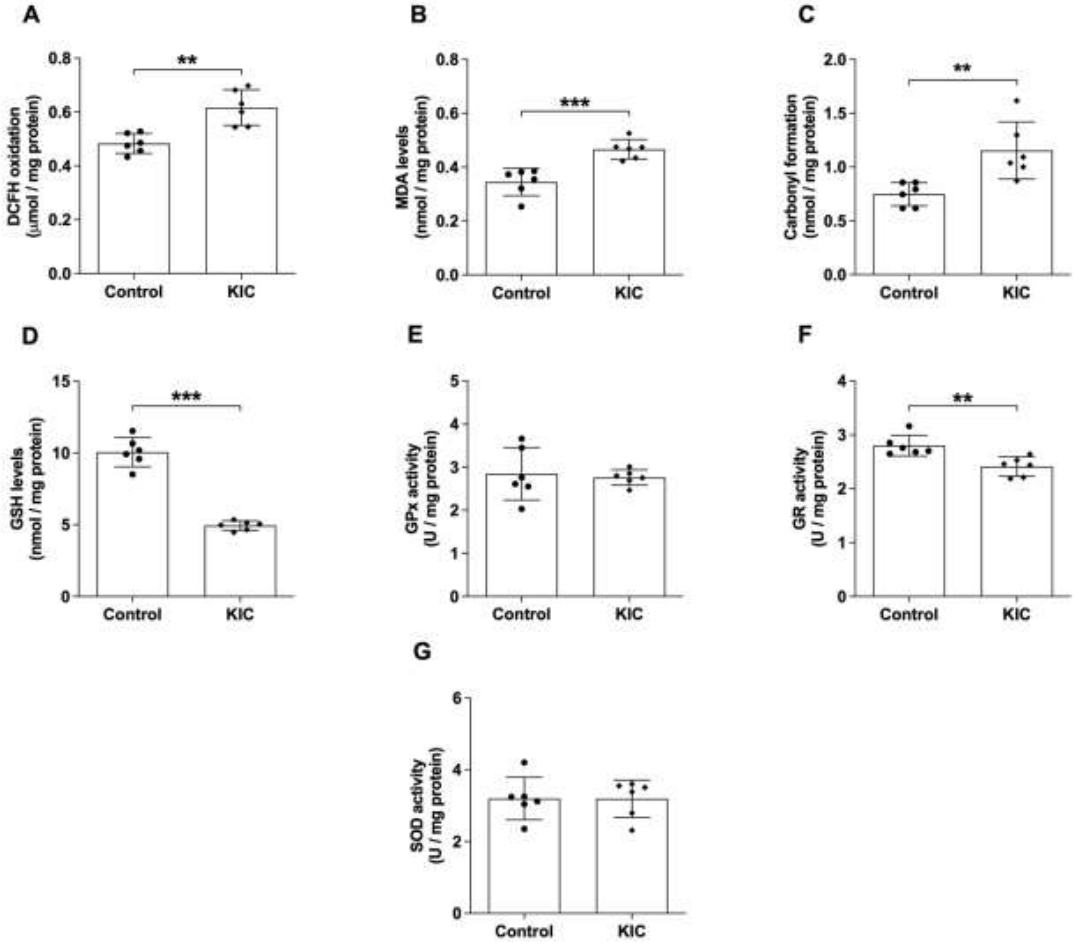


Fig. 2 Effects of an intracerebroventricular (icv) administration of KIC (1 µmol/g) to neonate rats on redox homeostasis in the cerebral cortex 6 hours after injection. 2′,7′-Dichlorofluorescein (DCFH) oxidation (**A**), malondialdehyde (MDA) levels (**B**), carbonyl formation (**C**), reduced glutathione (GSH) levels (**D**), and glutathione peroxidase (GPx) (**E**), glutathione reductase (GR) (**F**), and superoxide dismutase (SOD) (**G**) activities were determined. Values are mean ± standard deviation of six independent experiments (N) expressed as µmol/mg protein, nmol/mg protein or U/mg protein. $^{**}P < 0.01$, $^{***}P < 0.001$ compared to control (Student's *t* test for unpaired samples)

procedures were performed according to Seminotti et al. [33]. An overnight incubation at 4 °C with the following primary antibodies were then performed: mouse anti-neuronal nuclear protein (NeuN) (1:400, Millipore #MAB377), rabbit anti-glial fibrillary acidic protein (GFAP) (1:500, Thermo Fisher # MA5-12,023), mouse anti-myelin basic protein (MBP) (1:500, Merck #AMAb91064), and rabbit anti-2′,3′-cyclic-nucleotide 3′-phosphodiesterase (CNPase) (1:500, Cell Signaling #D83E10). Next, a 90-min incubation at room temperature with a secondary mouse or rabbit antibody was carried out (1:500, Thermo Fisher Scientific). Slices were then assembled with fluoroshield (Merck) and the images were captured by an Olympus FV300 confocal microscope using 488 and 546 nm wavelengths. NeuN-positive cells and the fluorescence intensity of GFAP, MPB, and CNPase were assessed in three randomly chosen fields per slice.

Determination of Protein Concentrations

Protein concentrations were measured by the method of Lowry and collaborators [44] with bovine serum albumin as standard.

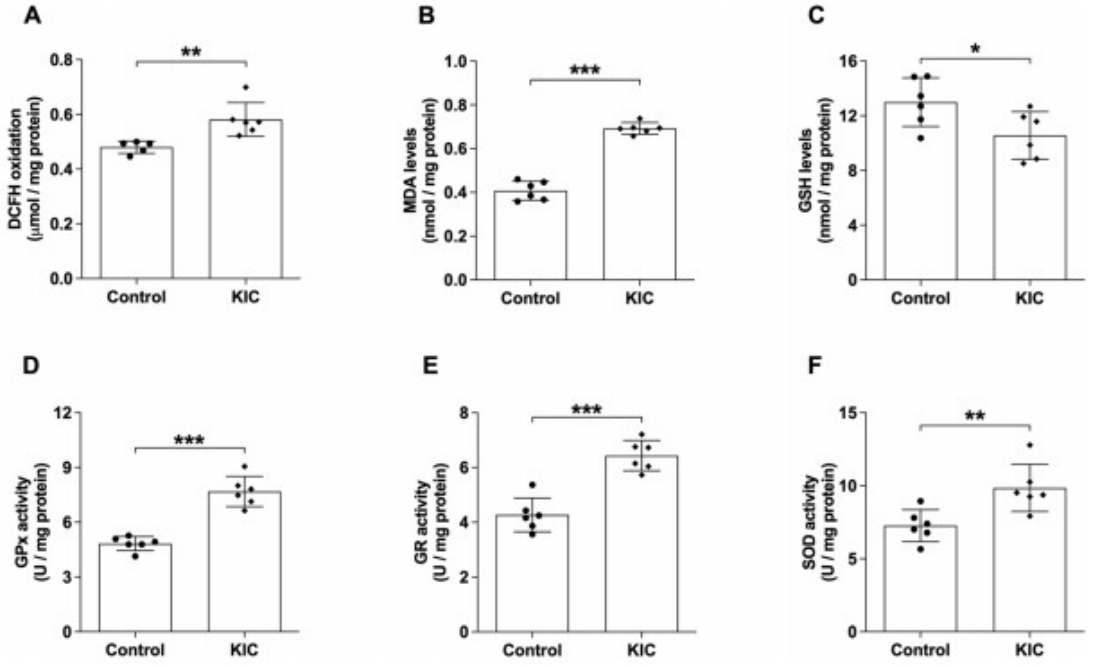


Fig. 3 Effects of an intracerebroventricular (icv) administration of KIC (1 µmol/g) to neonate rats on redox homeostasis in the striatum 6 hours after injection. 2′,7′-Dichlorofluorescein (DCFH) oxidation (**A**), malondialdehyde (MDA) levels (**B**), reduced glutathione (GSH) levels (**C**), and glutathione peroxidase (GPx) (**D**), glutathione reductase (GR) (**E**), and superoxide dismutase (SOD) (**F**) activities were determined. Values are mean ± standard deviation of five to six independent experiments (N) expressed as µmol/mg protein, nmol/mg protein, or U/mg protein. $^{*}P < 0.05$, $^{**}P < 0.01$, $^{***}P < 0.001$ compared to control (Student's *t* test for unpaired samples)

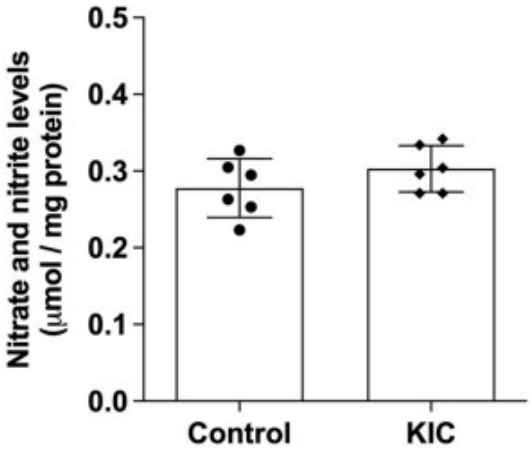


Fig. 4 Effects of an intracerebroventricular (icv) administration of KIC (1 µmol/g) to neonate rats on nitrate and nitrite concentrations in the forebrain 6 h after injection. Values are mean ± standard deviation of six independent experiments (N) expressed as µmol/mg protein. No significant differences were detected (Student's *t* test for unpaired samples)

Statistical Analysis

The normality of data distribution was initially assessed using the Shapiro-Wilk test, which showed a normal distribution pattern. Thus, the statistical analyses were one-way analysis of variance (ANOVA) followed by Tukey's post hoc test when more than two groups were compared, whereas Student's *t* test for unpaired samples was used to compare two groups. Results were expressed as mean ± standard deviation and differences rated significant when $P < 0.05$. All analyses were made in the GraphPad Prism 9.0 software.

Results

Markers of Redox Homeostasis

Cerebral cortex and striatum of neonate rats were assayed to determine a large spectrum of redox homeostasis parameters 6 h after KIC icv injection (1 µmol/g) or at PND 7.

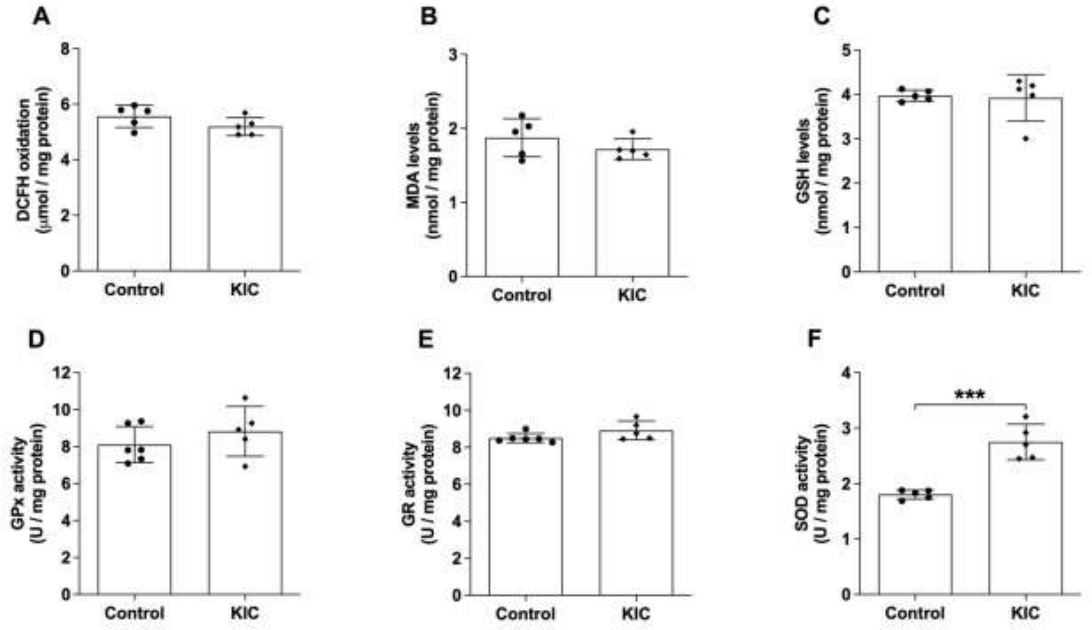


Fig. 5 Effects of an intracerebroventricular (icv) administration of KIC (1 µmol/g) to neonate rats on redox homeostasis in the cerebral cortex at postnatal day (PND) 7. 2',7'-Dichlorofluorescein (DCFH) oxidation (**A**), malondialdehyde (MDA) levels (**B**), reduced glutathione (GSH) levels (**C**), and glutathione peroxidase (GPx) (**D**), glutathione reductase (GR) (**E**), and superoxide dismutase (SOD) (**F**) activities were evaluated. Values are mean ± standard deviation of five to six independent experiments (N) expressed as µmol/mg protein, nmol/mg protein, and U/mg protein. ***$P < 0.001$ compared to control (Student's *t* test for unpaired samples)

icv Administration of KIC to Neonate Rats Disrupts Brain Redox Homeostasis

We initially observed that icv KIC administration caused significant increases of DCFH oxidation ($t_{(10)} = 4.329$, $P < 0.01$), MDA levels ($t_{(10)} = 4.769$, $P < 0.001$), and carbonyl content ($t_{(10)} = 3.458$, $P < 0.01$), besides a decrease of GSH levels ($t_{(10)} = 11.72$, $P < 0.001$), and GR activity ($t_{(10)} = 3.649$, $P < 0.01$) in the cerebral cortex of the neonate rats 6 h after icv injection. In contrast, SOD and GPx activities were not changed by this treatment (Fig. 2). Furthermore, increased DCFH oxidation ($t_{(9)} = 3.449$, $P < 0.01$) and MDA levels ($t_{(10)} = 13.72$, $P < 0.001$), and decreased GSH concentrations ($t_{(10)} = 2.4$, $P < 0.05$) were observed in the striatum of neonate rats following KIC treatment (Fig. 3). Increased activities of GPx ($t_{(10)} = 7.641$, $P < 0.001$), GR ($t_{(10)} = 6.389$, $P < 0.001$), and SOD ($t_{(10)} = 3.235$, $P < 0.01$) were also found in the striatum 6 h after KIC injection (Fig. 3). Finally, we found that nitrate and nitrite concentrations were not changed in the forebrain of neonate rats 6 h after the administration of the metabolite (Fig. 4). Taken together, these data clearly reveal that a single icv in vivo KIC injection causes short-lived oxidative stress in the brain of neonate rats probably secondary to increased ROS formation.

We also measured the effects of icv KIC injection to the neonate rats on redox homeostasis parameters in cerebral cortex and striatum at PND 7. We observed that KIC only significantly elevated SOD activity ($t_{(8)} = 6.392$, $P < 0.001$) in cerebral cortex, with no alterations of DCFH oxidation, MDA and GSH concentrations, as well as of GPx and GR activities (Fig. 5). Regarding the striatum, we found that all antioxidant enzymes had their activities increased by this treatment (GPx: $t_{(8)} = 9.987$, $P < 0.001$; GR: $t_{(8)} = 2.483$, $P < 0.05$; SOD: $t_{(8)} = 4.249$, $P < 0.01$), without any change in DCFH oxidation, MDA, and GSH levels (Fig. 6).

NAC and MEL Prevent the Alterations Induced by an icv Administration of KIC on Redox Homeostasis in Cerebral Cortex and Striatum of Neonate Rats

Next, we evaluated whether the antioxidants NAC and MEL (intraperitoneal injections 24 and 1 h before KIC administration) could prevent the alterations of the various redox homeostasis parameters caused by KIC administration 6 h after the injection. We found that MEL normalized DCFH

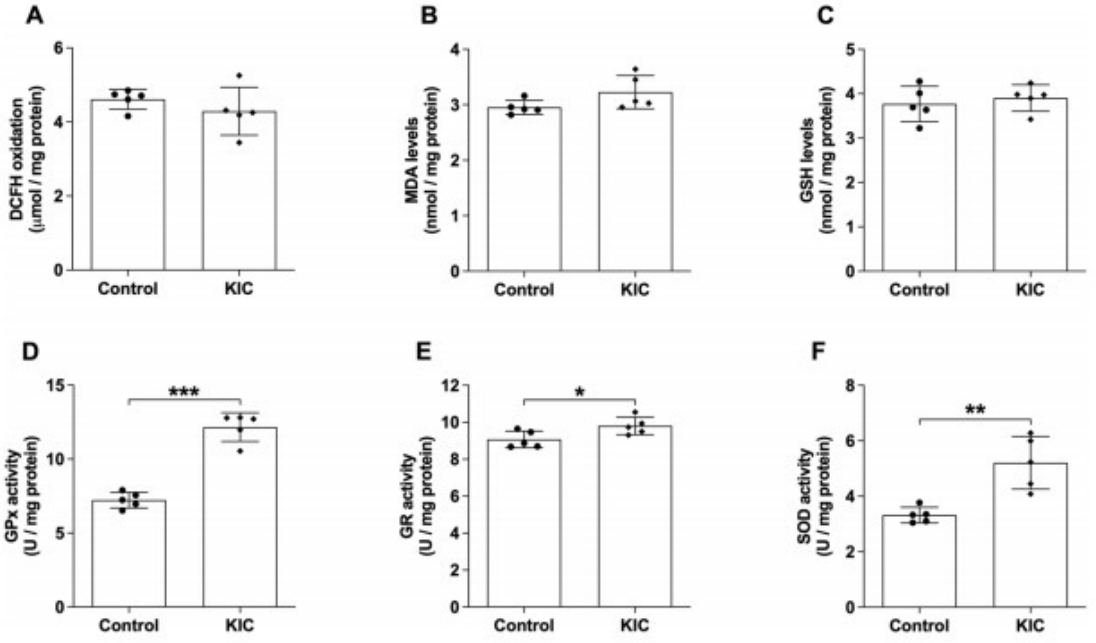


Fig. 6 Effects of an intracerebroventricular (icv) administration of KIC (1 µmol/g) to neonate rats on redox homeostasis in the striatum at postnatal day (PND) 7. 2′,7′-Dichlorofluorescein (DCFH) oxidation (**A**), malondialdehyde (MDA) levels (**B**), reduced glutathione (GSH) levels (**C**), and glutathione peroxidase (GPx) (**D**), glutathione reductase (GR) (**E**), and superoxide dismutase (SOD) (**F**) activities were evaluated. Values are mean ± standard deviation of five independent experiments (N) expressed as µmol/mg protein, nmol/mg protein, and U/mg protein. $^{*}P < 0.05$, $^{**}P < 0.01$, $^{***}P < 0.001$ compared to control (Student's *t* test for unpaired samples)

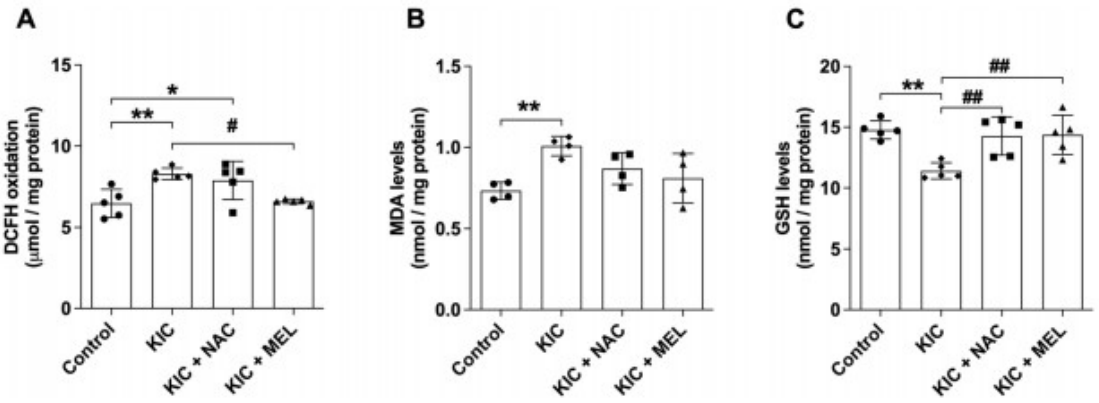


Fig. 7 Effects of the antioxidants N-acetylcysteine (NAC) and melatonin (MEL) on the alterations of redox homeostasis parameters caused by an intracerebroventricular (icv) administration of KIC (1 µmol/g) to neonate rats in the cerebral cortex 6 h after the injection. 2′,7′-Dichlorofluorescein (DCFH) oxidation (**A**), malondialdehyde (MDA) levels (**B**), and reduced glutathione (GSH) levels (**C**) were determined. Animals received two intraperitoneal injections of NAC (300 mg/kg and 400 mg/kg) or MEL (40 mg/kg) 24 and 1 h prior to KIC icv administration. Values are mean ± standard deviation of four to six independent experiments (N) expressed as µmol/mg protein and nmol/mg protein. $^{*}P < 0.05$, $^{**}P < 0.01$ compared to control. $^{\#}P < 0.05$, $^{\#\#}P < 0.01$ compared to KIC (one-way ANOVA, followed by post hoc Tukey's range test)

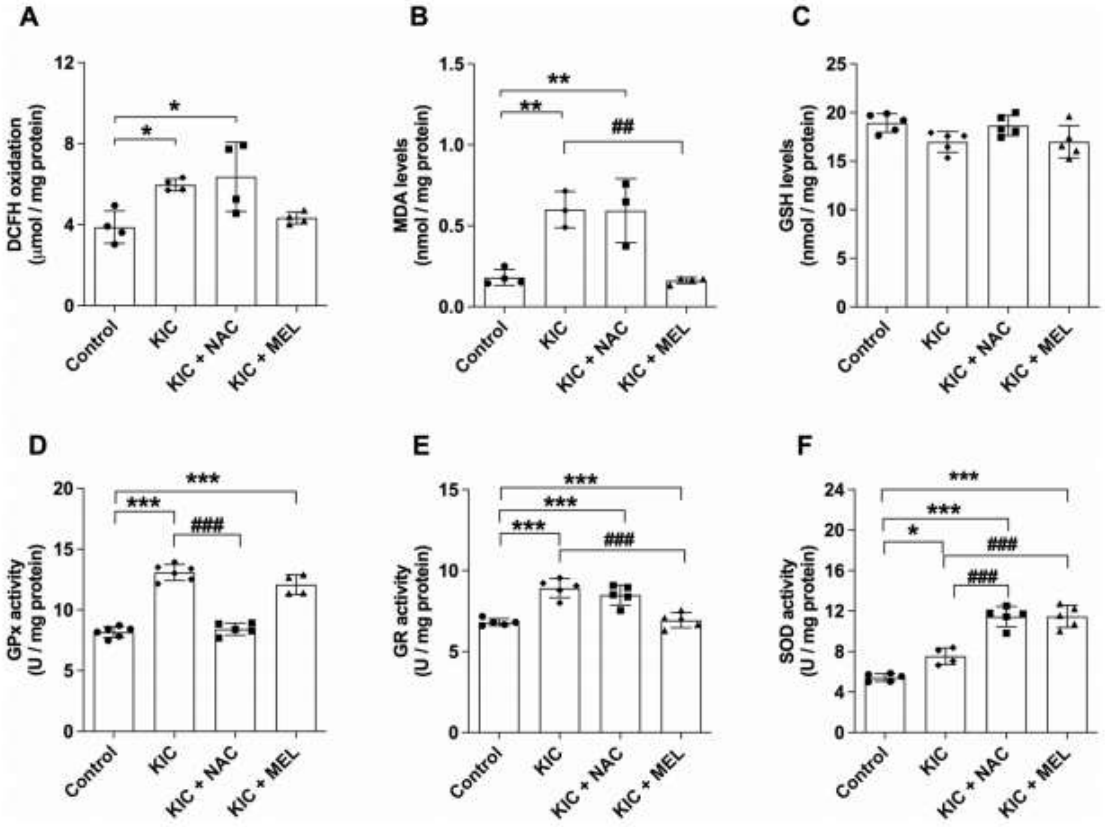


Fig. 8 Effects of the antioxidants N-acetylcysteine (NAC) and melatonin (MEL) on the alterations of redox homeostasis parameters caused by an intracerebroventricular (icv) administration of KIC (1 µmol/g) to neonate rats in the striatum 6 h after the injection. 2′,7′-Dichlorofluorescein (DCFH) oxidation (**A**), malondialdehyde (MDA) levels (**B**), reduced glutathione (GSH) levels (**C**), and the activities of glutathione peroxidase (GPx) (**D**), glutathione reductase (GR) (**E**), and superoxide dismutase (SOD) (**F**) were determined. Animals received two intraperitoneal injections of NAC (300 mg/kg and 400 mg/kg) or MEL (40 mg/kg) 24 and 1 h prior to KIC icv administration. Values are mean ± standard deviation of three to six independent experiments (N) expressed as µmol/mg protein, nmol/mg protein, or U/mg protein. $^{*}P < 0.05$, $^{**}P < 0.01$, $^{***}P < 0.001$ compared to control. $^{\#\#}P < 0.01$, $^{\#\#\#}P < 0.001$ compared to KIC (one-way ANOVA, followed by post hoc Tukey's range test)

oxidation, MDA levels, and GSH concentrations, whereas NAC totally prevented GSH decrease and the increase of MDA levels in the cerebral cortex (Fig. 7) (DCFH: $F_{(3,16)} = 7.359$, $P < 0.01$; MDA: $F_{(3,12)} = 5.555$, $P < 0.05$; GSH: $F_{(3,16)} = 7.861$, $P < 0.01$). Furthermore, MEL fully prevented DCFH oxidation, MDA, and GR activity increase, but did not change KIC-elicited increase of GPx, and exacerbated KIC-induced increase of SOD activity in the striatum. In turn, NAC normalized GPx activity, exacerbated KIC-induced SOD activity increase and did not change KIC-induced alterations on DCFH oxidation, MDA levels and GR activity (Fig. 8) (DCFH: $F_{(3,12)} = 6.313$, $P < 0.01$; MDA: $F_{(3,10)} = 18.67$, $P < 0.001$; GPx: $F_{(3,17)} = 94.67$, $P < 0.001$; GR: $F_{(3,16)} = 23.55$, $P < 0.001$; SOD: $F_{(3,15)} = 57.63$, $P < 0.001$).

icv Administration of KIC to Neonate Rats Induces HO-1 Production in Cerebral Cortex

To find out a possible signaling mechanism involved in the KIC-induced oxidative stress, we measured HO-1 protein levels, an enzyme with cytoprotective effects on oxidative stress by degrading free heme [45], in cerebral cortex of the KIC-treated neonate rats 6 h after injection. Figure 9 shows that the levels of HO-1, which are controlled by the nuclear factor erythroid 2-related factor

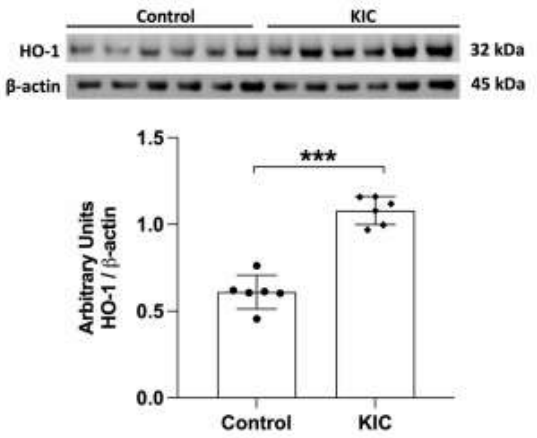


Fig. 9 Effect of an intracerebroventricular (icv) administration of α-ketoisocaproic acid (KIC, 1 μmol/g) to neonate rats on heme oxygenase-1 (HO-1) immunocontent in cerebral cortex 6 h after injection. Values are mean ± standard deviation of three to six independent experiments (N) expressed as arbitrary units. ***$P < 0.001$ compared to control (Student's *t* test for unpaired samples)

2 (Nrf2), were markedly increased after KIC administration ($t_{(10)} = 9.064$, $P < 0.001$).

Neurochemical Markers Measured by Immunofluorescence

We also measured the effects of icv administration of KIC (1 μmol/g) to neonate rats on NeuN, GFAP, MBP, and CNPase immunofluorescence that indicate neuronal number, reactive astrogliosis, and myelination, respectively, in cerebral cortex and striatum at PND 15.

icv Administration of KIC to Neonate Rats Provokes Long-Term Neuronal Loss, Astrocytic Reactivity, and Myelination Impairment at PND 15

Next, we investigated whether an icv administration of KIC to neonate rats could alter the immunofluorescence staining of neuronal (NeuN), astrocytic (GFAP), and myelin (MPB and CNPase) proteins at PND 15. It was found that KIC significantly decreased NeuN (cerebral cortex: $t_{(4)} = 3.301$, $P < 0.05$; striatum: $t_{(4)} = 12.04$, $P < 0.001$) (Fig. 10) and increased GFAP (cerebral cortex: $t_{(5)} = 2.829$, $P < 0.05$; striatum: $t_{(5)} = 2.087$, $P < 0.05$) (Fig. 11) immunofluorescence staining. In addition, MBP (striatum: $t_{(6)} = 2.026$, $P < 0.05$) (Fig. 12) and CNPase (striatum: $t_{(6)} = 2.870$, $P < 0.05$) (Fig. 13) staining were significantly reduced in the striatum of these animals. These results suggest long-term neuronal loss, astrocyte reactivity, and myelination injury in the brain following a single administration of KIC in the neonatal period.

Discussion

MSUD is a severe life-threatening inherited metabolic disease clinically characterized by neurological symptoms that worsen during crises of metabolic decompensation usually triggered by infections and other stressful conditions associated with fasting. These episodes are accompanied by a huge elevation in the levels of the BCKA and BCAA, mainly KIC and leucine, which are thought to be the major neurotoxic metabolites in MSUD [1, 2, 46]. MSUD children that survive the initial episodes of metabolic decompensation during the first weeks of life usually present long-term neurological sequelae, such as cortical atrophy and basal ganglia alterations, whose pathogenesis is still poorly established [8, 47]. In this particular, there is evidence suggesting that oxidative stress and neuroinflammation are associated with MSUD neurodegeneration [27–30, 48–50]. In line with this, various studies found that the metabolites accumulating in this disease disturb redox homeostasis and cause mitochondrial dysfunction in vivo in brain of young and adult rats [11, 13, 18, 22–24, 26]. Furthermore, in vivo icv injection of KIC to 30-day-old rats showed to cause oxidative stress [11], decrease of neurotrophic factors [12], and of respiratory chain complexes activities [13], as well as alterations of pro-inflammatory cytokines levels [14] in various cerebral regions. It is emphasized that most of these experimental works testing the effects of the BCAA and BCKA were carried out using 30-day-old or older rats. Investigating the role of these metabolites on neonatal brain seems therefore justified since MSUD patients manifest with neurological dysfunction in the first days of life.

Thus, the present investigation assessed biochemical markers of oxidative stress and neurochemical landmarks by immunofluorescence staining aiming to determine the number of neurons, astroglial reactivity, and myelination in the cerebral cortex and striatum following an acute cerebral overload of KIC to neonate rats in an effort to clarify the mechanisms responsible for brain injury in MSUD at this age. It is stressed that KIC can easily penetrate into the brain through the monocarboxylate transporter (MCT/SLC16A1) localized in the blood-brain barrier [51–53], being therefore able to accumulate in the central nervous system. We found that KIC caused short-term oxidative stress, as well as long-standing neurochemical alterations indicative of neuronal loss, astrogliosis, and hypo/demyelination in the brain of the treated animals. We also explored whether the antioxidants MEL and NAC could be protective against KIC-induced oxidative stress in these cerebral structures.

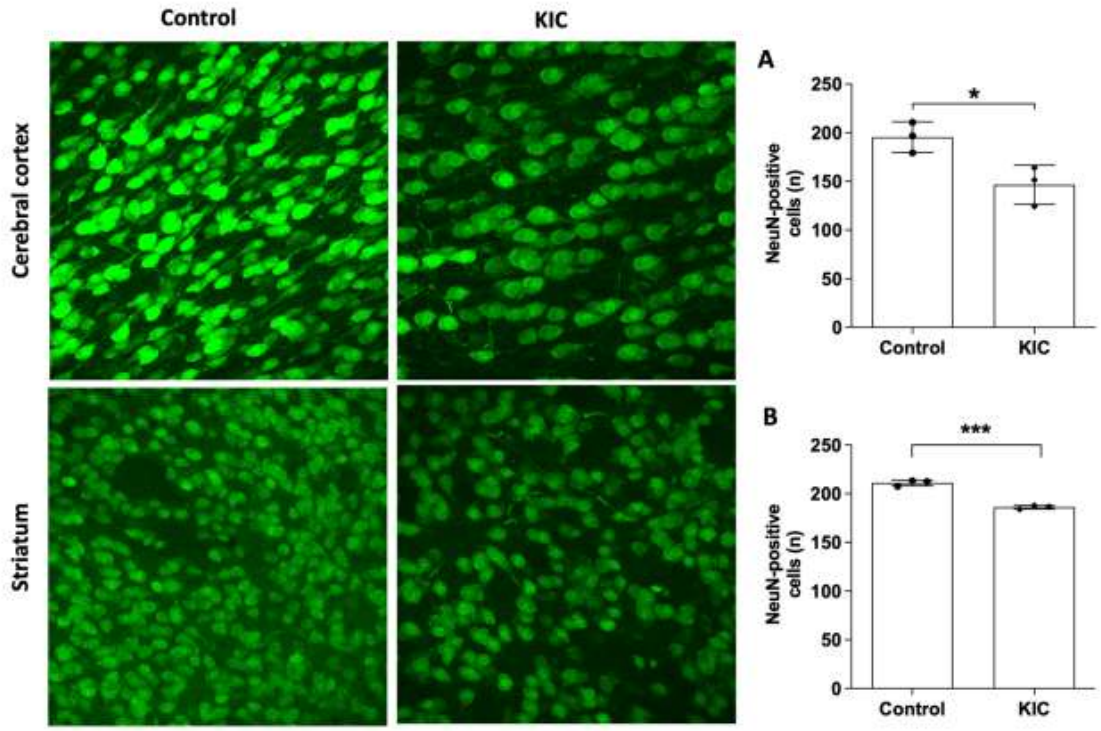


Fig. 10 Effects of an intracerebroventricular (icv) administration of KIC (1 μmol/g) to neonate rats on NeuN immunofluorescence in the cerebral cortex and striatum at postnatal day (PND) 15. Images are representative of three independent experiments (N). Quantitation of NeuN-positive cells was performed on 400× magnification images using the mean of three randomly selected fields of each brain structure per slice. Data were obtained using three slices (containing cerebral cortex and striatum) per rat brain from three animals in each experimental group and are expressed as mean ± standard deviation of NeuN-positive cells. $^{*}P < 0.05$, $^{***}P < 0.001$ compared to control (Student's t test for unpaired samples)

We initially found that KIC increased ROS generation (DCFH oxidation), induced lipid (MDA levels) and protein (carbonyl content) oxidative damage and decreased the GSH levels and GR activity in the cerebral cortex of the neonate rats. Similar findings were obtained in the striatum of these animals, except that all antioxidant enzymes evaluated (GPx, GR, and SOD) had their activities increased. It was also seen that nitrate and nitrite values were not changed by this treatment, ruling out a possible action of RNS in these effects. Noteworthy, since MDA is a lipoperoxidation-derived aldehyde, increases of its levels are indicative of lipid peroxidation, which may lead to severe cell damage, particularly to the brain that is rich in polyunsaturated fatty acids highly vulnerable to oxidation [54, 55]. With respect to the carbonyl groups, they result from the oxidation of amino acid side chain residues, indicating protein oxidation that is potentially harmful to cellular physiology [56, 57].

Regarding the decreased levels of GSH, the primary non-enzymatic antioxidant defense of the central nervous system that is critical to the clearance of free radicals [58], it is feasible that elevated levels of ROS could oxidize GSH, forming GSSG, but this should be confirmed since the oxidized form of GSH was not measured here. We might also suggest that the low capacity to prevent oxidative damage (GSH decrease) caused by KIC in the main structures injured in MSUD, may have contributed to lipid and protein oxidation. In turn, the decreased activity of GR in the cerebral cortex, which is a crucial enzyme to restore GSH concentrations, may also have a role in the diminution of GSH levels. Otherwise, we do not know yet the exact mechanisms for the increased antioxidant enzyme activities in the striatum following KIC injection, but our data showing that this organic acid also increased HO-1 protein content suggest that KIC leads to the upregulation of antioxidant defense genes possibly in an attempt to overcome the redox imbalance generated in this cerebral structure, reflecting therefore a cytoprotective strategy [59, 60].

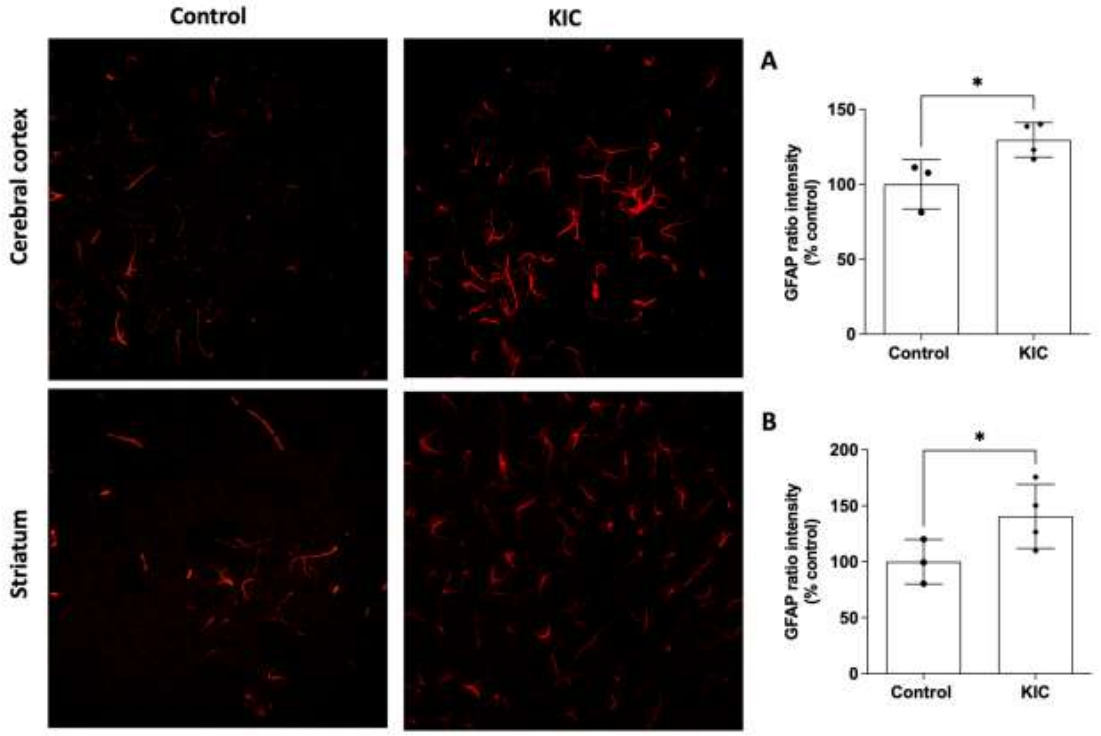


Fig. 11 Effects of an intracerebroventricular (icv) administration of KIC (1 µmol/g) to neonate rats on GFAP immunofluorescence in the cerebral cortex and striatum at postnatal day (PND) 15. Images are representatives of three independent experiments (N). Quantitation of GFAP ratio intensity was performed on 400× magnification images using the mean of three randomly selected fields of each brain structure per slice. Data were obtained using three slices (containing cerebral cortex and striatum) per rat brain from three to four animals in each experimental group and are expressed as mean ± standard deviation of GFAP ratio intensity (% of control). *$P < 0.05$ compared to control (Student's *t* test for unpaired samples)

With respect to SOD, since this enzyme converts the superoxide radical to hydrogen peroxide mainly to preserve GSH [61, 62], it is possible that SOD increased activity could result from its transcriptional overproduction to combat the increase in the anion superoxide radical [63]. The same reasoning could explain GPx activity augment in the striatum, to counterattack hydrogen peroxide species.

Since oxidative stress represents an unbalance between reactive species generation and antioxidant defenses [63], our present findings indicate that KIC induces oxidative stress in the brain of neonate rats, which to our mind was not yet described at this early development stage.

Our results also revealed that pre-treatment of neonate rats with the antioxidants NAC and MEL before KIC injection prevented or attenuated most of the altered biochemical markers of redox homeostasis. Therefore, we presume that particularly NAC, which is used in other pathologies to restore cell redox homeostasis [64–66], could serve as an adjuvant therapy to avoid, or ameliorate acute or chronic oxidative damage to critical cell macromolecules in MSUD.

In this regard, NAC is an effective antioxidant, neutralizing ROS and RNS [67]. This compound has a direct effect due to its free thiol group and it is an essential substrate for the enzyme γ-glutamylcysteine synthetase in the synthesis of GSH [68]. NAC has also anti-inflammatory properties by suppressing the nuclear factor κ B (NF-κB), diminishing the production of tumor necrosis factor-α, interleukin-1, and interleukin-6 (pro-inflammatory cytokines) [69].

MEL, a neurohormone secreted by the pineal gland, acts primarily on circadian rhythms [70], but has been shown to have neuroprotective effects [71, 72] mainly attributed to its antioxidant activity and improvement of mitochondrial function [70, 73–80]. In this context, MEL was demonstrated to mitigate oxidative stress induction by regulating the Nrf2 signaling pathway [81–83], which is mainly responsible for modulating the expression of many antioxidant genes [84].

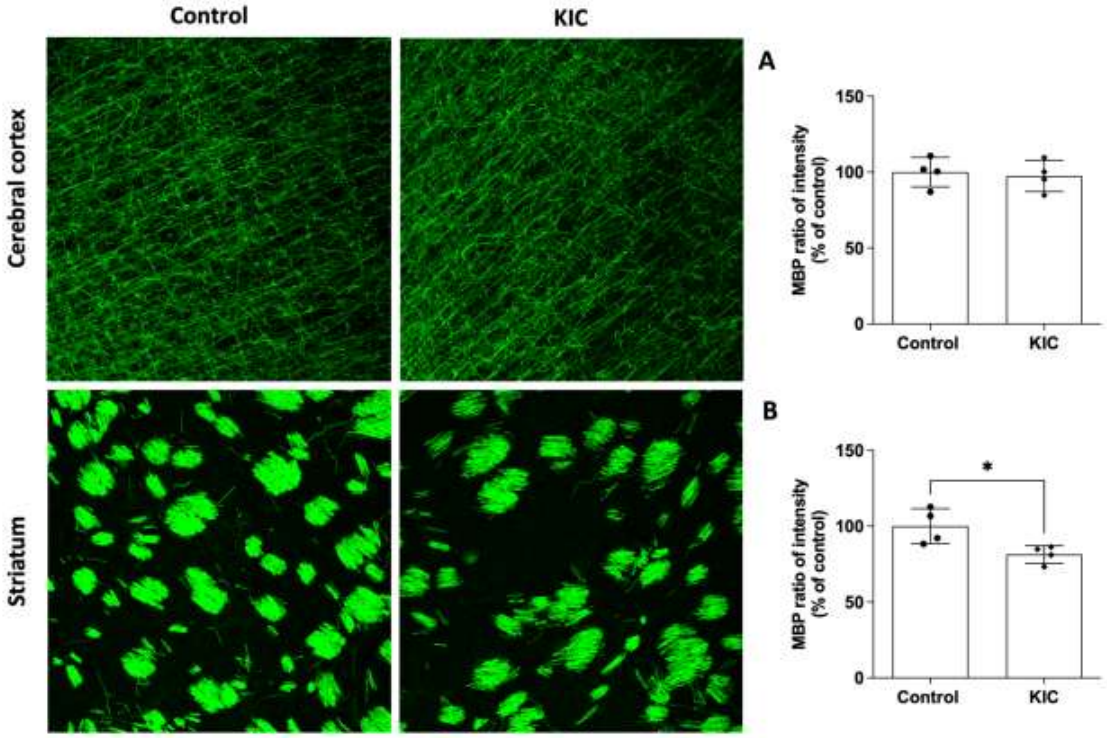


Fig. 12 Effects of an intracerebroventricular (icv) administration of KIC (1 µmol/g) to neonate rats on MBP immunofluorescence in the cerebral cortex (**A**) and striatum (**B**) at postnatal day (PND) 15. Images are representatives of four independent experiments (N). Quantitation of MBP ratio intensity was performed on 200× magnification images using the mean of three randomly selected fields of each brain structure per slice. Data were obtained using three slices (containing cerebral cortex and striatum) per rat brain from four animals in each experimental group and are expressed as mean ± standard deviation of MBP ratio intensity (% of control). *$P < 0.05$ compared to control (Student's *t* test for unpaired samples)

Another interesting observation of this work was that oxidative stress induction following KIC injection at neonatal period was much less evident at PND 7, implying a short-lived effect of this metabolite on brain redox status.

The present data obtained very early during rat development, at an age where severe neurological symptoms appear in humans, are in agreement with previous results that reported increased MDA levels, protein carbonylation, DCFH oxidation, DNA oxidative damage, and SOD activity induced by KIC icv administration in the brain of young rats [11, 13], as well as with in vitro studies demonstrating that KIC disturbs brain redox homeostasis in young rats [15], C6 astroglial cells [16], human leukocytes [85, 86], and hippocampal neuronal cells [13]. Oxidative damage to lipids and proteins has been also shown in plasma of MSUD patients [27–30], corroborating with the in vivo and in vitro animal studies.

We also evaluated whether the injection of KIC to neonate rats could provoke neuronal damage, astrocyte reactivity, and myelination injury in striatum and cerebral cortex at PND 15 since there is no report on whether an acute intracerebral KIC overload during this period of life could cause histopathological alterations along development.

KIC administration led to a long-standing (PND 15) neuronal damage or/and loss (decreased NeuN positive cells) and astroglial reactivity (elevation of the astrocytic marker GFAP) in the cerebral cortex and striatum, whereas significant decreases of the immunoreactivity of the myelin proteins MBP and CNPase, indicating myelination injury, were found in the striatum.

It is emphasized that a moderate activation of astrocytes usually represents a mechanism of protection to surrounding neurons, whereas exacerbated glial reactivity may be deleterious to neurons, as evidenced in various neurodegenerative pathologies [87–89]. Noteworthy, GFAP, which is the main protein constituting astrocyte intermediate filaments, has been considered a classic marker of reactive astrocytes [90, 91]. In this scenario, the present investigation also showed a

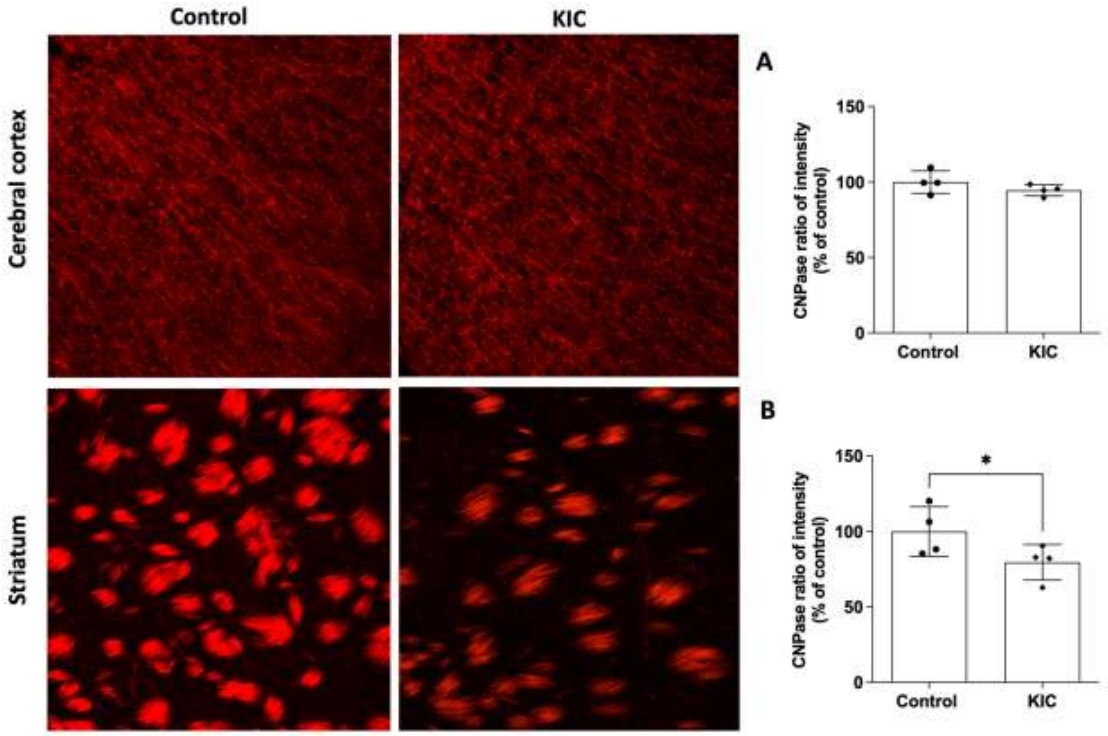


Fig. 13 Effects of an intracerebroventricular (icv) administration of KIC (1 μmol/g) to neonate rats on CNPase immunofluorescence in the cerebral cortex (**A**) and striatum (**B**) at postnatal day (PND) 15. Images are representatives of four independent experiments (N). Quantitation of CNPase ratio intensity was performed on 200× magnification images using the mean of three randomly selected fields of each brain structure per slice. Data were obtained using three slices (containing cerebral cortex and striatum) per rat brain from four animals in each experimental group and are expressed as mean ± standard deviation of CNPase ratio intensity (% of control). $^{*}P < 0.05$ compared to control (Student's *t* test for unpaired samples)

decrease of NeuN immunoreactivity in cerebral cortex and striatum, suggesting neuronal damage associated with glial reactivity in these cerebral structures that are mostly injured in MSUD.

In what concerns to myelination, we found a significant decrease of the content of sensitive protein markers of the myelination status in the striatum. A significant decrease in MBP immunoreactivity was observed in the striatum at PND 15, indicating myelin vulnerability secondary to neonatal intracerebral accumulation of KIC. Of note, the MBP is a sensitive marker of oligodendrocyte function and myelination status once it maintains myelin stability and integrity [92, 93]. In addition, MBP is involved in the maintenance of calcium and cell homeostasis [93]. The immunoreactivity of the CNPase protein, which is important in the regulation of oligodendrocyte process outgrowth [94, 95], was also significantly reduced in the striatum of these animals at PND 15, further indicating myelin injury in the rats neonatally injected with KIC. No significant effect of this treatment towards myelination was observed in the cerebral cortex, indicating that striatum is more vulnerable to myelin injury caused by an acute overload of KIC during the neonatal period that possibly mimics a metabolic episode of decompensation in MSUD affected neonates.

The present neurochemical findings corroborate with previous post-mortem studies carried out in MSUD patients showing defective myelination in various brain regions, including subcortical areas and basal ganglia [96, 97], as well as decrease of oligodendrocyte number in brain white matter [97–99], neuronal abnormalities in the cerebral cortex, and astrogliosis in the hippocampus and basal ganglia [100].

It should be also emphasized that the development and formation of a normal adult brain may be affected by injuries in the early postnatal period that lead to future neurologic symptoms and brain abnormalities. In this particular, it is interesting to note that all KIC-injected animals manifested with seizures immediately after its administration and

recovered after approximately 5 min, in contrast to the PBS-injected rats (controls) that had no seizures at all. These observations revealed that our model of MSUD was toxic to the animals. Based on the data of the present investigation, we postulate that intracerebral toxic levels of KIC at the neonatal period may imbalance cellular redox status, disturbing cellular functions, and ultimately leading to neuronal loss, astrocyte reactivity, and myelination impairment.

We cannot, however, rule out that other pathomechanisms of brain damage are caused by increased concentrations of KIC or of the other metabolites accumulated in MSUD, including mitochondrial dysfunction and increased inflammatory response [46], that may also play an important role in MSUD neuropathology. In this context, we highlight that oxidative stress and neuroinflammation are inter-connected pathogenic processes [101], so that it is feasible that increased pro-inflammatory cytokines in the neural cells might also contribute to the deleterious effects caused by KIC. Indeed, elevation of these inflammatory biomarkers was demonstrated in MSUD patients [48, 50] and in animal models of this disease [102, 103]. However, further studies are required to corroborate this hypothesis.

In conclusion, the findings obtained in this study indicate that KIC-induced oxidative stress early during development may represent a central deleterious mechanism involved in neurological injury in MSUD and that antioxidants may represent a potential new therapeutic strategy for patients affected by this disease. We emphasize that the main purpose of our experimental model using a single icv administration of KIC was to mimic the acute episodes of metabolic decompensation that take place during stressful situations in MSUD patients and are accompanied by high elevation of the brain levels of the accumulating metabolites, particularly KIC. It is also of note that in the affected patients KIC produced peripherally may enter the brain from the systemic circulation, being transported through the blood-brain barrier where it accumulates [53]. Furthermore, this organic acid can be also produced from leucine and accumulate inside the brain cells of MSUD patients, because of the deficient activity of the BCKDH complex in this tissue [53].

Acknowledgements We thank the Centro de Microscopia e Microanálise (UFRGS, RS, Brazil) for the support with the immunofluorescence analysis.

Author Contribution A.B.Z. performed experiments, prepared the figures, and analyzed the data; R.T.R. and C.V.P. performed experiments and analyzed the data; S.A.C., T.Q.T., and E.T.C. provided assistance to the experiments; G.L. analyzed the data and corrected the manuscript text; M.W. and A.U.A. planned the experiments, analyzed the data, and wrote the main manuscript text. All authors read and approved the final manuscript.

Funding This work was supported by grants from Conselho Nacional de Desenvolvimento Científico e Tecnológico (CNPq, 402440/2021-8), Fundação de Amparo à Pesquisa do Estado do Rio Grande do Sul (FAPERGS, 19/2551-0001662-0), Instituto Nacional de Ciência e Tecnologia – Excitotoxicidade e Neuroproteção (INCT-EN, 465671/2014–4), and Instituto Nacional de Ciência e Tecnologia – Saúde Cerebral (INCT-SC, 406020/2022-1).

Data Availability The datasets generated during and/or analyzed during the current study are available from the corresponding author on reasonable request.

Declarations

Ethics Approval The experimental procedures of this study were approved by the Ethical Committee of UFRGS (nº 42875) and performed according to the Guide for the Care and Use of Laboratory Animals (Eighth edition, 2011).

Consent to Participate Not applicable.

Consent to Publish Not applicable.

Competing Interests The authors declare no competing interests.

References

1. Chuang DT, Shih VE, Wynn RM (2019) Maple syrup urine disease (branched-chain ketoaciduria). In: Valle DL, Antonarakis S, Ballabio A, Beaudet AL, Mitchell GA (eds) The online metabolic and molecular bases of inherited disease. McGraw-Hill, New York City (NY), pp. 1–74. https://doi.org/10.1036/Ommbid.400
2. Strauss KA, Carson VJ, Soltys K et al (2020) Branched-chain α-ketoacid dehydrogenase deficiency (maple syrup urine disease): treatment, biomarkers, and outcomes. Mol Genet Metab 129:193–206. https://doi.org/10.1016/J.YMGME.2020.01.006
3. Chen T, Lu D, Xu F et al (2023) Newborn screening of maple syrup urine disease and the effect of early diagnosis. Clin Chim Acta 548:117483. https://doi.org/10.1016/J.CCA.2023.117483
4. Li L, Mao X, Yang N et al (2023) Identification of gene mutations in six Chinese patients with maple syrup urine disease. Front Genet 14:1132364. https://doi.org/10.3389/FGENE.2023.1132364
5. Allahwala A, Ahmed S, Afroze B (2021) Maple syrup urine disease: magnetic resonance imaging findings in three patients. J Pak Med Assoc 71:1–11. https://doi.org/10.47391/JPMA.1341
6. Cheng A, Han L, Feng Y et al (2017) MRI and clinical features of maple syrup urine disease: preliminary results in 10 cases. Diagn Interv Radiol 23:398–402. https://doi.org/10.5152/DIR.2017.16466
7. Kathait AS, Puac P, Castillo M (2018) Imaging findings in maple syrup urine disease: a case report. J Pediatr Neurosci 13:103–105. https://doi.org/10.4103/JPN.JPN_38_17
8. Muelly ER, Moore GJ, Bunce SC et al (2013) Biochemical correlates of neuropsychiatric illness in maple syrup urine disease. J Clin Invest 123:1809–1820. https://doi.org/10.1172/JCI67217
9. Schönberger S, Schweiger B, Schwahn B et al (2004) Dysmyelination in the brain of adolescents and young adults with maple syrup urine disease. Mol Genet Metab 82:69–75. https://doi.org/10.1016/J.YMGME.2004.01.016
10. Vasques VDC, De Boer MA, Diligenti F et al (2004) Intrahippocampal administration of the α-keto acids accumulating in maple syrup urine disease provokes learning deficits in rats. Pharmacol Biochem Behav 77:183–190. https://doi.org/10.1016/j.pbb.2003.10.013

11. Taschetto L, Scaini G, Zapelini HG et al (2017) Acute and long-term effects of intracerebroventricular administration of α-ketoisocaproic acid on oxidative stress parameters and cognitive and noncognitive behaviors. Metab Brain Dis 32:1507–1518. https://doi.org/10.1007/S11011-017-0035-Z
12. Wisniewski MSW, Carvalho-Silva M, Gomes LM et al (2016) Intracerebroventricular administration of α-ketoisocaproic acid decreases brain-derived neurotrophic factor and nerve growth factor levels in brain of young rats. Metab Brain Dis 31:377–383. https://doi.org/10.1007/S11011-015-9768-8
13. Farias HR, Gabriel JR, Cecconi ML et al (2021) The metabolic effect of α-ketoisocaproic acid: in vivo and in vitro studies. Metab Brain Dis 36:185–192. https://doi.org/10.1007/S11011-020-00626-Y
14. Rabelo F, Lemos ID, Dal Toé CP et al (2023) Acute effects of intracerebroventricular administration of α-ketoisocaproic acid in young rats on inflammatory parameters. Metab Brain Dis 38:1573–1579. https://doi.org/10.1007/S11011-023-01193-8
15. Bridi R, Braun CA, Zorzi GK et al (2005) α-Keto acids accumulating in maple syrup urine disease stimulate lipid peroxidation and reduce antioxidant defences in cerebral cortex from young rats. Metab Brain Dis 20:155–167. https://doi.org/10.1007/s11011-005-4152-8
16. Funchal C, Latini A, Jacques-Silva MC et al (2006) Morphological alterations and induction of oxidative stress in glial cells caused by the branched-chain α-keto acids accumulating in maple syrup urine disease. Neurochem Int 49:640–650. https://doi.org/10.1016/J.NEUINT.2006.05.007
17. Patel MS, Auerbach VH, Grover WD, Wilbur DO (1973) Effect of the branched-chain α-keto acids on pyruvate metabolism by homogenates of human brain. J Neurochem 20:1793–1796. https://doi.org/10.1111/J.1471-4159.1973.TB00298.X
18. Ribeiro CA, Sgaravatti ÂM, Rosa RB et al (2008) Inhibition of brain energy metabolism by the branched-chain amino acids accumulating in maple syrup urine disease. Neurochem Res 33:114–124. https://doi.org/10.1007/S11064-007-9423-9
19. Amaral AU, Leipnitz G, Fernandes CG et al (2010) α-Ketoisocaproic acid and leucine provoke mitochondrial bioenergetic dysfunction in rat brain. Brain Res 1324:75–84. https://doi.org/10.1016/J.BRAINRES.2010.02.018
20. Sgaravatti AM, Rosa RB, Schuck PF et al (2003) Inhibition of brain energy metabolism by the α-keto acids accumulating in maple syrup urine disease. Biochim Biophys Acta 1639:232–238. https://doi.org/10.1016/J.BBADIS.2003.09.010
21. Bridi R, Araldi J, Sgarbi MB et al (2003) Induction of oxidative stress in rat brain by the metabolites accumulating in maple syrup urine disease. Int J Dev Neurosci 21:327–332. https://doi.org/10.1016/S0736-5748(03)00074-1
22. Mescka C, Moraes T, Rosa A et al (2011) In vivo neuroprotective effect of L-carnitine against oxidative stress in maple syrup urine disease. Metab Brain Dis 26:21–28. https://doi.org/10.1007/S11011-011-9238-X
23. Mescka CP, Rosa AP, Schirmbeck G et al (2016) L-Carnitine prevents oxidative stress in the brains of rats subjected to a chemically induced chronic model of MSUD. Mol Neurobiol 53:6007–6017. https://doi.org/10.1007/S12035-015-9500-Z
24. Scaini G, Jeremias IC, Morais MOS et al (2012) DNA damage in an animal model of maple syrup urine disease. Mol Genet Metab 106:169–174. https://doi.org/10.1016/J.YMGME.2012.04.009
25. Pilla C, De Oliveira Cardozo RF, Dutra-Filho CS et al (2003) Effect of leucine administration on creatine kinase activity in rat brain. Metab Brain Dis 18:17–25. https://doi.org/10.1023/A:1021974517837
26. Pilla C, De Oliveira Cardozo RF, Dutra-Filho CS et al (2003) Creatine kinase activity from rat brain is inhibited by branched-chain amino acids in vitro. Neurochem Res 28:675–679. https://doi.org/10.1023/A:1022876130038
27. Barschak AG, Sitta A, Deon M et al (2006) Evidence that oxidative stress is increased in plasma from patients with maple syrup urine disease. Metab Brain Dis 21:279–286. https://doi.org/10.1007/S11011-006-9030-5
28. Guerreiro G, Mescka CP, Sitta A et al (2015) Urinary biomarkers of oxidative damage in maple syrup urine disease: the L-carnitine role. Int J Dev Neurosci 42:10–14. https://doi.org/10.1016/J.IJDEVNEU.2015.02.003
29. Mescka CP, Wayhs CAY, Vanzin CS et al (2013) Protein and lipid damage in maple syrup urine disease patients: L-carnitine effect. Int J Dev Neurosci 31:21–24. https://doi.org/10.1016/J.IJDEVNEU.2012.10.109
30. Mc Guire PJ, Parikh A, Diaz GA (2009) Profiling of oxidative stress in patients with inborn errors of metabolism. Mol Genet Metab 98:173–180. https://doi.org/10.1016/J.YMGME.2009.06.007
31. Olivera-Bravo S, Fernández A, Sarlabós MN et al (2011) Neonatal astrocyte damage is sufficient to trigger progressive striatal degeneration in a rat model of glutaric acidemia-I. PLoS One 6:e20831. https://doi.org/10.1371/JOURNAL.PONE.0020831
32. Ribeiro RT, Seminotti B, Zanatta Â et al (2021) Neuronal death, glial reactivity, microglia activation, oxidative stress and bioenergetics impairment caused by intracerebroventricular administration of D-2-hydroxyglutaric acid to neonatal rats. Neuroscience 471:115–132. https://doi.org/10.1016/J.NEUROSCIENCE.2021.07.024
33. Seminotti B, Zanatta Â, Ribeiro RT et al (2019) Disruption of brain redox homeostasis, microglia activation and neuronal damage induced by intracerebroventricular administration of s-adenosylmethionine to developing rats. Mol Neurobiol 56:2760–2773. https://doi.org/10.1007/S12035-018-1275-6
34. Moura AP, Parmeggiani B, Grings M et al (2016) Intracerebral glycine administration impairs energy and redox homeostasis and induces glial reactivity in cerebral cortex of newborn rats. Mol Neurobiol 53:5864–5875. https://doi.org/10.1007/S12035-015-9493-7
35. Ribeiro RT, Zanatta Â, Amaral AU et al (2018) Experimental evidence that in vivo intracerebral administration of L-2-hydroxyglutaric acid to neonatal rats provokes disruption of redox status and histopathological abnormalities in the brain. Neurotox Res 33:681–692. https://doi.org/10.1007/S12640-018-9874-6
36. LeBel CP, Ischiropoulos H, Bondy SC (1992) Evaluation of the probe 2',7'-dichlorofluorescin as an indicator of reactive oxygen species formation and oxidative stress. Chem Res Toxicol 5:227–231. https://doi.org/10.1021/TX00026A012
37. Navarro-Gonzálvez JA, García-Benayas C, Arenas J (1998) Semiautomated measurement of nitrate in biological fluids. Clin Chem 44:679–681. https://doi.org/10.1093/CLINCHEM/44.3.679
38. Yagi K (1998) Simple procedure for specific assay of lipid hydroperoxides in serum or plasma. Methods Mol Biol 108:107–110. https://doi.org/10.1385/0-89603-472-0:107
39. Reznick AZ, Packer L (1994) Oxidative damage to proteins: spectrophotometric method for carbonyl assay. Methods Enzymol 233:357–363. https://doi.org/10.1016/S0076-6879(94)33041-7
40. Browne RW, Armstrong D (1998) Reduced glutathione and glutathione disulfide. Methods Mol Biol 108:347–352. https://doi.org/10.1385/0-89603-472-0:347
41. Wendel A (1981) Glutathione peroxidase. Methods Enzymol 77:325–333. https://doi.org/10.1016/S0076-6879(81)77046-0

42. Carlberg I, Mannervik B (1985) [59] Glutathione reductase. Methods Enzymol 113:484–490. https://doi.org/10.1016/S0076-6879(85)13062-4
43. Marklund SL (1985) Product of extracellular-superoxide dismutase catalysis. FEBS Lett 184:237–239. https://doi.org/10.1016/0014-5793(85)80613-X
44. Lowry OH, Rosebrough NJ, Farr AL, Randall RJ (1951) Protein measurement with the Folin phenol reagent. J Biol Chem 193:265–275. https://doi.org/10.1016/S0021-9258(19)52451-6
45. Ryter SW, Alam J, Choi AMK (2006) Heme oxygenase-1/carbon monoxide: from basic science to therapeutic applications. Physiol Rev 86:583–650. https://doi.org/10.1152/PHYSREV.00011.2005
46. Amaral AU, Wajner M (2022) Pathophysiology of maple syrup urine disease: focus on the neurotoxic role of the accumulated branched-chain amino acids and branched-chain α-keto acids. Neurochem Int 157:105360. https://doi.org/10.1016/J.NEUINT.2022.105360
47. Strauss KA, Puffenberger EG, Carson VJ (2020) Maple syrup urine disease. In: Adam MP, Ardinger HH, Pagon RA, Wallace SE, Bean LJ, Mirzaa G, Amemiya A (eds) GeneReviews® [Internet]. University of Washington, Seattle (WA), pp. 1–33
48. Mescka CP, Guerreiro G, Donida B et al (2015) Investigation of inflammatory profile in MSUD patients: benefit of L-carnitine supplementation. Metab Brain Dis 30:1167–1174. https://doi.org/10.1007/S11011-015-9686-9
49. Scaini G, Tonon T, de Souza CFM et al (2016) Serum markers of neurodegeneration in maple syrup urine disease. MolNeurobiol 54:5709–5719. https://doi.org/10.1007/S12035-016-0116-8
50. Scaini G, Tonon T, Moura de Souza CF et al (2018) Evaluation of plasma biomarkers of inflammation in patients with maple syrup urine disease. J Inherit Metab Dis 41:631–640. https://doi.org/10.1007/S10545-018-0188-X
51. Boado RJ, Li JY, Nagaya M et al (1999) Selective expression of the large neutral amino acid transporter at the blood-brain barrier. Proc Natl Acad Sci U S A 96:12079–12084. https://doi.org/10.1073/PNAS.96.21.12079
52. Killian DM, Chikhale PJ (2001) Predominant functional activity of the large, neutral amino acid transporter (LAT1) isoform at the cerebrovasculature. Neurosci Lett 306:1–4. https://doi.org/10.1016/S0304-3940(01)01810-9
53. Sperringer JE, Addington A, Hutson SM (2017) Branched-chain amino acids and brain metabolism. Neurochem Res 42:1697–1709. https://doi.org/10.1007/S11064-017-2261-5
54. Ayala A, Muñoz MF, Argüelles S (2014) Lipid peroxidation: production, metabolism, and signaling mechanisms of malondialdehyde and 4-hydroxy-2-nonenal. Oxidative Med Cell Longev 2014:360438. https://doi.org/10.1155/2014/360438
55. Gaschler MM, Stockwell BR (2017) Lipid peroxidation in cell death. Biochem Biophys Res Commun 482:419–425. https://doi.org/10.1016/J.BBRC.2016.10.086
56. Dalle-Donne I, Rossi R, Giustarini D et al (2003) Protein carbonyl groups as biomarkers of oxidative stress. Clin Chim Acta 329:23–38. https://doi.org/10.1016/S0009-8981(03)00003-2
57. Levine RL, Williams JA, Stadtman EP, Shacter E (1994) [37] Carbonyl assays for determination of oxidatively modified proteins. Methods Enzymol 233:346–357. https://doi.org/10.1016/S0076-6879(94)33040-9
58. Kwon DH, Cha HJ, Lee H et al (2019) Protective effect of glutathione against oxidative stress-induced cytotoxicity in RAW 264.7 macrophages through activating the nuclear factor erythroid 2-related factor-2/heme oxygenase-1 pathway. Antioxidants 8:82. https://doi.org/10.3390/ANTIOX8040082
59. Vijayan V, Wagener FADTG, Immenschuh S (2018) The macrophage heme-heme oxygenase-1 system and its role in inflammation. Biochem Pharmacol 153:159–167. https://doi.org/10.1016/J.BCP.2018.02.010
60. Szabo IL, Kenyeres A, Szegedi A, Szollosi AG (2018) Heme oxygenase and the skin in health and disease. Curr Pharm Des 24:2303–2310. https://doi.org/10.2174/1381612824666180717155953
61. Pope SAS, Milton R, Heales SJR (2008) Astrocytes protect against copper-catalysed loss of extracellular glutathione. Neurochem Res 33:1410–1418. https://doi.org/10.1007/S11064-008-9602-3
62. Stewart VC, Stone R, Gegg ME et al (2002) Preservation of extracellular glutathione by an astrocyte derived factor with properties comparable to extracellular superoxide dismutase. J Neurochem 83:984–991. https://doi.org/10.1046/J.1471-4159.2002.01216.X
63. Halliwell B, Gutteridge JMC (2015) Antioxidant defenses synthesized in vivo. Free Radic Biol Med 77–152. https://doi.org/10.1093/ACPROF:OSO/9780198717478.003.0003
64. Arab JP, Roblero JP, Altamirano J et al (2019) Alcohol-related liver disease: clinical practice guidelines by the Latin American Association for the Study of the Liver (ALEH). Ann Hepatol 18:518–535. https://doi.org/10.1016/J.AOHEP.2019.04.005
65. Angelovski M, Hadzi-Petrushev N, Mitrokhin V et al (2023) Myocardial infarction and oxidative damage in animal models: objective and expectations from the application of cysteine derivatives. Toxicol Mech Methods 33:1–17. https://doi.org/10.1080/15376516.2022.2069530
66. Schoeps VA, Graves JS, Stern WA et al (2022) N-Acetyl cysteine as a neuroprotective agent in progressive multiple sclerosis (NACPMS) trial: study protocol for a randomized, double-blind, placebo-controlled add-on phase 2 trial. Contemp Clin Trials 122:106941. https://doi.org/10.1016/J.CCT.2022.106941
67. Santus P, Danzo F, Zuffi A et al (2022) Oxidative stress and viral infections: rationale, experiences, and perspectives on N-acetylcysteine. Eur Rev Med Pharmacol Sci 26:8582–8590. https://doi.org/10.26355/EURREV_202211_30395
68. Morris G, Anderson G, Dean O et al (2014) The glutathione system: a new drug target in neuroimmune disorders. Mol Neurobiol 50:1059–1084. https://doi.org/10.1007/S12035-014-8705-X
69. Pawlas N, Nierwińska K, Stolecka A et al (2009) Effects of N-acetylcysteine and ebselen on arachidonic acid release from astrocytes and neurons cultured in normoxic or simulated ischemic conditions. Pharmacol Rep 61:941–946. https://doi.org/10.1016/S1734-1140(09)70153-7
70. Rodriguez C, Mayo JC, Sainz RM et al (2004) Regulation of antioxidant enzymes: a significant role for melatonin. J Pineal Res 36:1–9. https://doi.org/10.1046/J.1600-079X.2003.00092.X
71. Malhotra S, Sawhney G, Pandhi P (2004) The therapeutic potential of melatonin: a review of the science. Medscape Gen Med 6:46
72. Tordjman S, Chokron S, Delorme R et al (2017) Melatonin: pharmacology, functions and therapeutic benefits. Curr Neuropharmacol 15:434–443. https://doi.org/10.2174/1570159X14666161228122115
73. Schaefer M, Hardeland R (2009) The melatonin metabolite N1-acetyl-5-methoxykynuramine is a potent singlet oxygen scavenger. J Pineal Res 46:49–52. https://doi.org/10.1111/J.1600-079X.2008.00614.X
74. Reiter RJ, Tan DX, Osuna C, Gitto E (2000) Actions of melatonin in the reduction of oxidative stress. A review. J Biomed Sci 7:444–458. https://doi.org/10.1007/BF02253360
75. Reiter RJ, Mayo JC, Tan DX et al (2016) Melatonin as an antioxidant: under promises but over delivers. J Pineal Res 61:253–278. https://doi.org/10.1111/JPI.12360
76. Hoppe JB, Frozza RL, Horn AP et al (2010) Amyloid-β neurotoxicity in organotypic culture is attenuated by melatonin: involvement of GSK-3β, tau and neuroinflammation. J Pineal Res 48:230–238. https://doi.org/10.1111/J.1600-079X.2010.00747.X

77. Manchester LC, Coto-Montes A, Boga JA et al (2015) Melatonin: an ancient molecule that makes oxygen metabolically tolerable. J Pineal Res 59:403–419. https://doi.org/10.1111/JPI.12267
78. Tan DX, Manchester LC, Esteban-Zubero E et al (2015) Melatonin as a potent and inducible endogenous antioxidant: synthesis and metabolism. Molecules 20:18886–18906. https://doi.org/10.3390/MOLECULES201018886
79. Wen J, Ariyannur PS, Ribeiro R et al (2016) Efficacy of N-acetylserotonin and melatonin in the EAE model of multiple sclerosis. J NeuroImmune Pharmacol 11:763–773. https://doi.org/10.1007/S11481-016-9702-9
80. Muhammad T, Ali T, Ikram M et al (2019) Melatonin rescue oxidative stress-mediated neuroinflammation/neurodegeneration and memory impairment in scopolamine-induced amnesia mice model. J NeuroImmune Pharmacol 14:278–294. https://doi.org/10.1007/S11481-018-9824-3
81. Shah SA, Khan M, Jo MH et al (2017) Melatonin stimulates the SIRT1/Nrf2 signaling pathway counteracting lipopolysaccharide (LPS)-induced oxidative stress to rescue postnatal rat brain. CNS Neurosci Ther 23:33–44. https://doi.org/10.1111/CNS.12588
82. Yarmohammadi F, Barangi S, Aghaee-Bakhtiari SH et al (2023) Melatonin ameliorates arsenic-induced cardiotoxicity through the regulation of the Sirt1/Nrf2 pathway in rats. BioFactors 49:620–635. https://doi.org/10.1002/BIOF.1934
83. Ali T, Hao Q, Ullah N et al (2020) Melatonin act as an antidepressant via attenuation of neuroinflammation by targeting Sirt1/Nrf2/HO-1 signaling. Front Mol Neurosci 13:96. https://doi.org/10.3389/FNMOL.2020.00096
84. Gan L, Johnson JA (2014) Oxidative damage and the Nrf2-ARE pathway in neurodegenerative diseases. Biochim Biophys Acta 1842:1208–1218. https://doi.org/10.1016/J.BBADIS.2013.12.011
85. Hauschild TC, Guerreiro G, Mescka CP et al (2019) DNA damage induced by alloisoleucine and other metabolites in maple syrup urine disease and protective effect of l-carnitine. Toxicol in Vitro 57:194–202. https://doi.org/10.1016/J.TIV.2019.03.007
86. Mescka CP, Wayhs CAY, Guerreiro G et al (2014) Prevention of DNA damage by l-carnitine induced by metabolites accumulated in maple syrup urine disease in human peripheral leukocytes in vitro. Gene 548:294–298. https://doi.org/10.1016/J.GENE.2014.07.051
87. Hol EM, Pekny M (2015) Glial fibrillary acidic protein (GFAP) and the astrocyte intermediate filament system in diseases of the central nervous system. Curr Opin Cell Biol 32:121–130. https://doi.org/10.1016/J.CEB.2015.02.004
88. Pekny M, Pekna M (2014) Astrocyte reactivity and reactive astrogliosis: costs and benefits. Physiol Rev 94:1077–1098. https://doi.org/10.1152/PHYSREV.00041.2013
89. Olivera-Bravo S, Barbeito L (2015) A role of astrocytes in mediating postnatal neurodegeneration in glutaric acidemia-type 1. FEBS Lett 589:3492–3497. https://doi.org/10.1016/J.FEBSLET.2015.09.010
90. Escartin C, Galea E, Lakatos A et al (2021) Reactive astrocyte nomenclature, definitions, and future directions. Nat Neurosci 24:312–325. https://doi.org/10.1038/s41593-020-00783-4
91. Janigro D, Mondello S, Posti JP, Unden J (2022) GFAP and S100B: what you always wanted to know and never dared to ask. Front Neurol 13:835597. https://doi.org/10.3389/FNEUR.2022.835597
92. Boggs JM, Rangaraj G, Heng YM et al (2011) Myelin basic protein binds microtubules to a membrane surface and to actin filaments in vitro: effect of phosphorylation and deimination. Biochim Biophys Acta 1808:761–773. https://doi.org/10.1016/J.BBAMEM.2010.12.016
93. Harauz G, Boggs JM (2013) Myelin management by the 18.5-kDa and 21.5-kDa classic myelin basic protein isoforms. J Neurochem 125:334–361. https://doi.org/10.1111/JNC.12195
94. Lee J, Gravel M, Zhang R et al (2005) Process outgrowth in oligodendrocytes is mediated by CNP, a novel microtubule assembly myelin protein. J Cell Biol 170:661–673. https://doi.org/10.1083/JCB.200411047
95. Fulton D, Paez PM, Campagnoni AT (2010) The multiple roles of myelin protein genes during the development of the oligodendrocyte. ASN Neuro 2:25–37. https://doi.org/10.1042/AN20090051
96. Martin JJ, Schlote W (1972) Central nervous system lesions in disorders of amino-acid metabolism: a neuropathological study. J Neurol Sci 15:49–76. https://doi.org/10.1016/0022-510X(72)90121-9
97. Menkes JH, Philippart M, Fiol RE (1965) Cerebral lipids in maple syrup disease. J Pediatr 66:584–594. https://doi.org/10.1016/S0022-3476(65)80122-6
98. Crome L, Dutton G, Ross CF (1961) Maple syrup urine disease. J Pathol Bacteriol 81:379–384. https://doi.org/10.1002/PATH.1700810209
99. Silberman J, Dancis J, Feigin I (1961) Neuropathological observations in maple syrup urine disease: branched-chain ketoaciduria. Arch Neurol 5:351–363. https://doi.org/10.1001/ARCHNEUR.1961.00450160001001
100. Kamei A, Takashima S, Chan F, Becker LE (1992) Abnormal dendritic development in maple syrup urine disease. Pediatr Neurol 8:145–147. https://doi.org/10.1016/0887-8994(92)90038-Z
101. Popa-Wagner A, Mitran S, Sivanesan S et al (2013) ROS and brain diseases: the good, the bad, and the ugly. Oxidative Med Cell Longev 2013:963520. https://doi.org/10.1155/2013/963520
102. Rosa L, Galant LS, Dall'Igna DM et al (2016) Cerebral oedema, blood–brain barrier breakdown and the decrease in Na+,K+-ATPase activity in the cerebral cortex and hippocampus are prevented by dexamethasone in an animal model of maple syrup urine disease. Mol Neurobiol 53:3714–3723. https://doi.org/10.1007/S12035-015-9313-0
103. Wessler LB, de Miranda RV, Bittencourt Pasquali MA et al (2019) Administration of branched-chain amino acids increases the susceptibility to lipopolysaccharide-induced inflammation in young Wistar rats. Int J Dev Neurosci 78:210–214. https://doi.org/10.1016/J.IJDEVNEU.2019.07.007

Publisher's Note Springer Nature remains neutral with regard to jurisdictional claims in published maps and institutional affiliations.

Springer Nature or its licensor (e.g. a society or other partner) holds exclusive rights to this article under a publishing agreement with the author(s) or other rightsholder(s); author self-archiving of the accepted manuscript version of this article is solely governed by the terms of such publishing agreement and applicable law.

4. Capítulo II

α-Ketoisocaproic Acid Disrupts Mitochondrial Bioenergetics in the Brain of Neonate Rats: Molecular Modeling Studies of α-ketoglutarate Dehydrogenase Subunits Inhibition

Ângela Beatris Zemniaçak, Rafael Teixeira Ribeiro, Gustavo Machado das Neves, Sâmela de Azevedo Cunha, Tailine Quevedo Tavares, Andrey Vinícios Soares Carvalho, Carlos Alexandre Netto, Roger Frigério Castilho, Moacir Wajner, Alexandre Umpierrez Amaral

Artigo científico publicado em

Neurochemical Research (2025) 50:76

Neurochemical Research (2025) 50:76
https://doi.org/10.1007/s11064-024-04328-0

RESEARCH

α-Ketoisocaproic Acid Disrupts Mitochondrial Bioenergetics in the Brain of Neonate Rats: Molecular Modeling Studies of α-ketoglutarate Dehydrogenase Subunits Inhibition

Ângela Beatris Zemniaçak[1] · Rafael Teixeira Ribeiro[1] · Gustavo Machado das Neves[2] · Sâmela de Azevedo Cunha[1] · Tailine Quevedo Tavares[1] · Andrey Vinícios Soares Carvalho[1] · Carlos Alexandre Netto[1,3] · Roger Frigério Castilho[4] · Moacir Wajner[1,3,5] · Alexandre Umpierrez Amaral[1,6]

Received: 1 October 2024 / Revised: 21 November 2024 / Accepted: 23 December 2024
© The Author(s), under exclusive licence to Springer Science+Business Media, LLC, part of Springer Nature 2024

Abstract
Brain accumulation of the branched-chain α-keto acids α-ketoisocaproic acid (KIC), α-keto-β-methylvaleric acid (KMV), and α-ketoisovaleric acid (KIV) occurs in maple syrup urine disease (MSUD), an inherited intoxicating metabolic disorder caused by defects of the branched-chain α-keto acid dehydrogenase complex. Patients commonly suffer life-threatening acute encephalopathy in the newborn period and develop chronic neurological sequelae of still undefined pathogenesis. Therefore, this work investigated the in vitro influence of pathological concentrations of KIC (5 mM), KMV (1 mM), and KIV (1 mM) on mitochondrial bioenergetics in the cerebral cortex of neonate (one-day-old) rats. KIC, but not KMV and KIV, decreased phosphorylating (stimulated by ADP) and uncoupled (induced by CCCP) mitochondrial respiration supported by pyruvate, malate, and glutamate, indicating metabolic inhibition. These effects were less evident after supplementing the medium with succinate. KIC also mildly increased non-phosphorylating respiration (in the presence of oligomycin) using pyruvate plus malate or glutamate plus malate as substrates, suggesting an uncoupling effect. Moreover, KIC markedly inhibited the activity of α-ketoglutarate dehydrogenase noncompetitively and decreased ATP synthesis. Finally, docking simulations demonstrated that KIC preferentially interacts with E2 and E3 subunits of α-ketoglutarate dehydrogenase at the dihydrolipoamide binding site and into an allosteric site of E1. The present data strongly indicate that KIC compromises mitochondrial bioenergetics in the neonatal rat brain, supporting the hypothesis that disruption of energy homeostasis caused by brain KIC accumulation in the first days of life may be implicated in the neuropathology of MSUD.

Keywords Maple syrup urine disease · α-Ketoisocaproic acid · Brain · Bioenergetics · Docking simulations

✉ Alexandre Umpierrez Amaral
alexandreamaral@uricer.edu.br

[1] Programa de Pós-Graduação em Ciências Biológicas: Bioquímica, Instituto de Ciências Básicas da Saúde, Universidade Federal do Rio Grande do Sul, Porto Alegre, RS, Brazil

[2] Laboratório de Síntese Orgânica Medicinal (LaSOM), Faculdade de Farmácia, Universidade Federal do Rio Grande do Sul, Porto Alegre, RS, Brazil

[3] Departamento de Bioquímica, Instituto de Ciências Básicas da Saúde, Universidade Federal do Rio Grande do Sul, Porto Alegre, RS, Brazil

[4] Departamento de Patologia, Faculdade de Ciências Médicas, Universidade Estadual de Campinas, Campinas, SP, Brazil

[5] Serviço de Genética Médica, Hospital de Clínicas de Porto Alegre, Porto Alegre, RS, Brazil

[6] Programa de Pós-Graduação em Atenção Integral à Saúde (UNICRUZ/URI-Erechim/UNIJUÍ), Universidade Regional Integrada do Alto Uruguai e das Missões, Erechim, RS, Brazil

Published online: 09 January 2025

Abbreviations

AF	AlphaFold
ANOVA	One-way analysis of variance
BCAA	Branched-chain amino acids
BCKA	Branched chain α-keto acids
BCKDH	Branched-chain α-keto acid dehydrogenase
BSA	Bovine serum albumin
CAC	Citric acid cycle
COA	Coenzyme A
CS	Citrate synthase
DCIP	2,6-dichloroindophenol
DHLPM	Dihydrolipoamide
DTNB	5,5'-Dithiobis-(2-Nitrobenzoic Acid)
EMA	Ethylmalonic acid
FAD	Oxidized flavin adenine dinucleotide
$FADH_2$	Reduced flavin adenine dinucleotide
GM	Glutamate plus malate
IDH1	Cytosolic NADP-dependent isocitrate dehydrogenase
IDH2	Mitochondrial NADP-dependent isocitrate dehydrogenase
IDH3	NAD-dependent isocitrate dehydrogenase
KG	α-Ketoglutarate
KGDH	α-Ketoglutarate dehydrogenase
KIC	α-Ketoisocaproic acid
KIV	α-Ketoisovaleric acid
KMV	α-Keto-β-methylvaleric acid
LPM	Lipoamide
MDH1	Cytosolic malate dehydrogenase
MDH2	Mitochondrial malate dehydrogenase
MSUD	Maple syrup urine disease
NAD^+	Oxidized nicotinamide adenine dinucleotide
NADH	Reduced nicotinamide adenine dinucleotide
PDB	Protein data bank
PM	Pyruvate plus malate
PMG	Pyruvate, malate and glutamate
RMSD	Root mean square deviation
SDH	Succinate dehydrogenase
SMILES	Simplified molecular-input line-entry system
SUIT	Substrate-uncoupler inhibitor titration
TD7	Enamine-TPP intermediate
TPP	Thiamine pyrophosphate

Introduction

Maple syrup urine disease (MSUD) (MIM 248600) is an autosomal recessive intoxicating metabolic disorder with a worthwhile prevalence of 1:185,000 live births. It results from mutations in the branched-chain α-ketoacid dehydrogenase complex (BCKDH, EC 1.2.4.4), severely reducing its activity. This causes tissue and plasma accumulation of the branched-chain α-ketoacids (BCKA) α-ketoisocaproic acid (KIC), α-keto-β-methylvaleric acid (KMV), and α-ketoisovaleric acid (KIV), as well as their respective branched-chain amino acids (BCAA) leucine, isoleucine, and valine [1, 2].

MSUD is classified into distinct variants; the classic form (neonatal MSUD) is the most severe and frequent [3, 4]. Infants with this form typically exhibit metabolic intoxication in the first days of life, reflected by irritability, somnolence, anorexia, vomiting, dehydration, and ketoacidosis, which rapidly progress to neurological manifestations as lethargy, coma, apnea, opisthotonos, and cytotoxic cerebral edema. Chronic neurological sequelae frequently occur as the disease progresses and are mainly manifested by intellectual disability, movement disorders, and neuropsychiatric features [1, 5, 6]. Neuropathological studies reveal brain atrophy [5, 7], hypomyelination, and cytotoxic edema across various brain regions, particularly in the basal ganglia and cerebral cortex [8–10].

The BCKA and the BCAA are potential neurotoxins in MSUD since neurological symptoms worsen with brain accumulation of these metabolites. This mainly occurs in situations of metabolic decompensation accompanied by intense proteolysis, such as fever, infections, and fasting [1]. Thus, therapy aims to reduce the accumulation of toxic metabolites through a protein/BCAA-restricted diet and prevent catabolic events [6]. Many studies have shown that the BCAA accumulating in MSUD can damage the central nervous system through distinct mechanisms [11–16]. However, the underlying neurotoxic role of the BCKA has been poorly explored, particularly at the early stages of development.

Previous studies conducted in rat brains have shown that the BCKA disturbed redox homeostasis in vitro by inducing lipid oxidative damage and impairing antioxidant defenses [17, 18]. These compounds were also shown to inhibit α-ketoglutarate dehydrogenase (KGDH) [19], pyruvate dehydrogenase [20], and respiratory complexes I-III activities [21], besides decreasing CO_2 production and increasing lactate release [21]. The BCKA also inhibited creatine kinase activity in C6 astroglial cells [18, 22]. Furthermore, KIC reduced mitochondrial phosphorylating respiration and decreased NAD(P)H content and membrane potential in brain mitochondria [19].

Notably, all these in vitro studies were performed in the brains of 30-day-old or older rats. Considering that the neurological findings in MSUD patients are usually manifested in the newborn period, further studies using the neonatal brain are needed to understand better the role of BCKA on the pathogenesis of brain injury in MSUD at the early stages of development. Therefore, in the present study, we aimed to investigate the effects of KIC, KMV, and KIV on critical

parameters of mitochondrial bioenergetics in the brains of neonate (1-day-old) rats. Additionally, we conducted an in silico study on α-ketoglutarate dehydrogenase (KGDH), which was markedly inhibited by KIC, with the aim of identifying the structural binding sites involved in the interaction between KIC and the enzyme.

Materials and Methods

Animals and Reagents

A total of 46 neonates aged one-day were used in the experiments. The rats were obtained from Centro de Reprodução e Experimentação de Animais de Laboratório (CREAL) at the Federal University of Rio Grande do Sul (UFRGS), Porto Alegre, Brazil, were used in this study. Animals were kept on a 12:12 h light/dark cycle at 24±1°C. Free water and commercial chow with 20% (w/w) protein were available. Neonate rats remained with their dams until the experiments began.

All reagents were highly analytical and purchased from Merck (St. Louis, MO, USA). The solutions were prepared on the day of the experiments and had their pH adjusted to 7.4.

Preparation of Cerebral Cortex Crude Homogenates

One-day-old Wistar rats were euthanized by decapitation; the cerebral cortex was dissected and manually homogenized in the same buffer used for the determination of respiratory parameters and ATP production at a proportion of 20 mg tissue. mL^{-1} for the experiments using pyruvate, malate and glutamate (PMG) plus succinate as substrates, and 80 mg tissue. mL^{-1} for the experiments using GM or PM as substrates.

Mitochondrial Respiratory Parameters

The mitochondrial respiratory parameters were measured in an OROBOROS Oxygraph-2k (Innsbruck, Austria) by monitoring the oxygen consumption rate at 37ºC [23]. KIC (5 mM), KIV (1 mM) and KMV (1 mM) were added to the incubation medium (20 mM HEPES buffer, pH 7.4, containing 0.11 M sucrose, 10 mM KH_2PO_4, 0.5 mM EGTA, 0.1 mg/mL bovine serum albumin - BSA, 60 mM lactobionate, 20 mM taurine, and 3 mM $MgCl_2$) containing the cerebral cortex crude homogenates (2 mg tissue. mL^{-1}), and the substrate-uncoupler inhibitor titration (SUIT) protocol was applied [24]. The doses of the BCKA used in the present work correspond to those of patients affected by classic MSUD during metabolic decompensation [1, 2, 25, 26]. In this protocol, the medium was supplemented with the NADH-linked respiratory substrates PMG at concentrations of 5 mM, 0.5 mM and 10 mM, respectively, and the $FADH_2$-linked succinate (10 mM). The respiratory parameters state 3 (phosphorylating), state 4 (non-phosphorylating), and uncoupled respirations were measured by additions of ADP (1 mM), oligomycin (1 µg. mL^{-1}), and CCCP (two pulses of 0.5 µM each), respectively. The respiratory control ratio (RCR) was obtained by the quotient of state 3/state 4. The experiments were also carried out in cerebral cortex crude homogenates (8 mg tissue. mL^{-1}) supported by the combination of glutamate plus malate (GM, 2.5 mM each) or pyruvate plus malate (PM, 2.5 mM each) in an incubation medium containing 0.3 M sucrose, 5 mM KH_2PO_4, 1 mM EGTA, 0.1 mg mL^{-1} BSA, and 5 mM MOPS, pH 7.4. Oxygen consumption was quantified in the DatLab 8.0.2 (Oroboros Instruments) and expressed as pmol O_2 flux. s^{-1}. mg of $tissue^{-1}$. We also tested the effect of digitonin (30 µM), which permeabilizes synaptosomal membranes, on respiratory parameters in the presence or absence of 5 mM KIC, using crude cerebral cortex homogenates (2 mg tissue. mL^{-1}) and the SUIT protocol.

ATP Production

ATP production was measured using the firefly luciferin–luciferase assay, according to Lemasters and Hackenbrock [27]. KIC (2 and 5 mM) was added to the incubation medium (20 mM HEPES buffer, pH 7.4, containing 0.11 M sucrose, 10 mM KH_2PO_4, 0.5 mM EGTA, 0.1 mg/mL BSA, 60 mM lactobionate, 20 mM taurine, and 3 mM $MgCl_2$), at 37 °C, containing the cerebral cortex crude homogenates (2 mg tissue. mL^{-1}). The NADH-linked substrates PMG (5, 0.5, and 10 mM, respectively) were used to support respiration. ADP (0.5 mM) was supplemented to the incubation medium to initiate the reaction, which was stopped two minutes later by adding 120 mM $HClO_4$. ATP production was then quantified in a SpectraMax I3 microplate (luminescence mode) and expressed as nmol ATP. min^{-1}. mg of $tissue^{-1}$.

Citric Acid Cycle Enzyme (CAC) Activities

For the determination of citric acid cycle (CAC) enzyme activities, the cerebral cortex from 1-day-old rats was homogeneized (1:10, w: v) in appropriate buffer (250 mM sucrose, 2 mM EDTA, and 10 mM Trizma base, pH 7.4), centrifuged at 750 *g* for 10 min, and the supernatants (homogenates) used in the assays (citrate synthase– CS: 0.015 mg protein.mL^{-1}; mitochondrial NADP-dependent isocitrate dehydrogenase - IDH2: 0.025 mg protein.mL^{-1}; NAD-dependent isocitrate dehydrogenase - IDH3: 0.6 mg protein.mL^{-1}; α-ketoglutarate dehydrogenase - KGDH:

0.9 mg protein.mL^{-1}; malate dehydrogenase - MDH: 0.005 mg protein.mL^{-1}; succinate dehydrogenase - SDH: 0.15 mg protein.mL^{-1}). Before the measurements, the cerebral cortex homogenates were pre-incubated at 37 °C for 30 min in the presence of KIC (5 mM).

The activities of KGDH and IDH3 were determined by following NAD^+ reduction and expressed as nmol NADH. min^{-1}. mg protein^{-1} [28]. IDH1 (cytosolic) plus IDH2 (mitochondrial) activities were assessed in the cortical homogenates by measuring $NADP^+$ reduction and were expressed as nmol NADPH. min^{-1}. mg protein^{-1} [29], whereas MDH1 (cytosolic) plus MDH2 (mitochondrial) activities were determined in the homogenates by following NADH oxidation and were expressed as nmol NAD^+. min^{-1}. mg protein^{-1} [30]. CS activity was assayed by observing 5,5'-dithiobis-(2-nitrobenzoic acid) (DTNB) reduction and expressed as µmol. min^{-1}. mg protein^{-1} [31]. SDH activity was measured following 2,6-dichloroindophenol (DCIP) reduction and expressed as µmol. min^{-1}. mg protein^{-1} [32]. Triton X-100 (0.1%) was used to permabilize synaptosomal and mitochondrial membranes before measuring CAC enzyme activities, except for SDH, for which the samples were subjected to three freeze-thaw cycles.

The activity of KGDH was also evaluated in the presence or absence of calcium (20 µM) using commercially purified KGDH from porcine heart (0.1 unit. mL^{-1}, K1502, Merck), and was expressed as nmol NADH. min^{-1}. unit^{-1}. Furthermore, kinetic analysis of KGDH (absence of calcium) was determined using the purified KGDH from porcine heart (0.1 unit. mL^{-1}, K1502, Merck) in a range of KIC concentrations from 2 to 5 mM and α-ketoglutarate (KG) from 0.15 to 1 mM. The Km, Vmax, and Ki (the dissociation constant of the enzyme-substrate–inhibitor complex) values were calculated using a nonlinear fitting (GraphPad Prism 9.0 software).

Determination of Protein Concentrations

Protein concentrations were measured by the method of Lowry and collaborators [33] with bovine serum albumin as standard.

Statistical Analysis

The normality of data distribution was initially assessed using the Shapiro-Wilk test, which showed a normal distribution pattern. Thus, the statistical analyses were one-way analysis of variance (ANOVA) followed by Tukey's post-hoc test when more than two groups were compared. In contrast, two tailed Student's t-test for unpaired samples was used to compare the two groups. Results were expressed as mean ± standard deviation, and differences were rated significant when $P < 0.05$. All analyses were made using the GraphPad Prism 9.0 software.

Molecular Modeling of KGDH Subunits

Subunit Structural Data Obtainment and Refinement

The subunits from porcine KGDH (E1, E2 and E3) were obtained from the AlphaFold (AF) models disposed at UniProt web server [34] considering the respective identification codes: F1SSH8, Q9N0F1 and P09623. The raw AlphaFold models had their protonation states determined at PDB2PQR web server [35] assuming a pH of 7.4 and AMBER forcefield. The protonated models had their geometry optimized at Yasara web server [36]. The raw AF and final optimized models were validated regarding their Ramachandran plot using the Procheck module [37] of the SAVES web server.

Each subunit required further improvement in its molecular structure, which included: (1) deletion of bad predicted and unmodeled tertiary structures from E2 (1-219) and E3 subunits (1–37); (2) ligand addition and (3) rebuilding of homodimer (E1 and E3 subunits) and homotrimer (E2 subunit) assembly. The refinement was accomplished by using the Matchmaker module of UCSF Chimera [38] to superpose the subunits with similar crystallographic structures disposed at Protein Data Bank (PDB) [39], as follows: (a) the E1 subunit model was superposed to the cryo-electron microscopic structure of human E1 (PDBID: 7WGR; identity: 98.66%; resolution: 2.92 Å); (b) the E2 subunit model was superposed to the cryo-EM homotrimer component (models 1, 5 and 9) from the biological assembly of pyruvate dehydrogenase from Azotobacter vinelandii in the "OUT" conformation (PDBID: 1EAB; identity: 34.16%; resolution: 2.60 Å), which allows the proper binding of substrate and cofactor without steric clashes [40]; (c) the E3 subunit model was superposed to the crystal structure of human dihydrolipoamide dehydrogenase (PDB: 1ZMD; identity: 96.41%; resolution: 2.08 Å). The final models were finally optimized using the Yasara web server and validated using the Procheck module from the SAVES web server.

Molecular Docking Simulations

The simplified molecular-input line-entry system (SMILES) notations of KIC and ethylmalonic acid (EMA) were obtained from PubChem web server [41] and their protonation states were determined by OpenBabel 2.3.2 [42] considering a pH of 7.4. EMA was used as a comparison compound because it exhibited inhibitory activity towards KGDH [43] and possesses a chemical structure similar to KIC. The tridimensional structures of both compounds

were modeled in Spartan'14 1.1.8 regarding a geometry optimization using MMFF forcefield followed by the PM6 semi-empirical method. Some co-crystallized compounds were used for validation and comparison purposes: (a) in the E1 subunit were used thiamine pyrophosphate (TPP) and enamine-TPP intermediate (TD7); (b) in the E2 subunit were used Coenzyme A (COA) and dihydrolipoamide (DHLPM); (c) in E3 subunit were used NADH and $FADH_2$.

The molecular docking protocols were performed at UCSF Chimera. The targets and the compounds had their charges added by the DockPrep module using Gasteiger charges. After the preparation, the docking was accomplished through Autodock Vina [44] with the grid location and size parameters described in Supplementary Table S1. The docking parameters were set as several modes equal to 10, exhaustiveness equal to 8, and an energy range of 3. The docking protocol was validated through redocking when the co-crystallized compound was available, considering a root mean square deviation (RMSD) cut-off of 2.0 Å for compounds with less than 5 rotatable bonds and 3.0 Å for compounds with more than 5 rotatable bonds. The poses of each ligand were visually examined and selected by means of the score and based on fundamental residue interactions deemed crucial for target inhibition, as outlined in literature and through comparison with crystallographic ligands. The figures were represented with PyMol 3.0.0 and Discovery Studio Visualizer 21.1.0.20298.

Binding Site Studies and Blind Docking Simulations

The binding site studies of the modeled KGDH subunits were conducted by DoGSiteScorer [45] and through FTMap [46] web servers. DoGSiteScorer identifies potential binding sites in the protein's three-dimensional structure using a grid-based method, which applies a Gaussian difference filter to calculate properties related to the size, shape, and chemical features. Finally, the program correlates these variables using a support vector machine to calculate a drug score (0 to 1), where higher values indicate a greater possibility of fitting. Meanwhile, FTMap maps the interacting regions of the protein and the 16 probes. These probes are docked through a rigid body approach that uses the fast Fourier transform correlation approach to accelerate the calculations. The subsequent poses are then measured using a detailed energy expression that includes van der Waals repulsion and attraction terms and electrostatic interaction energy based on Poisson-Boltzmann calculations. Finally, the poses are minimized and grouped into a specific consensus site (consensus site, CS).

Blind docking simulations were accomplished for all the modeled KGDH subunits and KIC through the ReverseDock web server [47]. The program executes a docking protocol via Autodock Vina with an automatically generated simulation box holding the respective target (a maximum of 1000 amino acids) and assuming an exhaustiveness of 64. Therefore, a modified version of chain A from the E1 subunit (120–1035) was used for the blind docking simulation.

The figures were represented with PyMol 3.0.0 and Discovery Studio Visualizer 21.1.0.20298.

Results

KIC Decreases Mitochondrial Oxygen Consumption in the Cerebral Cortex of Neonate Rats

We first investigated the in vitro effects of KIC (5 mM), KIV (1 mM), and KMV (1 mM) on respiratory parameters in cerebral cortex homogenates using the SUIT protocol. Fig. 1 shows that KIC significantly decreased state 3 respiration supported by NADH-linked substrates (PMG) [$F_{(3,20)}=13.14$, $P<0.001$], pointing to a metabolic inhibitory behavior. This effect was much less intense when succinate was added to the medium (PMG+S). State 4 and uncoupled respirations supported by PMG+S were not affected by KIC. Finally, none of these parameters were altered by KIV and KMV, suggesting a selective effect of KIC.

We also evaluated whether digitonin (30 µM) could change the respiratory parameters in the presence or absence of 5 mM KIC using crude cerebral cortex homogenates and the SUIT protocol. Digitonin permeabilizes the synaptosomes present in the cerebral homogenates. As shown in Fig. 2, the presence of digitonin only slightly increased the state 3 respiration in the control condition (absence of KIC). Furthermore, the extent of KIC-induced inhibition on mitochondrial respiration remained unchanged, reinforcing the inhibitory effect of this major accumulating organic acid [state 3 PMG: $F_{(3,20)}=42.49$, $P<0.001$; state 3 PMG+S: $F_{(3,20)}=12.49$, $P<0.001$] (Fig. 2).

To better clarify the KIC-induced alterations on mitochondrial respiration, we tested the effects of KIC on respiratory parameters in cerebral cortex homogenates using GM (Fig. 3) or PM (Fig. 4) as substrates. It can be seen in the figures that KIC reduced the state 3 and uncoupled respirations and the RCR using both GM [state 3: $t_{(8)}=3.18$, $P<0.05$; uncoupled: $t_{(8)}=2.782$, $P<0.05$; RCR: $t_{(8)}=4.839$, $P<0.01$] or PM [state 3: $t_{(10)}=3.451$, $P<0.01$; uncoupled: $t_{(10)}=4.522$, $P<0.01$; RCR: $t_{(10)}=7.316$, $P<0.001$], besides increasing state 4 respiration [GM: $t_{(8)}=2.422$, $P<0.05$; PM: $t_{(10)}=3.303$, $P<0.01$]. These results corroborate that KIC behaves as a metabolic inhibitor by impairing the oxidation of NADH-linked substrates in the cerebral cortex of neonate rats and show a mild uncoupling action of KIC with the mitochondrial respiring substrates PM.

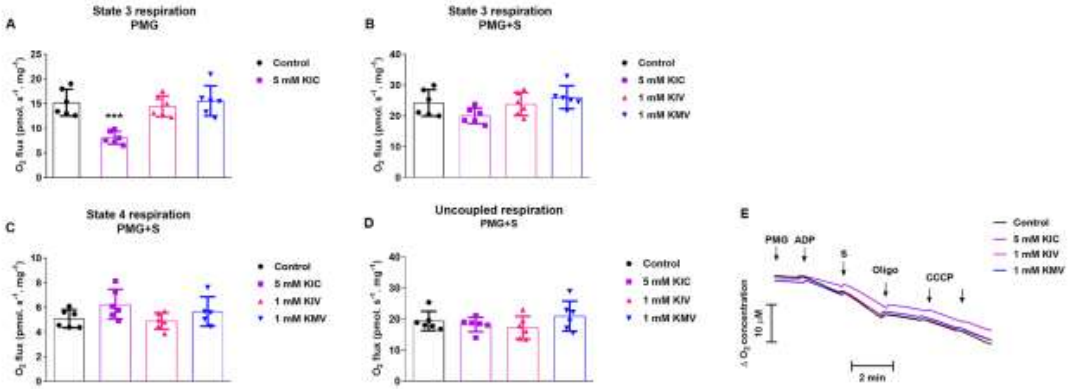


Fig. 1 Effects of α-ketoisocaproic acid (KIC), α-ketoisovaleric acid (KIV), and α-keto-β-methylvaleric acid (KMV) on respiratory parameters in cerebral cortex homogenates using the substrate-uncoupler inhibitor titration (SUIT) protocol. State 3 respiration (phosphorylating) (**A** and **B**), state 4 respiration (non-phosphorylating) (**C**), and uncoupled respiration (CCCP-stimulated) (**D**). Cerebral cortex homogenates (2 mg tissue. mL^{-1}) and KIC (5 mM), KIV (1 mM), or KMV (1 mM) were added to the incubation medium containing pyruvate (5 mM), malate (0.5 mM), and glutamate (10 mM) (PMG), which was later supplemented with succinate (10 mM) (PMG + S). Controls were performed in the absence of these organic acids. (**E**) Representative traces of the respiratory parameters measured by oxygen consumption. PMG (5 mM, 0.5 mM and 10 mM), ADP (1 mM), S (10 mM), oligomycin A (Oligo, 1 µg/mL), and CCCP (two pulses of 0.5 µM) were added as indicated by the arrows. Values are means ± standard deviation for five to six animals (N) performed in duplicates and are expressed as pmol O_2. s^{-1}. mg of $tissue^{-1}$. ***$P<0.001$ compared to Control (Tukey's range test)

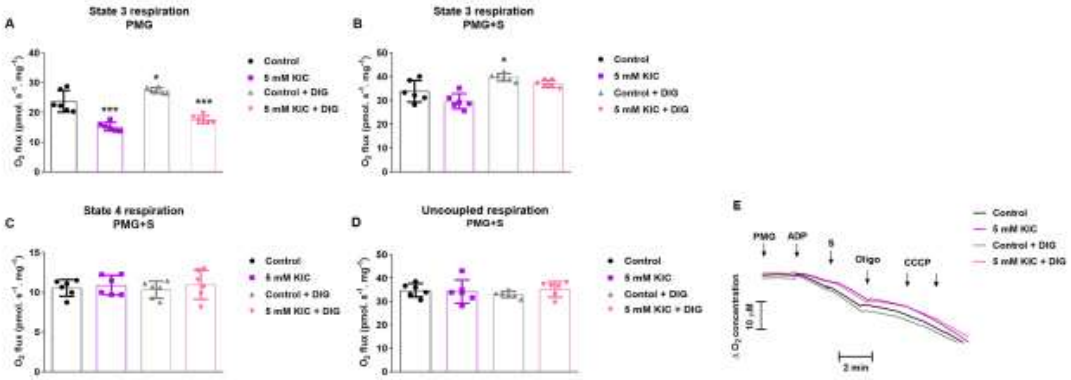


Fig. 2 Effects of α-ketoisocaproic acid (KIC) on respiratory parameters in cerebral cortex homogenates in the presence or absence of digitonin (DIG) using the substrate-uncoupler inhibitor titration (SUIT) protocol. State 3 respiration (phosphorylating) (**A** and **B**), state 4 respiration (non-phosphorylating) (**C**), and uncoupled respiration (CCCP-stimulated) (**D**). Cerebral cortex homogenates (2 mg tissue. mL^{-1}) and KIC (5 mM) and DIG (30 µM) were added to the incubation medium containing pyruvate (5 mM), malate (0.5 mM), and glutamate (10 mM) (PMG), which was later supplemented with succinate (10 mM) (PMG + S). Controls were performed in the absence of KIC. (**E**) Representative traces of the respiratory parameters measured by oxygen consumption. PMG (5 mM, 0.5 mM and 10 mM), ADP (1 mM), S (10 mM), oligomycin A (Oligo, 1 µg/mL), and CCCP (two pulses of 0.5 µM) were added as indicated by the arrows. Values are means ± standard deviation for six animals (N) performed in duplicates and are expressed as pmol O_2. s^{-1}. mg of $tissue^{-1}$. *$P<0.05$, ***$P<0.001$ compared to Control (Tukey's range test)

KIC Decreases ATP Production in the Cerebral Cortex of Neonate Rats

Next, we determined the effects of KIC on ATP production in cerebral cortex homogenates from neonate rats supported by PMG substrates. We observed that KIC significantly decreased ATP production (Fig. 5) [$F_{(3,16)}=72.01$, $P<0.001$] in a dose-dependent manner ($\beta=0.6326$, $P<0.001$), indicating mitochondrial bioenergetics failure and cell energy deprivation.

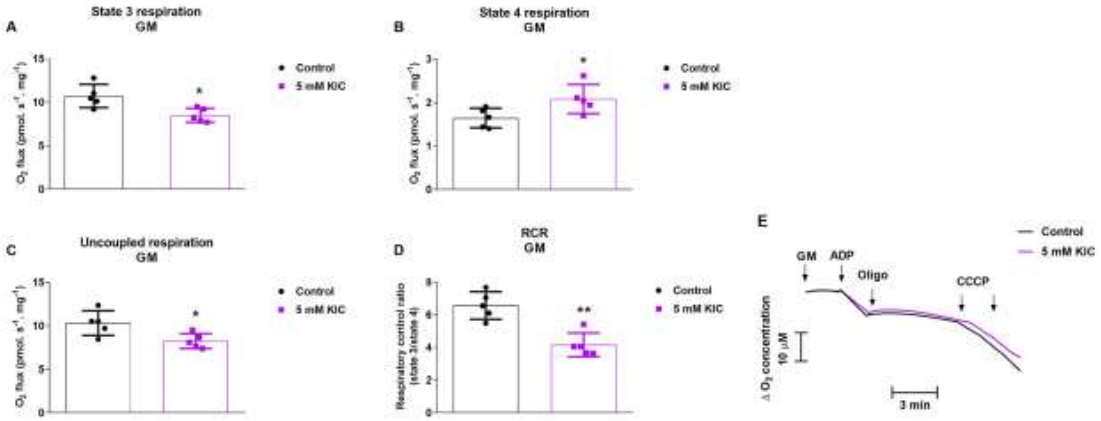


Fig. 3 Effects of α-ketoisocaproic acid (KIC) on respiratory parameters in cerebral cortex homogenates supported by glutamate plus malate. State 3 respiration (phosphorylating) (**A**), state 4 respiration (non-phosphorylating) (**B**), uncoupled respiration (CCCP-stimulated) (**C**), and respiratory control ratio (RCR, state 3/state 4) (**D**). Cerebral cortex homogenates (8 mg tissue. mL^{-1}) and KIC (5 mM) were added to the incubation medium containing glutamate plus malate (GM, 2.5 mM each) as substrates. Controls were performed in the absence of KIC. (**E**) Representative traces of the respiratory parameters measured by oxygen consumption. GM (2.5 mM each), ADP (1 mM), oligomycin A (Oligo, 1 µg/mL), and CCCP (two pulses of 0.5 µM) were added as indicated by the arrows. Values are means ± standard deviation for five animals (N) performed in duplicates and are expressed as pmol O_2. s^{-1}. mg of $tissue^{-1}$. $^{*}P<0.05$, $^{**}P<0.01$ compared to Control (Student's *t*-test)

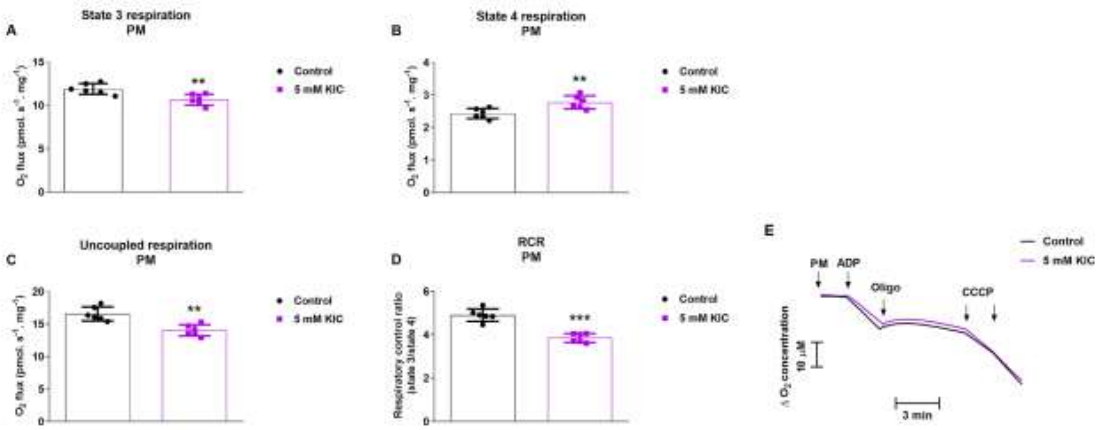


Fig. 4 Effects of α-ketoisocaproic acid (KIC) on respiratory parameters in cerebral cortex homogenates supported by pyruvate plus malate. State 3 respiration (phosphorylating) (**A**), state 4 respiration (non-phosphorylating) (**B**), uncoupled respiration (CCCP-stimulated) (**C**), and respiratory control ratio (RCR, state 3/state 4) (**D**). Cerebral cortex homogenates (8 mg tissue. mL^{-1}) and KIC (5 mM) were added to the incubation medium containing pyruvate plus malate (PM, 2.5 mM each) as substrates. Controls were performed in the absence of KIC. (**E**) Representative traces of the respiratory parameters measured by oxygen consumption. PM (2.5 mM each), ADP (1 mM), oligomycin A (Oligo, 1 µg/mL), and CCCP (two pulses of 0.5 µM) were added as indicated by the arrows. Values are means ± standard deviation for six animals (N) performed in duplicates and are expressed as pmol O_2. s^{-1}. mg of $tissue^{-1}$. $^{**}P<0.01$, $^{***}P<0.001$ compared to Control (Student's *t*-test)

KIC Inhibits KGDH Activity in the Cerebral Cortex of Neonate Rats

We also tested the effects of KIC on the activity of the CAC enzymes CS, IDH1 (cytosolic) plus IDH2 (mitochondrial), IDH3, KGDH, SDH, and MDH1 (cytosolic) plus MDH2 (mitochondrial) in cerebral cortex homogenates from neonate rats. KIC markedly inhibited KGDH activity [$t_{(10)}=9.433$, $P<0.001$] without altering the other enzyme activities (Fig. 6). The effect of KIC on the activity of a commercially highly purified KGDH was further tested in the presence or absence of 20 µM calcium. Overall, higher

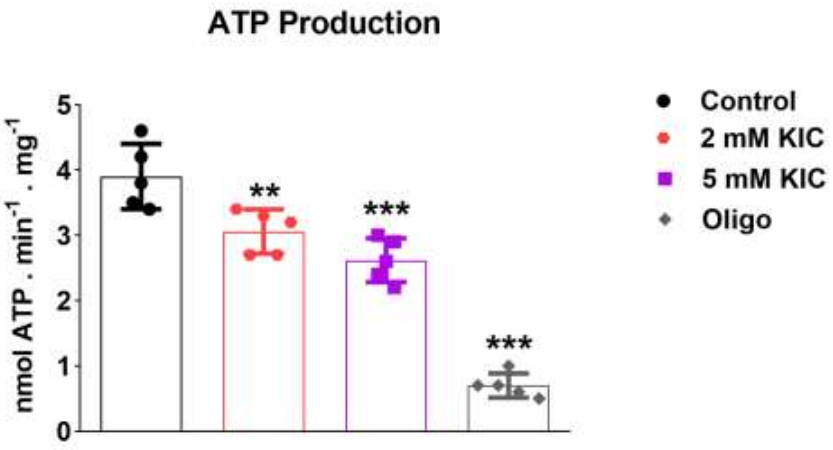


Fig. 5 Effects of α-ketoisocaproic acid (KIC) on ATP production in cerebral cortex homogenates. Experiments were performed in an incubation medium containing cerebral cortex homogenates (2 mg tissue. mL^{-1}) supported by pyruvate (5 mM), malate (0.5 mM), and glutamate (10 mM). KIC (2 and 5 mM) was added at the assays' beginning. The reaction was started by the addition of ADP (0.5 mM). Controls were performed in the absence of KIC. Oligomycin A (Oligo, 1 µg. mL^{-1}) was a positive control. Values are means ± standard deviation for five animals (N) performed in duplicates and are expressed as nmol ATP. min^{-1}. mg of $tissue^{-1}$. $^{**}P<0.01$, $^{***}P<0.001$ compared to Control (Tukey's range test)

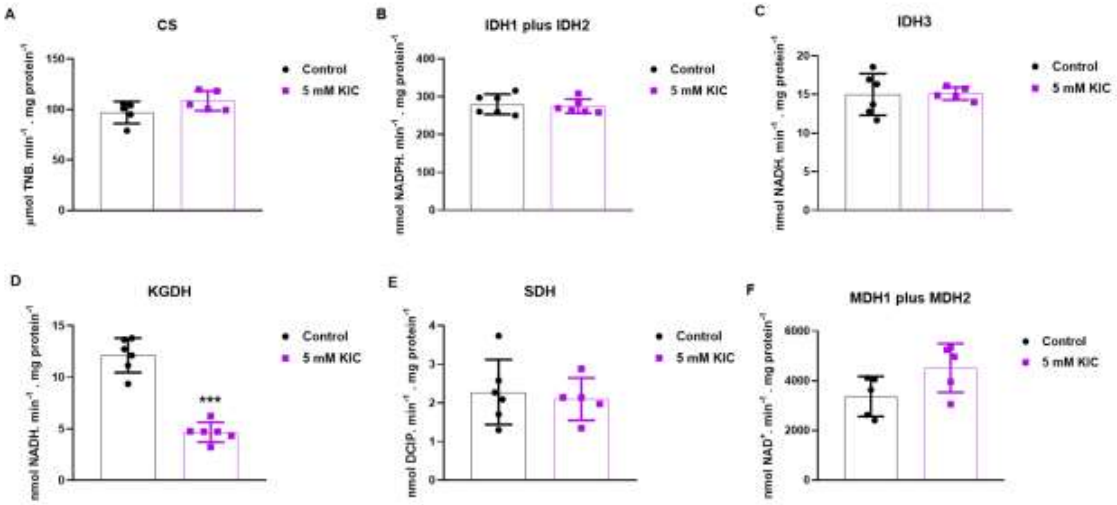


Fig. 6 Effects of α-ketoisocaproic acid (KIC) on citric acid cycle (CAC) enzymes activities in cerebral cortex homogenates. The activities of citrate synthase (CS, **A**), cytosolic and mitochondrial NADP-dependent isocitrate dehydrogenase (IDH1 plus IDH2, **B**), NAD-dependent isocitrate dehydrogenase (IDH3, **C**), α-ketoglutarate dehydrogenase (KGDH, **D**), succinate dehydrogenase (SDH, **E**), cytosolic and mitochondrial malate dehydrogenase (MDH1 plus MDH2, F) were measured in cerebral cortex homogenates pre-incubated in the presence of KIC (5 mM) for 30 min. Controls did not contain KIC in the incubation medium. Values are means ± standard deviation for five to six animals (N) performed in duplicates or triplicates and are expressed as µmol or nmol. min^{-1}. mg of $protein^{-1}$. $^{***}P<0.001$ compared to Control (Student's *t*-test)

KGDH activities were observed with the purified enzyme (Fig. 7). This figure also shows that KIC-induced inhibition of KGDH activity was similar in both calcium-free medium and medium supplemented with 20 µM calcium [$F_{(3,20)}=149.5$, $P<0.001$].

Kinetic analysis using commercially purified KGDH was performed on a concentration range of KG from 0.15 to 1 mM to determine the KIC-induced inhibition profile of this enzyme. The Lineweaver–Burk double-reciprocal graph showed that this inhibition was noncompetitive, with

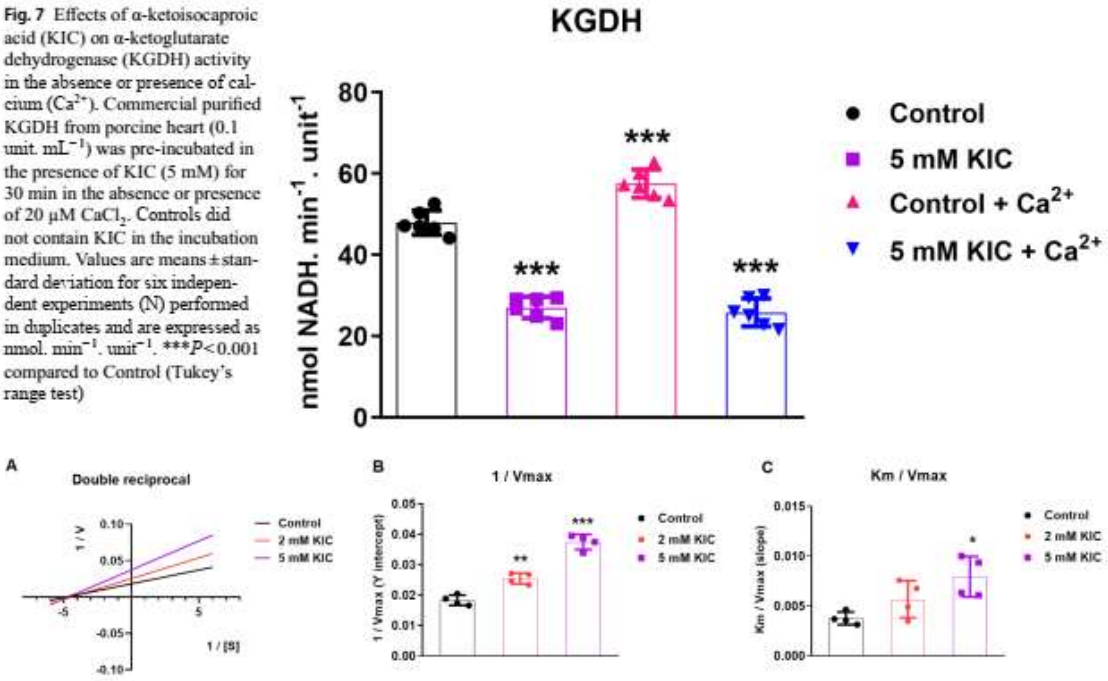


Fig. 7 Effects of α-ketoisocaproic acid (KIC) on α-ketoglutarate dehydrogenase (KGDH) activity in the absence or presence of calcium (Ca^{2+}). Commercial purified KGDH from porcine heart (0.1 unit. mL^{-1}) was pre-incubated in the presence of KIC (5 mM) for 30 min in the absence or presence of 20 µM $CaCl_2$. Controls did not contain KIC in the incubation medium. Values are means ± standard deviation for six independent experiments (N) performed in duplicates and are expressed as nmol. min^{-1}. $unit^{-1}$. ***$P<0.001$ compared to Control (Tukey's range test)

Fig. 8 Kinetic analysis of the α-ketoisocaproic acid (KIC)-induced inhibition of α-ketoglutarate dehydrogenase (KGDH) activity. A commercial purified KGDH from porcine heart (0.1 unit. mL^{-1}) was used in the assays. The graph displays a double-reciprocal plot of KGDH activity (nmol NADH. min^{-1}. $unit^{-1}$) for α-ketoglutarate (0.15–1 mM) [S] in the absence (Control) or presence of 2 and 5 mM KIC showing a noncompetitive profile of inhibition (A). All experiments were repeated four times (N) in triplicates, and the means of 1/Vmax (Y intercept) and Km/Vmax (slope) obtained by nonlinear regression were used to construct the Lineweaver-Burk graph. Raw kinetic data are provided in panels B (1/Vmax, Y intercept) and C (Km/Vmax, slope). *$P<0.05$, **$P<0.01$, ***$P<0.001$ compared to Control (Tukey's range test)

Vmax values of 54.92±4.99 (control), 39.46±2.83 (2 mM KIC) and 26.8±1.86 (5 mM KIC) nmol NADH. min^{-1}. $unit^{-1}$, without significantly altering the Km values (control = 0.21±0.052 mM; 2 mM KIC = 0.22±0.077 mM; 5 mM KIC = 0.21±0.060 mM) (Fig. 8). Moreover, the obtained Ki value for KIC, representing the dissociation constant of the enzyme-substrate–inhibitor complex, was 4.91±1.27 mM.

Molecular Modeling of KGDH Subunits

Subunit Structural Data Refinement

Next, we conducted in silico studies to support our in vitro biochemical data, demonstrating that KIC-induced inhibition of KGDH activity occurs noncompetitively and potentially identifies KIC binding sites on KGDH.

The subunit models built by AlphaFold displayed reasonable Ramachandran plot distribution, as seen in Table 1. All the raw models showed residues occupation close to 90% in the most favored region, except for the E2 subunit, which displayed 82.4% of residues in the most favored region. The following steps in the model refinement included protonation state definition and geometry optimization. For all the subunit models, the geometry optimization performed at Yasara web server improved the torsional angles of amino acid residues to the most favored regions. Moreover, it can be noticed that for E1 and E3 models, the optimization enhanced the most favored values above the cut-off of 90%, which is considered the reference for suitable crystallographic structures. The final procedures involved the removal of inadequate secondary structures at the very beginning of the models, such as unmodeled loops and the dimeric and trimeric structures. It was observed that the amino acid removal further improved the models, whereas the reconstruction of the dimeric and trimeric composition has kept the amino acid disposition strong.

Molecular Docking Simulations

The molecular docking simulations were validated through redocking for the three KGDH subunits according to Supplementary Table S1. The protocols for each target produced RMSD values that met the criteria, with at least one pose falling below the 2.0 Å cut-off for the E1 and E3

Table 1 Ramachandran plot distribution of the raw and minimized models for each KGDH subunit

E1 Subunit			Ramachandran plot (%)			
Name: Chain	Processing level	Residues	Most favored	Additional allowed	Generously allowed	Disallowed
AF-F1SSH8-F1:A	Raw	1-1035	89.0	9.5	0.9	0.7
AF-F1SSH8-F1:AB	Minimized	1-1035	89.9	9.1	0.4	0.6
E2 Subunit			**Ramachandran plot (%)**			
Name: Chain	**Processing level**	**Residues**	**Most favored**	**Additional allowed**	**Generously allowed**	**Disallowed**
AF-Q9N0F1-F1:A	Raw	1-455	82.4	13.0	1.8	2.8
AF-Q9N0F1-F1:A	Minimized	1-455	87.8	9.6	0.8	1.8
AF-Q9N0F1-F1:A	Minimized	220–455	94.8	5.2	0.0	0.0
AF-Q9N0F1-F1:ABC	Minimzed	220–455	94.0	6.0	0.0	0.0
E3 Subunit			**Ramachandran plot (%)**			
Name: Chain	**Processing level**	**Residues**	**Most favored**	**Additional allowed**	**Generously allowed**	**Disallowed**
AF-P09623-F1:A	Raw	1-509	88.9	9.7	0.7	0.7
AF-P09623-F1:A	Minimized	1-509	91.0	8.1	0.5	0.5
AF-P09623-F1:A	Minimized	37–509	92.8	7.2	0.0	0.0
AF-P09623-F1:AB	Minimized	37–509	92.8	7.2	0.0	0.0

AF: AlphaFold

Table 2 Best ligand docking simulations performed in the α-ketoglutarate dehydrogenase (KGDH) subunits E1, E2 and E3

Subunit	Binding site	Ligand name	Vinascore (kcal/mol)
E1	TPP site	TD7	-11.0
		TPP	-10.3
		EMA	-5.6
		KIC	-5.3
	KG site with TPP	Best scored KG	-3.5
		EMA	-3.4
		Best posed KG	-2.9
		KIC	-2.7
E2	COA site	COA	-7.5
		EMA	-3.8
		KIC	-3.8
	DHLPM site	KIC	-4.2
		Best scored DHLPM	-4.1
		EMA	-4.0
		Best posed DHLPM	-3.9
E3	FAD site	FAD	-13.8
		EMA	-5.2
		KIC	-5.2
	NADH site	NADH	-10.7
		KIC	-4.7
		EMA	-4.4
	DHLPM site	LPM	-6.0
		DHLPM	-5.7
		EMA	-5.3
		KIC	-5.2

COA: Coenzyme A; DHLPM: Dihydrolipoamide; EMA: Ethylmalonic acid; FAD: Oxidized flavin adenine dinucleotide; KG: α-Ketoglutarate; KIC: α-Ketoisocaproic acid; LPM: lipoamide; NADH: Reduced nicotinamide adenine dinucleotide; TD7: Enamine-TPP intermediate; TPP: Thiamine pyrophosphate

subunits. For the E2 subunit, one ligand (COA) overcomes the limit with a minimum RMSD value of 2.8 Å. Therefore, the protocols were considered suitable for molecular docking simulations.

The docking assays performed in the three KGDH subunits were evaluated mainly at substrate and cofactor binding sites (Table 2 and Supplementary Table S1). The docking scores obtained by Autodock Vina suggest that KIC may interact preferably with the binding sites related to DHLPM of E2 and E3 subunits, which showed values of -4.2 and −5.2, respectively. Moreover, the results suggested that KIC may not interact appropriately with the other binding sites since most of the compared ligands (substrates and cofactors) showed higher scoring values. The poses found for KIC at both DHLPM binding sites are depicted in Fig. 9A and B, compared to DHLPM Fig. 9C and D. The interaction profile found for KIC in the E2 subunit, considering the DHLPM binding site, revealed a similar pattern as compared to DHLPM concerning two interactions: a hydrogen bond interaction with Ile387 and a van der Waals interaction with Leu329, both residues from the B chain. Regarding the E3 subunit, KIC displayed a different pattern as compared to DHLPM, interacting mainly through van der Waals interactions, while DHLPM performed two hydrogen bonds with Gly77 from chain A and His487 from chain B; however, KIC showed an electrostatic interaction with Arg495 from the B chain, which may compensate the interaction value obtained by Autodock Vina.

Taken together, the analyses obtained from the molecular docking simulations indicate that KIC may potentially interact with E2, particularly with E3 subunits, at the DHLPM binding site.

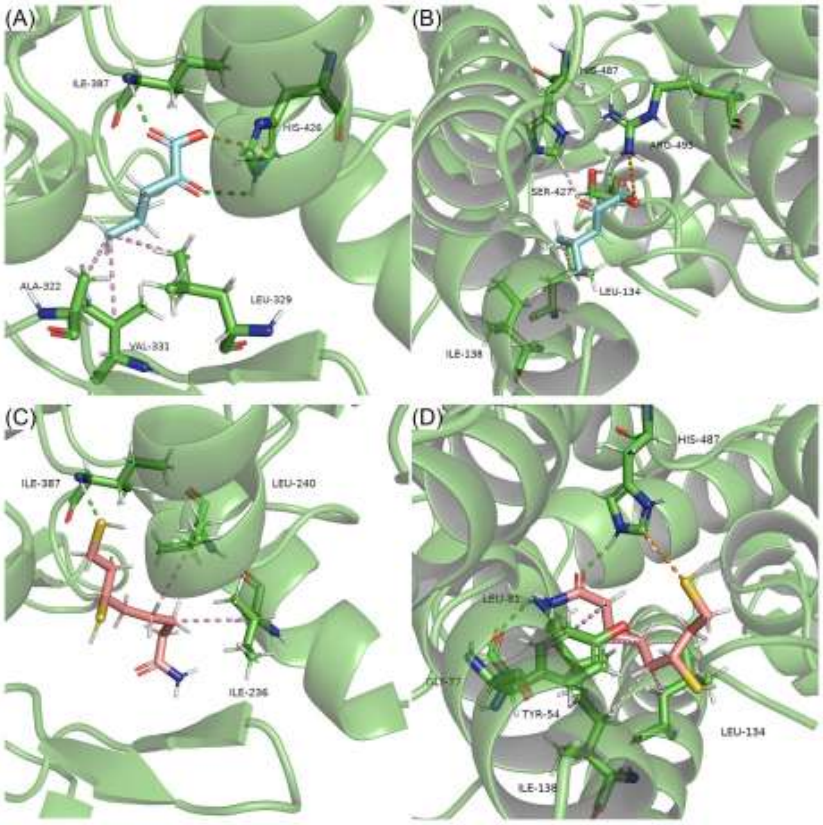


Fig. 9 Interaction profile for KIC (cyan carbons sticks) and DHLPM (salmon carbons sticks) at KGDH subunits. (**A**) KIC at the E2 subunit, (**B**) KIC at the E3 subunit, (**C**) DHLPM at the E2 subunit, and (**D**) DHLPM at the E3 subunit. Interactions legend: green (hydrogen bonds); pink (van der Waals); dark orange (electrostatic); orange (sulfur-π)

Binding Site Studies and Blind Docking Simulations

Next, a further investigation was carried out to evaluate other potential binding sites by the simultaneous analyses on three distinct web servers: DoGSiteScorer and FTMap for binding site characterization and Reverse Dock for blind docking simulations. The detailed data are described in Supplementary Table S2.

Regarding the binding site characterization, the best-characterized pocket of the E1 subunit was P1, which showed low hydrophobicity and a volume of 1843 $Å^3$. Furthermore, most KIC poses were predicted to bind at the P1 pocket, which is the orthosteric site for TPP and KG (Supplementary Fig. 1A). The analyses of the E2 subunit revealed three large pockets (P0, P1, and P3) associated with each monomer characterizing the DHLPM and part of COA sites from the three chain monomers (Supplementary Fig. 1B). The Reverse Dock approach fitted KIC preferentially in P3 with 4 poses with scores ranging from −4.1 to -4.0 kcal/mol. Accordingly, the docking simulations (blind and local docking) found the orthosteric site (DHLPM and COA pockets) to be the most favorable. Regarding the E3 subunit, the second largest pocket, P1 (1422 Å3), was the best characterized among the fourteen mapped. This pocket contains the FAD binding site and involves the nicotinamide moiety from NAD (Supplementary Fig. 1C).

Taken together, the analyses obtained from the blind docking simulations indicate that KIC may preferentially interact with an allosteric site of E1 (P10), the DHLPM site of E2 (P3), and the FAD site of E3 (P1).

Discussion

MSUD is a severe inherited metabolic disorder clinically characterized by potentially lethal encephalopathy associated with acute brain edema in the first days of life. Long-term neurological sequelae affecting the cerebral cortex and basal ganglia are manifested in patients who survive the neonatal period. Although the pathogenesis of acute and chronic brain injury in MSUD is still under debate, it is believed brain accumulation of KIC, one of the most neurotoxic metabolites in MSUD, may play a significant role. In this regard, previous studies have shown that KIC

compromises brain mitochondrial functions in vitro [19–21] and in vivo [48] in experiments performed using adult animals, and this may represent a mechanism of KIC neurotoxicity. However, practically nothing has been reported about the effects of KIC on bioenergetics in the brains of neonatal animals. Indeed, it seems relevant to investigate the impact of KIC on mitochondrial functions in the neonate brain, given that MSUD patients exhibit severe neurological dysfunction in the first days of life. Therefore, in this study, we evaluated the in vitro influence of KIC on mitochondrial respiration using different substrates, ATP production, and CAC enzyme activities in the cerebral cortex of neonatal rats.

We initially investigated mitochondrial respiratory parameters in cerebral cortex homogenates using the SUIT protocol, allowing us to sequentially assess different coupling states with various substrates in the mitochondrial cell microenvironment. Our data demonstrated that KIC inhibited the phosphorylating respiration supported by PMG, which was attenuated by adding succinate, indicating impairment of the mitochondrial metabolism of NADH-linked substrates. We also found that KIC significantly decreased ATP production in cerebral cortex homogenates supported by PMG, which may be possibly related to the decrease of mitochondrial respiration caused by this organic acid, ultimately leading to energy deprivation.

To better characterize KIC-induced disruption of cell respiration, we also measured the mitochondrial respiratory parameters in cerebral cortex homogenates supported by GM or PM as substrates. We found that KIC inhibited phosphorylating and uncoupled respirations using both combinations of respiratory substrates, confirming its metabolic inhibitory behavior and impairing the metabolism of NADH-linked substrates. These later experiments also revealed that KIC increased non-phosphorylation respiration and decreased RCR, suggesting a mild uncoupling activity. It should be noted that a sustained uncoupler effect might also be involved in the KIC-induced impairment of ATP synthesis. These results are in accordance with a previous study using brain mitochondria from 30-day-old rats [19].

Furthermore, KIC selectively and markedly inhibited the activity of KGDH noncompetitively without changing the activities of CS, IDH1 (cytosolic) plus IDH2 (mitochondrial), IDH3, SDH, MDH1 (cytosolic) plus MDH2 (mitochondrial) in cortical homogenates. Of note, KIC-induced decrease in KGDH activity was previously reported using brain mitochondria from young [19, 49] and adult [49] rats. The molecular modeling results revealed that KIC preferentially interacts with E2 and E3 subunits of KGDH at the DHLPM binding site, as shown by the molecular docking analyses. Other potential binding sites obtained from blind docking simulations suggest that KIC could also interact with an allosteric site of E1 with a similar docking score achieved for the local docking approach for the orthosteric site of E3 (DHLPM), as well as into the DHLPM site of E2 and the FAD site of E3. These data support our in vitro findings, which show that KIC inhibits KGDH non-competitively. In addition, KIC presented results similar to those of EMA [43], particularly regarding the interaction with the E1 catalytic site of the KGDH complex, reinforcing that KIC may not interact with this enzyme through a competitive binding mode. Nevertheless, the exact location of the KIC binding site, considering a noncompetitive inhibition, must be further characterized by experimental methods such as X-ray crystallography.

Since KGDH is a key CAC regulatory enzyme, it is feasible that the KIC-induced inhibition of KGDH may contribute to the alterations of mitochondrial respiration and particularly to the reduction of energy production caused by this organic acid. KGDH is also known to provide NADH for oxidative phosphorylation, and reduction of this enzyme activity was also associated with neurochemical pathological conditions, including oxidative stress induction [50–52], disruption of calcium homeostasis [53], glutamate-mediated neurotoxicity [54] and disturbed neurogenesis [51]. Accordingly, the diminution of KGDH activity has been related to neurodegenerative disorders, such as Alzheimer's disease [55–57]. Additionally, the effects of KIC on mitochondrial bioenergetics described here may also be associated with the inhibition of PDH activity by this compound, as observed in previous works [20, 58]. Since KGDH and PDH share a similar architecture, including a E3 subunit [59, 60] our docking simulation data suggest that KIC may also interact with PDH, particularly with its E3 subunit.

Our present findings are supported by other reports showing bioenergetics failure in MSUD patients, such as elevation of lactate concentrations [61–64] and decreased creatine levels [5, 61] in the brain, as well as lactic acidosis during metabolic crises in MSUD patients [65]. Additionally, the alterations of mitochondrial functions observed in fibroblasts of MSUD patients [66] and studies performed in the mouse model of the disease showed elevated concentrations of lactate and KG and decreased levels of pyruvate, phosphocreatine and ATP in the brain [67] support our present in vitro data of bioenergetics failure in MSUD.

Energy deprivation in the neonatal mammalian brain may impair neurotransmission and compromise neurogenesis, axonal and dendritic proliferation, and myelination, severely damaging brain development [68]. Although the pathophysiological relevance of our present data is uncertain because cerebral levels of KIC were not yet determined in MSUD, the KIC-induced mitochondrial bioenergetics deficiency may underscore the significance of our findings,

given that similar levels of KIV used in our study correspond to those found in the plasma of patients. Therefore, bioenergetics failure may be implicated in the acute and long-term neurological damage that frequently affects these individuals [1].

Conclusion

To the best of our knowledge, we demonstrate solid data showing disruption of brain bioenergetics provoked by pathological concentrations of KIC in the neonatal rat brain for the first time. In case our data can be extrapolated to the human condition, it is suggested that this pathomechanism may be involved in the pathogenesis of brain damage in MSUD during the newborn period, particularly in situations of metabolic decompensation crises where the blood and tissue levels of KIC dramatically increase [1].

Supplementary Information The online version contains supplementary material available at https://doi.org/10.1007/s11064-024-04328-0.

Author Contributions A.B.Z.: Investigation; Formal analysis; Methodology. R.T.R.: Investigation; Methodology. G.M.N.: Investigation; Methodology. S.A.C.: Investigation; Methodology. T.Q.T.: Investigation; Methodology. A.V.S.C.: Investigation; Methodology. C.A.N.: Investigation; Methodology. R.F.C.: Conceptualization; Writing– Review & Editing. M.W.: Conceptualization; Funding Acquisition; Project Administration; Supervision; Writing– Review & Editing. A.U.A.: Conceptualization; Funding Acquisition; Project Administration; Supervision; Writing– Original Draft Preparation.

Funding This work was supported by grants from Conselho Nacional de Desenvolvimento Científico e Tecnológico (CNPq, 402440/2021-8), Fundação de Amparo à Pesquisa do Estado do Rio Grande do Sul (FAPERGS, 24/2551-0001395-4), Fundação de Amparo à Pesquisa do Estado de São Paulo (FAPESP, 17/17728-8 and 23/00229-0), Instituto Nacional de Ciência e Tecnologia– Excitotoxicidade e Neuroproteção (INCT-EN, 465671/2014–4) and Instituto Nacional de Ciência e Tecnologia– Saúde Cerebral (INCT-SC, 406020/2022-1).

Data Availability The datasets generated and/or analysed during the current study are available from the corresponding author on reasonable request.

Declarations

Ethical Approval This research was conducted according to the National Research Council's Guide for the Care and Use of Laboratory Animals (8th edition, National Academies Press). Additionally, the experimental procedures received approval from the Ethics Committee on the Use of Animals at UFRGS (nº 42875).

Competing Interests The authors declare no competing interests.

References

1. Chuang DT, Shih VE, Wynn RM (2019) Maple syrup urine disease (branched-Chain Ketoaciduria). In: Valle DL, Antonarakis S, Ballabio A, Beaudet AL, Mitchell GA (eds) The online metabolic and molecular bases of inherited disease. McGraw-Hill, New York City (NY), pp 1–74
2. Strauss KA, Puffenberger EG, Carson VJ (2020) Maple syrup urine disease. In: Adam MP, Ardinger HH, Pagon RA, Wallace SE, Bean LJ, Mirzaa G, Amemiya A (eds) GeneReviews® [Internet]. University of Washington, Seattle (WA), pp 1–33
3. Chen T, Lu D, Xu F et al (2023) Newborn screening of maple syrup urine disease and the effect of early diagnosis. Clin Chim Acta 548:117483. https://doi.org/10.1016/J.CCA.2023.117483
4. Li L, Mao X, Yang N et al (2023) Identification of gene mutations in six Chinese patients with maple syrup urine disease. Front Genet 14:1132364. https://doi.org/10.3389/FGENE.2023.1132364
5. Muelly ER, Moore GJ, Bunce SC et al (2013) Biochemical correlates of neuropsychiatric illness in maple syrup urine disease. J Clin Invest 123:1809–1820. https://doi.org/10.1172/JCI67217
6. Strauss KA, Carson VJ, Soltys K et al (2020) Branched-chain α-ketoacid dehydrogenase deficiency (maple syrup urine disease): treatment, biomarkers, and outcomes. Mol Genet Metab 129:193–206. https://doi.org/10.1016/J.YMGME.2020.01.006
7. Schönberger S, Schweiger B, Schwahn B et al (2004) Dysmyelination in the brain of adolescents and young adults with maple syrup urine disease. Mol Genet Metab 82:69–75. https://doi.org/10.1016/j.ymgme.2004.01.016
8. Allahwala A, Ahmed S, Afroze B (2021) Maple syrup urine disease: magnetic resonance imaging findings in three patients. J Pak Med Assoc 71:1309–1313. https://doi.org/10.47391/JPMA.1341
9. Cheng A, Han L, Feng Y et al (2017) MRI and clinical features of maple syrup urine disease: preliminary results in 10 cases. Diagn Interv Radiol 23:398–402. https://doi.org/10.5152/DIR.2017.16466
10. Kathait AS, Puac P, Castillo M (2018) Imaging findings in maple syrup urine disease: a Case Report. J Pediatr Neurosci 13:103–105. https://doi.org/10.4103/JPN.JPN_38_17
11. Contrusciere V, Paradisi S, Matteucci A, Malchiodi-Albedi F (2010) Branched-chain amino acids induce neurotoxicity in rat cortical cultures. Neurotox Res 17:392–398. https://doi.org/10.1007/S12640-009-9115-0
12. Kasinski A, Doering CB, Danner DJ (2004) Leucine toxicity in a neuronal cell model with inhibited branched chain amino acid catabolism. Brain Res Mol Brain Res 122:180–187. https://doi.org/10.1016/J.MOLBRAINRES.2003.08.023
13. Mescka CP, Rosa AP, Schirmbeck G et al (2016) L-carnitine prevents oxidative stress in the brains of rats subjected to a chemically Induced Chronic Model of MSUD. Mol Neurobiol 53:6007–6017. https://doi.org/10.1007/S12035-015-9500-Z
14. Pilla C, De Oliveira Cardozo RF, Dutra-Filho CS et al (2003) Effect of leucine administration on creatine kinase activity in rat brain. Metab Brain Dis 18:17–25. https://doi.org/10.1023/A:1021974517837
15. Vilela TC, Scaini G, Furlanetto CB et al (2017) Apoptotic signaling pathways induced by acute administration of branched-chain amino acids in an animal model of maple syrup urine disease. Metab Brain Dis 32:115–122. https://doi.org/10.1007/S11011-016-9892-0
16. Wessler LB, Ise K, Lemos IC et al (2020) Melatonin ameliorates oxidative stress and DNA damage of rats subjected to a chemically induced chronic model of maple syrup urine disease. Metab Brain Dis 35:905–914. https://doi.org/10.1007/S11011-020-00572-9
17. Bridi R, Braun CA, Zorzi GK et al (2005) α-Keto acids accumulating in maple syrup urine disease stimulate lipid peroxidation

and reduce antioxidant defences in cerebral cortex from young rats. Metab Brain Dis 20:155–167. https://doi.org/10.1007/s11011-005-4152-8
18. Funchal C, Latini A, Jacques-Silva MC et al (2006) Morphological alterations and induction of oxidative stress in glial cells caused by the branched-chain α-keto acids accumulating in maple syrup urine disease. Neurochem Int 49:640–650. https://doi.org/10.1016/J.NEUINT.2006.05.007
19. Amaral AU, Leipnitz G, Fernandes CG et al (2010) α-Ketoisocaproic acid and leucine provoke mitochondrial bioenergetic dysfunction in rat brain. Brain Res 1324:75–84. https://doi.org/10.1016/J.BRAINRES.2010.02.018
20. Ribeiro CA, Sgaravatti ÂM, Rosa RB et al (2008) Inhibition of brain energy metabolism by the branched-chain amino acids accumulating in maple syrup urine disease. Neurochem Res 33:114–124. https://doi.org/10.1007/S11064-007-9423-9
21. Sgaravatti AM, Rosa RB, Schuck PF et al (2003) Inhibition of brain energy metabolism by the α-keto acids accumulating in maple syrup urine disease. Biochim Biophys Acta 1639:232–238. https://doi.org/10.1016/J.BBADIS.2003.09.010
22. Funchal C, Gottfried C, De Vieira LM et al (2004) Evidence that the branched chain α-keto acids accumulating in maple syrup urine disease induce morphological alterations and death in cultured astrocytes from rat cerebral cortex. Glia 48:230–240. https://doi.org/10.1002/glia.20072
23. Amaral AU, Cecatto C, Castilho RF, Wajner M (2016) 2-Methylcitric acid impairs glutamate metabolism and induces permeability transition in brain mitochondria. J Neurochem 137:62–75. https://doi.org/10.1111/JNC.13544
24. Makrecka-Kuka M, Krumschnabel G, Gnaiger E (2015) High-resolution respirometry for simultaneous measurement of Oxygen and Hydrogen Peroxide fluxes in permeabilized cells, tissue homogenate and isolated Mitochondria. Biomolecules 5:1319–1338. https://doi.org/10.3390/BIOM5031319
25. Langenbeck U, Wendel U, Mench-Hoinowski A et al (1978) Correlations between branched-chain amino acids and branched-chain alpha-keto acids in blood in maple syrup urine disease. Clin Chim Acta 88:283–291. https://doi.org/10.1016/0009-8981(78)90433-3
26. Snyderman SE, Goldstein F, Sansaricq C, Norton PM (1984) The relationship between the branched chain amino acids and their alpha-ketoacids in maple syrup urine disease. Pediatr Res 18:851–853. https://doi.org/10.1203/00006450-198409000-00009
27. Lemasters JJ, HackenbrockA CR (1976) Continuous measurement and rapid kinetics of ATP synthesis in rat liver mitochondria, mitoplasts and inner membrane vesicles determined by firefly-luciferase luminescence. Eur J Biochem 67:1–10. https://doi.org/10.1111/J.1432-1033.1976.TB10625.X
28. Tretter L, Adam-Vizi V (2004) Generation of reactive oxygen species in the reaction catalyzed by alpha-ketoglutarate dehydrogenase. J Neurosci 24:7771–7778. https://doi.org/10.1523/JNEUROSCI.1842-04.2004
29. Figueira TR, Francisco A, Ronchi JA et al (2021) NADPH supply and the contribution of NAD(P)+transhydrogenase (NNT) to H2O2 balance in skeletal muscle mitochondria. Arch Biochem Biophys 707:108934. https://doi.org/10.1016/J.ABB.2021.108934
30. Kitto GB (1969) [19] intra- and extramitochondrial malate dehydrogenases from chicken and tuna heart: [EC 1.1.1.37 l-Malate: NAD oxidoreductase]. Methods Enzymol 13:106–116. https://doi.org/10.1016/0076-6879(69)13023-2
31. Srere PA (1969) [1] citrate synthase: [EC 4.1.3.7. Citrate oxaloacetate-lyase (CoA-acetylating)]. Methods Enzymol 13:3–11. https://doi.org/10.1016/0076-6879(69)13005-0
32. Fischer JC, Ruitenbeek W, Berden JA et al (1985) Differential investigation of the capacity of succinate oxidation in human skeletal muscle. Clin Chim Acta 153:23–36. https://doi.org/10.1016/0009-8981(85)90135-4
33. Lowry OH, Rosebrough NJ, Farr AL, Randall RJ (1951) Protein measurement with the folin phenol reagent. J Biol Chem 193:265–275. https://doi.org/10.1016/S0021-9258(19)52451-6
34. Bateman A (2019) UniProt: a worldwide hub of protein knowledge. Nucleic Acids Res 47:D506–D515. https://doi.org/10.1093/NAR/GKY1049
35. Unni S, Huang Y, Hanson RM et al (2011) Web servers and services for electrostatics calculations with APBS and PDB2PQR. J Comput Chem 32:1488. https://doi.org/10.1002/JCC.21720
36. Krieger E, Joo K, Lee J et al (2009) Improving physical realism, stereochemistry and side-chain accuracy in homology modeling: four approaches that performed well in CASP8. Proteins 77:114. https://doi.org/10.1002/PROT.22570
37. Laskowski RA, MacArthur MW, Moss DS, Thornton JM (1993) PROCHECK: a program to check the stereochemical quality of protein structures. J Appl Crystallogr 26:283–291. https://doi.org/10.1107/S0021889892009944
38. Pettersen EF, Goddard TD, Huang CC et al (2004) UCSF Chimera—A visualization system for exploratory research and analysis. J Comput Chem 25:1605–1612. https://doi.org/10.1002/JCC.20084
39. Berman HM, Westbrook J, Feng Z et al (2000) The Protein Data Bank. Nucleic Acids Res 28:235–242. https://doi.org/10.1093/NAR/28.1.235
40. Mattevi A, Obmolova G, Kalk KH et al (1993) Three-dimensional structure of lipoamide dehydrogenase from Pseudomonas fluorescens at 2.8 a resolution. Analysis of redox and thermostability properties. J Mol Biol 230:1200–1215. https://doi.org/10.1006/JMBI.1993.1236
41. Kim S, Chen J, Cheng T et al (2019) PubChem 2019 update: improved access to chemical data. Nucleic Acids Res 47:D1102–D1109. https://doi.org/10.1093/NAR/GKY1033
42. O'Boyle NM, Banck M, James CA et al (2011) Open Babel: an Open chemical toolbox. J Cheminform 3:1–14. https://doi.org/10.1186/1758-2946-3-33
43. de Moura Alvorcem L, Britto R, Cecatto C et al (2021) Ethylmalonic acid impairs bioenergetics by disturbing succinate and glutamate oxidation and induces mitochondrial permeability transition pore opening in rat cerebellum. J Neurochem 158:262–281. https://doi.org/10.1111/JNC.15363
44. Trott O, Olson AJ (2010) AutoDock Vina: improving the speed and accuracy of docking with a new scoring function, efficient optimization and multithreading. J Comput Chem 31:455. https://doi.org/10.1002/JCC.21334
45. Volkamer A, Kuhn D, Rippmann F, Rarey M (2012) DoGSiteScorer: a web server for automatic binding site prediction, analysis and druggability assessment. Bioinformatics 28:2074–2075. https://doi.org/10.1093/BIOINFORMATICS/BTS310
46. Kozakov D, Grove LE, Hall DR et al (2015) The FTMap family of web servers for determining and characterizing ligand-binding hot spots of proteins. Nat Protoc 10:733–755. https://doi.org/10.1038/nprot.2015.043
47. Krause F, Voigt K, Di Ventura B, Öztürk MA (2023) ReverseDock: a web server for blind docking of a single ligand to multiple protein targets using AutoDock Vina. Front Mol Biosci 10:1243970. https://doi.org/10.3389/FMOLB.2023.1243970
48. Farias HR, Gabriel JR, Cecconi ML et al (2021) The metabolic effect of α-ketoisocaproic acid: in vivo and in vitro studies. Metab Brain Dis 36:185–192. https://doi.org/10.1007/S11011-020-00626-Y
49. Patel MS (1974) Inhibition by the branched-chain 2-oxo acids of the 2-oxoglutarate dehydrogenase complex in developing rat and human brain. Biochem J 144:91–97. https://doi.org/10.1042/BJ1440091

50. Artiukhov AV, Graf AV, Kazantsev AV et al (2022) Increasing inhibition of the rat brain 2-Oxoglutarate dehydrogenase decreases glutathione Redox State, elevating anxiety and perturbing stress adaptation. Pharmaceuticals (Basel) 15:182. https://doi.org/10.3390/PH15020182
51. Chen H, Denton TT, Xu H et al (2016) Reductions in the mitochondrial enzyme α-ketoglutarate dehydrogenase complex in neurodegenerative disease– beneficial or detrimental? J Neurochem 139:823–838. https://doi.org/10.1111/jnc.13836
52. Wagner M, Bertero E, Nickel A et al (2020) Selective NADH communication from α-ketoglutarate dehydrogenase to mitochondrial transhydrogenase prevents reactive oxygen species formation under reducing conditions in the heart. Basic Res Cardiol 115:1–16. https://doi.org/10.1007/S00395-020-0815-1
53. Chen H, Cross AC, Thakkar A et al (2021) Selective linkage of mitochondrial enzymes to intracellular calcium stores differs between human-induced pluripotent stem cells, neural stem cells, and neurons. J Neurochem 156:867–879. https://doi.org/10.1111/jnc.15160
54. Weidinger A, Milivojev N, Hosmann A et al (2023) Oxoglutarate dehydrogenase complex controls glutamate-mediated neuronal death. Redox Biol 62:102669. https://doi.org/10.1016/J.REDOX.2023.102669
55. Gibson GE, Peterson C (1987) Calcium and the aging nervous system. Neurobiol Aging 8:329–343. https://doi.org/10.1016/0197-4580(87)90072-8
56. Gibson GE, Hirsch JA, Cirio RT et al (2013) Abnormal thiamine-dependent processes in Alzheimer's Disease. Lessons from diabetes. Mol Cell Neurosci 55:17–25. https://doi.org/10.1016/J.MCN.2012.09.001
57. Gibson GE, Sheu KR, Blass JP et al (1988) Reduced activities of thiamine-dependent enzymes in the brains and peripheral tissues of patients with Alzheimer's disease. Arch Neurol 45:836–840. https://doi.org/10.1001/ARCHNEUR.1988.00520320022009
58. Patel MS, Auerbach VH, Grover WD, Wilbur DO (1973) Effect of the branched-chain alpha-keto acids on pyruvate metabolism by homogenates of human brain. J Neurochem 20:1793–1796. https://doi.org/10.1111/J.1471-4159.1973.TB00298.X
59. Heublein M, Burguillos MA, Vögtle FN et al (2014) The novel component Kgd4 recruits the E3 subunit to the mitochondrial α-ketoglutarate dehydrogenase. Mol Biol Cell 25:3342–3349. https://doi.org/10.1091/MBC.E14-07-1178
60. Szabo E, Nagy B, Czajlik A et al (2024) Mitochondrial alpha-keto acid dehydrogenase complexes: recent developments on structure and function in Health and Disease. Subcell Biochem 104:295–381. https://doi.org/10.1007/978-3-031-58843-3_13
61. Felber SR, Sperl W, Chemelli A et al (1993) Maple syrup urine disease: metabolic decompensation monitored by proton magnetic resonance imaging and spectroscopy. Ann Neurol 33:396–401. https://doi.org/10.1002/ANA.410330412
62. Jan W, Zimmerman RA, Wang ZJ et al (2003) MR diffusion imaging and MR spectroscopy of maple syrup urine disease during acute metabolic decompensation. Neuroradiology 45:393–399. https://doi.org/10.1007/S00234-003-0955-7
63. Srinivasan KG, Ramprabananth S, Ushanandhini KP, Srividya S (2009) Typical neuroradiological diagnosis of maple syrup urine disease as a precursor to clinical diagnosis. Neuroradiol J 22:564–567. https://doi.org/10.1177/197140090902200509
64. Terek D, Koroglu O, Yalaz M et al (2013) Diagnostic tools of early brain disturbances in an asymptomatic neonate with maple syrup urine disease. Neuropediatrics 44:208–212. https://doi.org/10.1055/S-0032-1332741/ID/JR120855SC-12
65. Yang C, Linpeng S, Cao Y, Wu L (2019) Identification of six novel mutations in five infants with suspected maple syrup urine disease based on blood and urine metabolism screening. Gene 710:9–16. https://doi.org/10.1016/J.GENE.2019.04.086
66. Strand JM, Skinnes R, Scheffler K et al (2014) Genome instability in maple syrup urine Disease correlates with impaired mitochondrial biogenesis. Metabolism 63:1063–1070. https://doi.org/10.1016/j.metabol.2014.05.003
67. Zinnanti WJ, Lazovic J, Griffin K et al (2009) Dual mechanism of brain injury and novel treatment strategy in maple syrup urine disease. Brain 132:903. https://doi.org/10.1093/BRAIN/AWP024
68. Erecinska M, Cherian S, Silver IA (2004) Energy metabolism in mammalian brain during development. Prog Neurobiol 73:397–445. https://doi.org/10.1016/J.PNEUROBIO.2004.06.003

Publisher's Note Springer Nature remains neutral with regard to jurisdictional claims in published maps and institutional affiliations.

Springer Nature or its licensor (e.g. a society or other partner) holds exclusive rights to this article under a publishing agreement with the author(s) or other rightsholder(s); author self-archiving of the accepted manuscript version of this article is solely governed by the terms of such publishing agreement and applicable law.

REFERÊNCIAS

1. Del Rio RM (1962) Aminoacidopatias congenitas y sus repercusiones en el desarrolo del SNC. Madrid
2. Menkes JH, Hurst PL, Craig JM (1954) A new syndrome: progressive familial infantile cerebral dysfunction associated with an ususual urinary substance. Pediatrics 14:462–467. https://doi.org/10.1542/PEDS.14.5.462
3. Westall RG, Dancis J, Miller S (1957) Maple syrup urine disease. The American Journal of Diseases of Children 94:571–572
4. Menkes JH (1959) Maple syrup urine disease. Isolation and identification of organic acids in the urine. Pediatrics 23:348–353
5. Chuang DavidT, Shih VE, Wynn MR Maple Syrup Urine Disease (Branched-Chain Ketoaciduria) | The Online Metabolic and Molecular Bases of Inherited Disease | OMMBID | McGraw Hill Medical. https://ommbid.mhmedical.com/content.aspx?bookId=2709&sectionId=225084607. Accessed 17 Aug 2023
6. Nobukuni Y, Mitsubuchi H, Ohta K, et al (1992) Molecular diagnosis of maple syrup urine disease: screening and identification of gene mutations in the branched-chain alpha-ketoacid dehydrogenase multienzyme complex. J Inherit Metab Dis 15:827–833. https://doi.org/10.1007/BF01800029
7. Shigematsu Y, Kikuchi K, Momoi T, et al (1983) Organic acids and branched-chain amino acids in body fluids before and after multiple exchange transfusions in maple syrup urine disease. J Inherit Metab Dis 6:183–189. https://doi.org/10.1007/BF02310879/METRICS
8. Danner DJ, Elsas LJ (1989) Disorders of branched chain amino acid and keto acid metabolism. In: The Metabolic Basis of Inherited Disease, 6th ed. New York, pp 671–692
9. Schadewalt PL, Wenderl U (1997) Metabolism of branched-chain amino acids in maple syrup urine disease. Eur J Pediatr 56:62–66
10. Peinemann F, Danner DJ (1994) Maple syrup urine disease 1954-1993. J Inherit Metab Dis 17:3–15
11. Muelly ER, Moore GJ, Bunce SC, et al (2013) Biochemical correlates of neuropsychiatric illness in maple syrup urine disease. J Clin Invest 123:1809–1820. https://doi.org/10.1172/JCI67217
12. Shellmer DA, Devito Dabbs A, Dew MA, et al (2011) Cognitive and adaptive functioning after liver transplantation for maple syrup urine disease: A case series. Pediatr Transplant 15:58–64. https://doi.org/10.1111/J.1399-3046.2010.01411.X
13. Strauss KA, Puffenberger EG, Carson VJ (2020) Maple Syrup Urine Disease. Gene Reviews

14. Fischer MH, Gerritsen T (1971) Biochemical studies on a variant of branched chain ketoaciduria in a 19-year-old female. Pediatrics 48:795–801. https://doi.org/10.1542/peds.48.5.795

15. Gonzalez-Rios M del C, Chuang DT, Cox RP, et al (1985) A distinct variant of intermediate maple syrup urine disease. Clin Genet 27:153–159. https://doi.org/10.1111/J.1399-0004.1985.TB00203.X

16. Müller H, Bickel H, Feist D, Lutz P (1971) [Maple syrup urine disease with an intermittent relatively benign course]. Dtsch Med Wochenschr 96:1552–1557. https://doi.org/10.1055/S-0028-1110178

17. Allahwala A, Ahmed S, Afroze B (2021) Maple syrup urine disease: magnetic resonance imaging findings in three patients. J Pak Med Assoc 71:1309–1313. https://doi.org/10.47391/JPMA.1341

18. Cheng A, Han L, Feng Y, et al (2017) MRI and clinical features of maple syrup urine disease: preliminary results in 10 cases. https://doi.org/10.5152/dir.2017.16466

19. Kathait AS, Puac P, Castillo M (2018) Imaging Findings in Maple Syrup Urine Disease: A Case Report. J Pediatr Neurosci 13:103–105. https://doi.org/10.4103/JPN.JPN_38_17

20. Ha JS, Kim TK, Eun BL, et al (2004) Maple syrup urine disease encephalopathy: a follow-up study in the acute stage using diffusion-weighted MRI. Pediatr Radiol 34:163–166. https://doi.org/10.1007/S00247-003-1058-7

21. Schönberger S, Schweiger B, Schwahn B, et al (2004) Dysmyelination in the brain of adolescents and young adults with maple syrup urine disease. Mol Genet Metab 82:69–75. https://doi.org/10.1016/j.ymgme.2004.01.016

22. Kamei A, Takashima S, Chan F, Becker LE (1992) Abnormal dendritic development in maple syrup urine disease. Pediatr Neurol 8:145–147. https://doi.org/10.1016/0887-8994(92)90038-Z

23. Martin JJ, Schlote W (1972) Central nervous system lesions in disorders of amino-acid metabolism: A neuropathological study. J Neurol Sci 15:49–76. https://doi.org/10.1016/0022-510X(72)90121-9

24. Menkes JH, Philippart M, Fiol RE (1965) Cerebral lipids in maple syrup disease. J Pediatr 66:584–594. https://doi.org/10.1016/S0022-3476(65)80122-6

25. Crome L, Dutton G, Ross CF (1961) Maple syrup urine disease. J Pathol Bacteriol 81:379–384. https://doi.org/10.1002/PATH.1700810209

26. Silberman J, Dancis J, Feigin I (1961) Neuropathological Observations in Maple Syrup Urine Disease: Branched-Chain Ketoaciduria. Arch Neurol 5:351–363. https://doi.org/10.1001/ARCHNEUR.1961.00450160001001

27. Snyderman SE, Norton PM, Roitman E, Holt LE (1964) Maple syrup urine disease, with particular reference to dietotherapy. Pediatrics 34:454–472. https://doi.org/10.1542/peds.34.4.454

28. Celik N, Kelly B, Soltys K, et al (2019) Technique and outcome of domino liver transplantation from patients with maple syrup urine disease: Expanding the donor pool for live donor liver transplantation. Clin Transplant 33:e13721. https://doi.org/10.1111/CTR.13721

29. Strauss KA, Carson VJ, Soltys K, et al (2020) Branched-chain α-ketoacid dehydrogenase deficiency (maple syrup urine disease): Treatment, biomarkers, and outcomes. Mol Genet Metab 129:193–206. https://doi.org/10.1016/J.YMGME.2020.01.006

30. Rogers QR, Spolter PD, Harper AE (1962) Effect of leucine-lsoleucine antagonism on plasma amino acid pattern of rats. Arch Biochem Biophys 97:497–504. https://doi.org/10.1016/0003-9861(62)90113-3

31. Wendel U, Langenbeck U, Lombeck I, Bremer HJ (1982) Maple syrup urine disease--therapeutic use of insulin in catabolic states. Eur J Pediatr 139:172–175. https://doi.org/10.1007/BF01377350

32. Muelly ER, Moore GJ, Bunce SC, et al (2013) Biochemical correlates of neuropsychiatric illness in maple syrup urine disease. Journal of Clinical Investigation 123:1809–1820. https://doi.org/10.1172/JCI67217

33. Smith QR, Momma S, Aoyagi M, Rapoport SI (1987) Kinetics of Neutral Amino Acid Transport Across the Blood-Brain Barrier. J Neurochem 49:1651–1658. https://doi.org/10.1111/J.1471-4159.1987.TB01039.X

34. Barschak AG, Sitta A, Deon M, et al (2006) Evidence that oxidative stress is increased in plasma from patients with maple syrup urine disease. Metab Brain Dis 21:279–286. https://doi.org/10.1007/S11011-006-9030-5/FIGURES/3

35. Holmes Morton D, Strauss KA, Robinson DL, et al (2002) Diagnosis and Treatment of Maple Syrup Disease: A Study of 36 Patients. Pediatrics 109:999–1008. https://doi.org/10.1542/PEDS.109.6.999

36. Scaini G, Tonon T, de Souza CFM, et al (2016) Serum Markers of Neurodegeneration in Maple Syrup Urine Disease. Molecular Neurobiology 2016 54:7 54:5709–5719. https://doi.org/10.1007/S12035-016-0116-8

37. Wajner M, Coelho DM, Barschak AG, et al (2000) Reduction of large neutral amino acid concentrations in plasma and CSF of patients with maple syrup urine disease during crises. J Inherit Metab Dis 23:505–512. https://doi.org/10.1023/A:1005668431926

38. Prensky AL, Moser HW (1966) Brain lipids, proteolipids, and free amino acids in maple syrup urine disease. J Neurochem 13:863–874. https://doi.org/10.1111/J.1471-4159.1966.TB05882.X

39. Yudkoff M, Daikhin Y, Nissim I, et al (1994) Inhibition of astrocyte glutamine production by alpha-ketoisocaproic acid. J Neurochem 63:1508–1515. https://doi.org/10.1046/J.1471-4159.1994.63041508.X

40. Zinnanti WJ, Lazovic J, Griffin K, et al (2009) Dual mechanism of brain injury and novel treatment strategy in maple syrup urine disease. Brain 132:903. https://doi.org/10.1093/BRAIN/AWP024

41. Amaral AU, Wajner M (2022) Pathophysiology of maple syrup urine disease: Focus on the neurotoxic role of the accumulated branched-chain amino acids and branched-chain α-keto acids. Neurochem Int 157:105360. https://doi.org/10.1016/J.NEUINT.2022.105360

42. Skvorak KJ, Hager EJ, Arning E, et al (2009) Hepatocyte transplantation (HTx) corrects selected neurometabolic abnormalities in murine intermediate maple syrup urine disease (iMSUD). Biochimica et Biophysica Acta (BBA) - Molecular Basis of Disease 1792:1004–1010. https://doi.org/10.1016/J.BBADIS.2009.08.006

43. Sitta A, Barschak AG, Deon M, et al (2009) L-carnitine blood levels and oxidative stress in treated phenylketonuric patients. Cell Mol Neurobiol 29:211–218. https://doi.org/10.1007/S10571-008-9313-Y

44. Medina G, Nosworthy MG, Petkau JC, et al (2022) Alteration of the dietary methionine: Cysteine ratio modulates the inflammatory response to an inter-peritoneal injection of lipopolysaccharide in wistar rats. J Nutr Biochem 102:108937. https://doi.org/10.1016/J.JNUTBIO.2022.108937

45. Nelson, D.L. and Cox, M.M. (2017) Lehninger Principles of Biochemistry. 7th Edition, W.H. Freeman, New York, 1328. - References - Scientific Research Publishing. https://www.scirp.org/reference/referencespapers?referenceid=2103234. Accessed 13 Jun 2026

46. Bock FJ, Tait SWG (2020) Mitochondria as multifaceted regulators of cell death. Nat Rev Mol Cell Biol 21:85–100. https://doi.org/10.1038/S41580-019-0173-8;SUBJMETA

47. Faas MM, de Vos P (2020) Mitochondrial function in immune cells in health and disease. Biochimica et Biophysica Acta (BBA) - Molecular Basis of Disease 1866:165845. https://doi.org/10.1016/J.BBADIS.2020.165845

48. Javadov S, Kozlov A V., Camara AKS (2020) Mitochondria in Health and Diseases. Cells 2020, Vol 9, Page 1177 9:1177. https://doi.org/10.3390/CELLS9051177

49. Nunnari J, Suomalainen A (2012) Mitochondria: In Sickness and in Health. Cell 148:1145–1159. https://doi.org/10.1016/J.CELL.2012.02.035

50. Onishi M, Yamano K, Sato M, et al (2021) Molecular mechanisms and physiological functions of mitophagy. EMBO J 40:EMBJ2020104705-. https://doi.org/10.15252/EMBJ.2020104705/FIGURES/5

51. Popov LD (2020) Mitochondrial biogenesis: An update. J Cell Mol Med 24:4892–4899. https://doi.org/10.1111/JCMM.15194

52. Nicholls DG, Ferguson S (2013) Bioenergetics: Fourth Edition. Bioenergetics: Fourth Edition 1–419. https://doi.org/10.1016/C2010-0-64902-9

53. Vakifahmetoglu-Norberg H, Ouchida AT, Norberg E (2017) The role of mitochondria in metabolism and cell death. Biochem Biophys Res Commun 482:426–431. https://doi.org/10.1016/J.BBRC.2016.11.088

54. Nicholls DG (2021) Mitochondrial proton leaks and uncoupling proteins. Biochim Biophys Acta Bioenerg 1862: 148428. https://doi.org/10.1016/J.BBABIO.2021.148428

55. Halliwell B, Gutteridge J (2015) Oxidative stress and redox regulation: adaptation, damage, repair, senescence, and death. In: Free Radicals in Biology and Medicine. Oxford University Press, New York, pp 199–2083

56. SOUTHORN PA, POWIS G (1988) Free radicals in medicine. I. Chemical nature and biologic reactions. Mayo Clin Proc 63:381–389. https://doi.org/10.1016/S0025-6196(12)64861-7

57. Aratani Y, Miura N, Ohno N, Suzuki K (2012) [Role of neutrophil-derived reactive oxygen species in host defense and inflammation]. Med Mycol J 53:123–128. https://doi.org/10.3314/MMJ.53.123

58. Delanty N, Dichter MA (1998) Oxidative injury in the nervous system. Acta Neurol Scand 98:145–153. https://doi.org/10.1111/J.1600-0404.1998.TB07285.X

59. Hamann I, Petroll K, Grimm L, et al (2014) Insulin-like modulation of Akt/FoxO signaling by copper ions is independent of insulin receptor. Arch Biochem Biophys 558:42–50. https://doi.org/10.1016/J.ABB.2014.06.004

60. Irani K (2000) Oxidant signaling in vascular cell growth, death, and survival : a review of the roles of reactive oxygen species in smooth muscle and endothelial cell mitogenic and apoptotic signaling. Circ Res 87:179–183. https://doi.org/10.1161/01.RES.87.3.179

61. Wall SB, Oh JY, Diers AR, Landar A (2012) Oxidative modification of proteins: an emerging mechanism of cell signaling. Front Physiol 369. https://doi.org/10.3389/FPHYS.2012.00369

62. Webb R, Hughes MG, Thomas AW, Morris K (2017) The Ability of Exercise-Associated Oxidative Stress to Trigger Redox-Sensitive Signalling Responses. Antioxidants (Basel) 6 (3): 63. https://doi.org/10.3390/ANTIOX6030063

63. Halliwell B, Gutteridge J (2015) Antioxidants from the diet. In: : Free Radicals in Biology and Medicine. Oxford University Press , New York, pp 153–197

64. Halliwell B, Gutteridge JMC (2015) Antioxidant defences synthesized in vivo. Free Radicals in Biology and Medicine 77–152. https://doi.org/10.1093/ACPROF:OSO/9780198717478.003.0003

65. Halliwell B (2006) Reactive species and antioxidants. Redox biology is a fundamental theme of aerobic life. Plant Physiol 141:312–322. https://doi.org/10.1104/PP.106.077073

66. Cipolla-Neto J, Do Amaral FG (2018) Melatonin as a Hormone: New Physiological and Clinical Insights. Endocr Rev 39:990–1028. https://doi.org/10.1210/ER.2018-00084

67. Pieri C, Marra M, Moroni F, et al (1994) Melatonin: a peroxyl radical scavenger more effective than vitamin E. Life Sci 55: 271-276. https://doi.org/10.1016/0024-3205(94)00666-0

68. Reiter RJ, Mayo JC, Tan DX, et al (2016) Melatonin as an antioxidant: under promises but over delivers. J Pineal Res 61:253–278. https://doi.org/10.1111/JPI.12360

69. Gulcin I, Buyukokuroglu ME, Kufrevioglu OI (2003) Metal chelating and hydrogen peroxide scavenging effects of melatonin. J Pineal Res 34:278–281. https://doi.org/10.1034/J.1600-079X.2003.00042.X

70. Reiter RJ, Tan D-X, Rosales-Corral S, Manchester LC (2013) The Universal Nature, Unequal Distribution and Antioxidant Functions of Melatonin and Its Derivatives. Mini-Reviews in Medicinal Chemistry 13:373–384. https://doi.org/10.2174/1389557511313030006

71. Ribeiro RT, Seminotti B, Zanatta Â, et al (2021) Neuronal Death, Glial Reactivity, Microglia Activation, Oxidative Stress and Bioenergetics Impairment Caused by Intracerebroventricular Administration of D-2-hydroxyglutaric Acid to Neonatal Rats. Neuroscience 471:115–132. https://doi.org/10.1016/J.NEUROSCIENCE.2021.07.024

72. Seminotti B, Zanatta Â, Ribeiro RT, et al (2019) Disruption of Brain Redox Homeostasis, Microglia Activation and Neuronal Damage Induced by Intracerebroventricular Administration of S-Adenosylmethionine to Developing Rats. Mol Neurobiol 56:2760–2773. https://doi.org/10.1007/S12035-018-1275-6/FIGURES/10

73. Duarte MB, Medeiros BZ, da Silva Lemos I, et al (2023) Melatonin improves behavioral parameters and oxidative stress in zebrafish submitted to a leucine-induced MSUD protocol. Metab Brain Dis 38:2105–2114. https://doi.org/10.1007/S11011-023-01220-8

74. Aldini G, Altomare A, Baron G, et al (2018) N-Acetylcysteine as an antioxidant and disulphide breaking agent: the reasons why. Free Radic Res 52:751–762. https://doi.org/10.1080/10715762.2018.1468564

75. Prescott LF (1983) New approaches in managing drug overdosage and poisoning. Br Med J (Clin Res Ed) 287:274–276. https://doi.org/10.1136/BMJ.287.6387.274

76. Pedre B, Barayeu U, Ezeriņa D, Dick TP (2021) The mechanism of action of N-acetylcysteine (NAC): The emerging role of H2S and sulfane sulfur species. Pharmacol Ther 228:107916. https://doi.org/10.1016/J.PHARMTHERA.2021.107916

77. Ribas GS, Vargas CR, Wajner M (2014) l-carnitine supplementation as a potential antioxidant therapy for inherited neurometabolic disorders. Gene 533:469–476. https://doi.org/10.1016/J.GENE.2013.10.017

78. Walter JH (1996) L-Carnitine. Arch Dis Child 74:475–478. https://doi.org/10.1136/ADC.74.6.475

79. Girardi J, Faverzani JL, Lopes FF, et al (2025) Neuroprotective, antioxidant and anti-inflammatory effect of carnitine in patients with Maple syrup urine disease: branched-chain amino acids and branched-chain keto acids levels. Metab Brain Dis 40(8):314. https://doi.org/10.1007/S11011-025-01747-Y

80. dos Reis BG, Becker GS, Marchetti DP, et al (2024) Neurodegenerative biomarkers and inflammation in patients with propionic and methylmalonic acidemias: effect of L-carnitine treatment. Metab Brain Dis 40(1):6. https://doi.org/10.1007/S11011-024-01475-9

81. Faverzani JL, Guerreiro G, Hammerschmidt TG, et al (2023) Increased peripheral of brain-derived neurotrophic factor levels in phenylketonuric patients treated with L-carnitine. Arch Biochem Biophys 749:109792. https://doi.org/10.1016/j.abb.2023.109792

82. Ramos JMP, Bussi C, Gaviglio EA, et al (2017) Type I IFNs Are Required to Promote Central Nervous System Immune Surveillance through the Recruitment of Inflammatory Monocytes upon Systemic Inflammation. Front Immunol 8:1666. https://doi.org/10.3389/FIMMU.2017.01666

83. Lenz KM, Nelson LH (2018) Microglia and Beyond: Innate Immune Cells As Regulators of Brain Development and Behavioral Function. Front Immunol 9:698. https://doi.org/10.3389/FIMMU.2018.00698

84. Yang I, Han SJ, Kaur G, et al (2010) The role of microglia in central nervous system immunity and glioma immunology. Journal of Clinical Neuroscience 17:6–10. https://doi.org/10.1016/j.jocn.2009.05.006

85. Hines DJ, Hines RM, Mulligan SJ, Macvicar BA (2009) Microglia processes block the spread of damage in the brain and require functional chloride channels. Glia 57:1610–1618. https://doi.org/10.1002/GLIA.20874

86. Kreutzberg GW (1996) Microglia: a sensor for pathological events in the CNS. Trends Neurosci 19:312–318. https://doi.org/10.1016/0166-2236(96)10049-7

87. Norden DM, Trojanowski PJ, Villanueva E, et al (2016) Sequential activation of microglia and astrocyte cytokine expression precedes increased Iba-1 or GFAP immunoreactivity following systemic immune challenge. Glia 64:300–316. https://doi.org/10.1002/GLIA.22930

88. Hovens IB, Nyakas C, Schoemaker RG (2014) A novel method for evaluating microglial activation using ionized calcium-binding adaptor protein-1 staining: cell body to cell size ratio. Neuroimmunology Neuroinflammation 1:82–88

89. Fu R, Shen Q, Xu P, et al (2014) Phagocytosis of microglia in the central nervous system diseases. Mol Neurobiol 49:1422–1434. https://doi.org/10.1007/S12035-013-8620-6

90. Kwon DH, Cha HJ, Lee H, et al (2019) Protective Effect of Glutathione against Oxidative Stress-induced Cytotoxicity in RAW 264.7 Macrophages through Activating the Nuclear Factor Erythroid 2-Related Factor-2/Heme Oxygenase-1 Pathway. Antioxidants 2019, Vol 8, Page 82 8:82. https://doi.org/10.3390/ANTIOX8040082

91. Oksanen M, Lehtonen S, Jaronen M, et al (2019) Astrocyte alterations in neurodegenerative pathologies and their modeling in human induced pluripotent stem cell platforms. Cell Mol Life Sci 76:2739–2760. https://doi.org/10.1007/S00018-019-03111-7

92. Colombo E, Farina C (2016) Astrocytes: Key Regulators of Neuroinflammation. Trends Immunol 37:608–620. https://doi.org/10.1016/J.IT.2016.06.006

93. Carter SF, Herholz K, Rosa-Neto P, et al (2019) Astrocyte Biomarkers in Alzheimer's Disease. Trends Mol Med 25:77–95. https://doi.org/10.1016/J.MOLMED.2018.11.006

94. Smith JA, Das A, Ray SK, Banik NL (2012) Role of pro-inflammatory cytokines released from microglia in neurodegenerative diseases. Brain Res Bull 87:10–20. https://doi.org/10.1016/J.BRAINRESBULL.2011.10.004

95. Aguilar Delgado C, Hammerschmidt T, Faverzini JL, et al (2023) Inflammatory process and oxidative/nitrative stress: in vivo study in mucopolysaccharidosis type IV A patients under long-term enzyme replacement therapy. Arch Biochem Biophys 737: 109541. https://doi.org/10.1016/J.ABB.2023.109541

96. Amaral AU, Cecatto C, Da Silva JC, et al (2016) cis-4-Decenoic and decanoic acids impair mitochondrial energy, redox and Ca2 + homeostasis and induce mitochondrial permeability transition pore opening in rat brain and liver: Possible implications for the pathogenesis of MCAD deficiency. Biochimica et Biophysica Acta (BBA) - Bioenergetics 1857:1363–1372. https://doi.org/10.1016/J.BBABIO.2016.05.007

97. Faverzani JL, Hammerschmidt TG, Mescka CP, et al (2023) Increased cytokine levels induced by high phenylalanine concentrations in late diagnosis PKU patients compared to early diagnosis: Anti-inflammatory effect of L-carnitine. Cell Biochem Funct 41:490–500. https://doi.org/10.1002/CBF.3800

98. Hammerschmidt TG, Donida B, Faverzani JL, et al (2022) Cytokine profile and cholesterol levels in patients with Niemann-Pick type C disease presenting neurological symptoms: in vivo effect of miglustat and in vitro effect of N-acetylcysteine and coenzyme Q10. Exp Cell Res 416:2. https://doi.org/10.1016/J.YEXCR.2022.113175

99. Jacques CED, Donida B, Mescka CP, et al (2016) Oxidative and nitrative stress and pro-inflammatory cytokines in Mucopolysaccharidosis type II patients: effect

of long-term enzyme replacement therapy and relation with glycosaminoglycan accumulation. Biochim Biophys Acta 1862:1608–1616. https://doi.org/10.1016/J.BBADIS.2016.05.021

100. Marchetti DP, Donida B, Jacques CE, et al (2018) Inflammatory profile in X-linked adrenoleukodystrophy patients: Understanding disease progression. J Cell Biochem 119:1223–1233. https://doi.org/10.1002/JCB.26295

101. Leon CG, Tory R, Jia J, et al (2008) Discovery and Development of Toll-Like Receptor 4 (TLR4) Antagonists: A New Paradigm for Treating Sepsis and Other Diseases. Pharm Res 25:1751–1761. https://doi.org/10.1007/s11095-008-9571-x

102. Janeway CA, Medzhitov R (2002) Innate Immune Recognition. Annu Rev Immunol 20:197–216. https://doi.org/10.1146/annurev.immunol.20.083001.084359

103. Glezer I, Simard AR, Rivest S (2007) Neuroprotective role of the innate immune system by microglia. Neuroscience 147:867–883. https://doi.org/10.1016/j.neuroscience.2007.02.055

104. Hashimoto C, Hudson KL, Anderson K V. (1988) The Toll gene of drosophila, required for dorsal-ventral embryonic polarity, appears to encode a transmembrane protein. Cell 52:269–279. https://doi.org/10.1016/0092-8674(88)90516-8

105. Uematsu S, Akira S (2006) Toll-like receptors and innate immunity. J Mol Med (Berl) 84:712–725. https://doi.org/10.1007/S00109-006-0084-Y

106. Carpentier PA, Duncan DS, Miller SD (2008) Glial toll-like receptor signaling in central nervous system infection and autoimmunity. Brain Behav Immun 22:140–147. https://doi.org/10.1016/J.BBI.2007.08.011

107. Kipp M, Norkute A, Johann S, et al (2008) Brain-Region-Specific Astroglial Responses In Vitro After LPS Exposure. Journal of Molecular Neuroscience 35:235–243. https://doi.org/10.1007/s12031-008-9057-7

108. Johann S, Kampmann E, Denecke B, et al (2008) Expression of Enzymes Involved in the Prostanoid Metabolism by Cortical Astrocytes after LPS-induced Inflammation. Journal of Molecular Neuroscience 34:177–185. https://doi.org/10.1007/s12031-007-9028-4

109. Zhou H, Lapointe BM, Clark SR, et al (2006) A Requirement for Microglial TLR4 in Leukocyte Recruitment into Brain in Response to Lipopolysaccharide. The Journal of Immunology 177:8103–8110. https://doi.org/10.4049/jimmunol.177.11.8103

110. Henry CJ, Huang Y, Wynne AM, Godbout JP (2009) Peripheral lipopolysaccharide (LPS) challenge promotes microglial hyperactivity in aged mice that is associated with exaggerated induction of both pro-inflammatory IL-1β and anti-inflammatory IL-10 cytokines. Brain Behav Immun 23:309–317. https://doi.org/10.1016/j.bbi.2008.09.002

111. Mitsubuchi H, Owada M, Endo F (2005) Markers associated with inborn errors of metabolism of branched-chain amino acids and their relevance to upper levels of intake in healthy people: An implication from clinical and molecular investigations on maple syrup urine disease. Journal of Nutrition 135:1565S-70S. https://doi.org/10.1093/jn/135.6.1565s

112. Amaral AU, Wajner M (2022) Pathophysiology of maple syrup urine disease: Focus on the neurotoxic role of the accumulated branched-chain amino acids and branched-chain α-keto acids. Neurochem Int 157: 105360. https://doi.org/10.1016/j.neuint.2022.105360

113. Blackburn PR, Gass JM, Pinto e Vairo F, et al (2017) Maple syrup urine disease: mechanisms and management. Appl Clin Genet 10:57. https://doi.org/10.2147/TACG.S125962

114. Vogel KR, Arning E, Wasek BL, et al (2014) Brain–blood amino acid correlates following protein restriction in murine maple syrup urine disease. Orphanet Journal of Rare Diseases 2014 9:1 9:73. https://doi.org/10.1186/1750-1172-9-73

115. McKenna MC, Sonnewald U, Huang X, et al (1998) Alpha-ketoisocaproate alters the production of both lactate and aspartate from [U-13C]glutamate in astrocytes: a 13C NMR study. J Neurochem 70:1001–1008. https://doi.org/10.1046/J.1471-4159.1998.70031001.X

116. Amaral AU, Leipnitz G, Fernandes CG, et al (2010) α-Ketoisocaproic acid and leucine provoke mitochondrial bioenergetic dysfunction in rat brain. Brain Res 1324:75–84. https://doi.org/10.1016/J.BRAINRES.2010.02.018

117. Farias HR, Gabriel JR, Cecconi ML, et al (2021) The metabolic effect of α-ketoisocaproic acid: in vivo and in vitro studies. Metab Brain Dis 36:185–192. https://doi.org/10.1007/S11011-020-00626-Y

118. Lemos I da S, Alano CG, Canarim RO, et al (2025) Donepezil treatment mitigates cholinergic system alterations, oxidative stress, neuroinflammation and memory impairment induced by branched-chain amino acid administration in rats. Behavioural Brain Research 480:115359. https://doi.org/10.1016/J.BBR.2024.115359

119. Taschetto L, Scaini G, Zapelini HG, et al (2017) Acute and long-term effects of intracerebroventricular administration of α-ketoisocaproic acid on oxidative stress parameters and cognitive and noncognitive behaviors. Metab Brain Dis 32:1507–1518. https://doi.org/10.1007/S11011-017-0035-Z

120. Funchal C, Latini A, Jacques-Silva MC, et al (2006) Morphological alterations and induction of oxidative stress in glial cells caused by the branched-chain α-keto acids accumulating in maple syrup urine disease. Neurochem Int 49:640–650. https://doi.org/10.1016/j.neuint.2006.05.007

121. Farias HR, Gabriel JR, Cecconi ML, et al (2021) The metabolic effect of α-ketoisocaproic acid: in vivo and in vitro studies. Metab Brain Dis 36:185–192. https://doi.org/10.1007/S11011-020-00626-Y

122. Bridi R, Araldi J, Sgarbi MB, et al (2003) Induction of oxidative stress in rat brain by the metabolites accumulating in maple syrup urine disease. International Journal of Developmental Neuroscience 21:327–332. https://doi.org/10.1016/S0736-5748(03)00074-1

123. Fontella FU, Gassen E, Pulrolnik V, et al (2002) Stimulation of lipid peroxidation in vitro in rat brain by the metabolites accumulating in maple syrup urine disease. Met Brain Dis 17:47–54. https://doi.org/10.1023/a:1014004414733

124. Bridi R, Braun CA, Zorzi GK, et al (2005) α-Keto acids accumulating in maple syrup urine disease stimulate lipid peroxidation and reduce antioxidant defences in cerebral cortex from young rats. Metab Brain Dis 20:155–167. https://doi.org/10.1007/s11011-005-4152-8

125. Sitta A, Ribas GS, Mescka CP, et al (2014) Neurological damage in MSUD: the role of oxidative stress. Cell Mol Neurobiol 34:157–165. https://doi.org/10.1007/S10571-013-0002-0

126. Barschak AG, Sitta A, Deon M, et al (2009) Amino acids levels and lipid peroxidation in maple syrup urine disease patients. Clin Biochem 42:462–466. https://doi.org/10.1016/J.CLINBIOCHEM.2008.12.005

127. Leipnitz G, Amaral AU, Zanatta Â, et al (2010) Neurochemical evidence that phytanic acid induces oxidative damage and reduces the antioxidant defenses in cerebellum and cerebral cortex of rats. Life Sci 87:275–280. https://doi.org/10.1016/J.LFS.2010.06.015

128. Barschak AG, Sitta A, Deon M, et al (2006) Evidence that oxidative stress is increased in plasma from patients with maple syrup urine disease. Metab Brain Dis 21:279–286. https://doi.org/10.1007/S11011-006-9030-5

129. Barschak AG, Sitta A, Deon M, et al (2008) Oxidative stress in plasma from maple syrup urine disease patients during treatment. Metab Brain Dis 23:71–80. https://doi.org/10.1007/S11011-007-9077-Y

130. Guerreiro G, Mescka CP, Sitta A, et al (2015) Urinary biomarkers of oxidative damage in Maple syrup urine disease: the L-carnitine role. Int J Dev Neurosci 42:10–14. https://doi.org/10.1016/J.IJDEVNEU.2015.02.003

131. Volpe JJ. (2018) Volpe's neurology of the newborn. Elsevier, 6ed. https://doii.org/10.1016/C2010-0-68825-0

132. Hagberg H, Mallard C, Ferriero DM, et al (2015) The role of inflammation in perinatal brain injury. Nat Rev Neurol 11:192–208. https://doi.org/10.1038/NRNEUROL.2015.13

133. Loboda A, Damulewicz M, Pyza E, et al (2016) Role of Nrf2/HO-1 system in development, oxidative stress response and diseases: an evolutionarily conserved mechanism. Cell Mol Life Sci 73:3221–3247. https://doi.org/10.1007/S00018-016-2223-0

134. Kensler TW, Wakabayashi N, Biswal S (2007) Cell survival responses to environmental stresses via the Keap1-Nrf2-ARE pathway. Annu Rev Pharmacol Toxicol 47:89–116. https://doi.org/10.1146/ANNUREV.PHARMTOX.46.120604.141046

135. Indiran V, Gunaseelan RE (2013) Neuroradiological findings in maple syrup urine disease. J Pediatr Neurosci 8:31. https://doi.org/10.4103/1817-1745.111419

136. Muelly ER, Moore GJ, Bunce SC, et al (2013) Biochemical correlates of neuropsychiatric illness in maple syrup urine disease. J Clin Invest 123:1809–1820. https://doi.org/10.1172/JCI67217

137. Jan W, Zimmerman RA, Wang ZJ, et al (2003) MR diffusion imaging and MR spectroscopy of maple syrup urine disease during acute metabolic decompensation. Neuroradiology 45:393–399. https://doi.org/10.1007/S00234-003-0955-7

138. Pekny M, Pekna M (2014) Astrocyte reactivity and reactive astrogliosis: costs and benefits. Physiol Rev 94:1077–1098. https://doi.org/10.1152/PHYSREV.00041.2013

139. Escartin C, Galea E, Lakatos A, et al (2021) Reactive astrocyte nomenclature, definitions, and future directions. Nature Neuroscience 2021 24:3 24:312–325. https://doi.org/10.1038/s41593-020-00783-4

140. Sener RN (2007) Maple syrup urine disease: Diffusion MRI, and proton MR spectroscopy findings. Computerized Medical Imaging and Graphics 31:106–110. https://doi.org/10.1016/j.compmedimag.2006.11.005

141. Nave KA, Werner HB (2014) Myelination of the nervous system: mechanisms and functions. Annu Rev Cell Dev Biol 30:503–533. https://doi.org/10.1146/ANNUREV-CELLBIO-100913-013101

142. Fields RD (2008) White matter in learning, cognition and psychiatric disorders. Trends Neurosci 31:361–370. https://doi.org/10.1016/j.tins.2008.04.001

143. Frazier DM, Allgeier C, Homer C, et al (2014) Nutrition management guideline for maple syrup urine disease: An evidence- and consensus-based approach. Mol Genet Metab 112:210–217. https://doi.org/10.1016/j.ymgme.2014.05.006

144. Funchal C, Zamoner A, Dos Santos AQ, et al (2005) Evidence that intracellular Ca2+ mediates the effect of alpha-ketoisocaproic acid on the phosphorylating system of cytoskeletal proteins from cerebral cortex of immature rats. J Neurol Sci 283:75–82. https://doi.org/10.1016/j.jns.2005.06.013

145. Tretter L, Adam-Vizi V (2004) Generation of reactive oxygen species in the reaction catalyzed by alpha-ketoglutarate dehydrogenase. J Neurosci 24:7771–7778. https://doi.org/10.1523/JNEUROSCI.1842-04.2004

146. Gibson GE, Blass JP, Beal MF, Bunik V (2005) The alpha-ketoglutarate-dehydrogenase complex: a mediator between mitochondria and oxidative stress

in neurodegeneration. Mol Neurobiol 31:43–63. https://doi.org/10.1385/MN:31:1-3:043

147. Bunik VI, Mkrtchyan G, Grabarska A, et al (2016) Inhibition of mitochondrial 2-oxoglutarate dehydrogenase impairs viability of cancer cells in a cell-specific metabolism-dependent manner. Oncotarget 7:26400–26421. https://doi.org/10.18632/ONCOTARGET.8387

148. McLain AL, Szweda PA, Szweda LI (2010) α-Ketoglutarate dehydrogenase: A mitochondrial redox sensor. Free Radic Res 45:29. https://doi.org/10.3109/10715762.2010.534163

149. Reed LJ (2001) A Trail of Research from Lipoic Acid to α-Keto Acid Dehydrogenase Complexes. Journal of Biological Chemistry 276:38329–38336. https://doi.org/10.1074/jbc.R100026200

150. McCormack JG, Halestrap AP, Denton RM (1990) Role of calcium ions in regulation of mammalian intramitochondrial metabolism. Physiol Rev 70:391–425. https://doi.org/10.1152/PHYSREV.1990.70.2.391

151. Denton RM (2009) Regulation of mitochondrial dehydrogenases by calcium ions. Biochim Biophys Acta Bioenerg 1787:1309–1316. https://doi.org/10.1016/j.bbabio.2009.01.005

152. Ribeiro CA, Sgaravatti ÂM, Rosa RB, et al (2008) Inhibition of brain energy metabolism by the branched-chain amino acids accumulating in maple syrup urine disease. Neurochem Res 33:114–124. https://doi.org/10.1007/S11064-007-9423-9

153. Sgaravatti AM, Rosa RB, Schuck PF, et al (2003) Inhibition of brain energy metabolism by the α-keto acids accumulating in maple syrup urine disease. Biochimica et Biophysica Acta (BBA) - Molecular Basis of Disease 1639:232–238. https://doi.org/10.1016/J.BBADIS.2003.09.010

154. Barschak AG, Marchesan C, Sitta A, et al (2008) Maple syrup urine disease in treated patients: Biochemical and oxidative stress profiles. Clin Biochem 41:317–324. https://doi.org/10.1016/J.CLINBIOCHEM.2007.11.015

155. Vasques VDC, De Boer MA, Diligenti F, et al (2004) Intrahippocampal administration of the α-keto acids accumulating in maple syrup urine disease provokes learning deficits in rats. Pharmacol Biochem Behav 77:183–190. https://doi.org/10.1016/j.pbb.2003.10.013

156. Mescka C, Moraes T, Rosa A, et al (2011) In vivo neuroprotective effect of L-carnitine against oxidative stress in maple syrup urine disease. Metab Brain Dis 26:21–28. https://doi.org/10.1007/S11011-011-9238-X/FIGURES/2

157. Mescka CP, Rosa AP, Schirmbeck G, et al (2016) L-carnitine Prevents Oxidative Stress in the Brains of Rats Subjected to a Chemically Induced Chronic Model of MSUD. Mol Neurobiol 53:6007–6017. https://doi.org/10.1007/S12035-015-9500-Z

158. Gibson GE, Hirsch JA, Cirio RT, et al (2013) Abnormal thiamine-dependent processes in Alzheimer's Disease. Lessons from diabetes. Mol Cell Neurosci 55:17–25. https://doi.org/10.1016/J.MCN.2012.09.001

159. Mailloux RJ, Bériault R, Lemire J, et al (2007) The tricarboxylic acid cycle, an ancient metabolic network with a novel twist. PLoS One 2(8):e690. https://doi.org/10.1371/JOURNAL.PONE.0000690

160. Kawai T, Akira S (2006) TLR signaling. Cell Death Differ 13:816–825. https://doi.org/10.1038/SJ.CDD.4401850;KWRD

161. Allan SM, Tyrrell PJ, Rothwell NJ (2005) Interleukin-1 and neuronal injury. Nat Rev Immunol 5:629–640. https://doi.org/10.1038/NRI1664

162. Perry VH, Cunningham C, Holmes C (2007) Systemic infections and inflammation affect chronic neurodegeneration. Nat Rev Immunol 7:161–167. https://doi.org/10.1038/NRI2015

163. Erta M, Quintana A, Hidalgo J (2012) Interleukin-6, a Major Cytokine in the Central Nervous System. Int J Biol Sci 8:1254–1266. https://doi.org/10.7150/IJBS.4679

164. Vezzani A, French J, Bartfai T, Baram TZ (2011) The role of inflammation in epilepsy. Nat Rev Neurol 7:31–40. https://doi.org/10.1038/NRNEUROL.2010.178

165. Heneka MT, Kummer MP, Latz E (2014) Innate immune activation in neurodegenerative disease. Nat Rev Immunol 14:463–477. https://doi.org/10.1038/NRI3705

166. Rosa L, Galant LS, Dall'Igna DM, et al (2016) Cerebral Oedema, Blood-Brain Barrier Breakdown and the Decrease in Na(+),K(+)-ATPase Activity in the Cerebral Cortex and Hippocampus are Prevented by Dexamethasone in an Animal Model of Maple Syrup Urine Disease. Mol Neurobiol 53:3714–3723. https://doi.org/10.1007/S12035-015-9313-0

167. Wessler LB, de Miranda Ramos V, Bittencourt Pasquali MA, et al (2019) Administration of branched-chain amino acids increases the susceptibility to lipopolysaccharide-induced inflammation in young Wistar rats. International Journal of Developmental Neuroscience 78:210–214. https://doi.org/10.1016/J.IJDEVNEU.2019.07.007

168. Minghetti L (2004) Cyclooxygenase-2 (COX-2) in inflammatory and degenerative brain diseases. J Neuropathol Exp Neurol 63:901–910. https://doi.org/10.1093/JNEN/63.9.901

169. Heneka MT, O'Banion MK (2007) Inflammatory processes in Alzheimer's disease. J Neuroimmunol 184:69–91. https://doi.org/10.1016/j.jneuroim.2006.11.017

170. Pacher P, Beckman JS, Liaudet L (2007) Nitric Oxide and Peroxynitrite in Health and Disease. https://doi.org/101152/physrev000292006 87:315–424. https://doi.org/10.1152/PHYSREV.00029.2006

171. Scaini G, Jeremias IC, Morais MOS, et al (2012) DNA damage in an animal model of maple syrup urine disease. Mol Genet Metab 106:169–174. https://doi.org/10.1016/J.YMGME.2012.04.009

172. Maes M, Galecki P, Chang YS, Berk M (2011) A review on the oxidative and nitrosative stress (O&NS) pathways in major depression and their possible contribution to the (neuro)degenerative processes in that illness. Prog Neuropsychopharmacol Biol Psychiatry 35:676–692. https://doi.org/10.1016/j.pnpbp.2010.05.004

173. Sies H, Berndt C, Jones DP (2017) Oxidative Stress. Annu Rev Biochem 86:715–748. https://doi.org/10.1146/ANNUREV-BIOCHEM-061516-045037

174. Narendra D, Tanaka A, Suen DF, Youle RJ (2008) Parkin is recruited selectively to impaired mitochondria and promotes their autophagy. J Cell Biol 183:795. https://doi.org/10.1083/JCB.200809125

175. Pickrell AM, Youle RJ (2015) The roles of PINK1, Parkin, and mitochondrial fidelity in parkinson's disease. Neuron 85:257–273. https://doi.org/10.1016/j.neuron.2014.12.007

176. Liu L, Feng D, Chen G, et al (2012) Mitochondrial outer-membrane protein FUNDC1 mediates hypoxia-induced mitophagy in mammalian cells. Nature Cell Biology 2012 14:2 14:177–185. https://doi.org/10.1038/ncb2422

177. West AP, Shadel GS, Ghosh S (2011) Mitochondria in innate immune responses. Nature Reviews Immunology 2011 11:6 11:389–402. https://doi.org/10.1038/nri2975

178. Sliter DA, Martinez J, Hao L, et al (2018) Parkin and PINK1 mitigate STING-induced inflammation. Nature 561:258–262. https://doi.org/10.1038/S41586-018-0448-9

179. Missiroli S, Genovese I, Perrone M, et al (2020) The Role of Mitochondria in Inflammation: From Cancer to Neurodegenerative Disorders. J Clin Med 9:740. https://doi.org/10.3390/JCM9030740

180. Morais FA, Lemos IS, Matiola RT, et al (2022) Coadministration of tianeptine alters behavioral parameters and levels of neurotrophins in a chronic model of Maple Syrup Urine disease. Metabolic Brain Disease 2022 37:5 37:1585–1596. https://doi.org/10.1007/S11011-022-00969-8

181. Lemos I da S, Torres CA, Alano CG, et al (2024) Memantine Improves Memory and Neurochemical Damage in a Model of Maple Syrup Urine Disease. Neurochem Res 49:758–770. https://doi.org/10.1007/S11064-023-04072-X

182. Valko M, Leibfritz D, Moncol J, et al (2007) Free radicals and antioxidants in normal physiological functions and human disease. International Journal of

Biochemistry and Cell Biology 39:44–84.
https://doi.org/10.1016/j.biocel.2006.07.001

183. Cobley JN, Fiorello ML, Bailey DM (2018) 13 reasons why the brain is susceptible to oxidative stress. Redox Biol 15:490–503.
https://doi.org/10.1016/j.redox.2018.01.008

ANEXOS

CARTA DE APROVAÇÃO COMISSÃO DE ÉTICA NO USO DE ANIMAIS

U F R G S
UNIVERSIDADE FEDERAL
DO RIO GRANDE DO SUL

PRÓ-REITORIA DE PESQUISA

Comissão De Ética No Uso De Animais

CEUA UFRGS

CARTA DE APROVAÇÃO

Comissão De Ética No Uso De Animais analisou o projeto:

Número: 42875
Título: EFEITOS DA ADMINISTRACAO INTRACEREBROVENTRICULAR DO ACIDO ALFA-CETOISOCAPROICO E DA LEUCINA EM RATOS NEONATOS SOBRE AS HOMEOSTASES MITOCONDRIAL E REDOX E SOBRE A HISTOPATOLOGIA CEREBRAL

Vigência: 01/11/2022 à 31/10/2026

Pesquisadores:

Equipe UFRGS:

MOACIR WAJNER - coordenador desde 01/11/2022
Júlia Gabrieli Bender - desde 01/11/2022
RAFAEL TEIXEIRA RIBEIRO - desde 01/11/2022
Alexandre Umpierrez Amaral - pesquisador desde 01/11/2022
Vanessa Trindade Bortoluzzi - pesquisador desde 01/11/2022
Ângela Beatris Zemniaçak - Farmacêutico desde 01/11/2022

Comissão De Ética No Uso De Animais aprovou o projeto nº 42875 - EFEITOS DA ADMINISTRACAO INTRACEREBROVENTRICULAR DO ACIDO ALFA-CETOISOCAPROICO E DA LEUCINA EM RATOS NEONATOS SOBRE AS HOMEOSTASES MITOCONDRIAL E REDOX E SOBRE A HISTOPATOLOGIA CEREBRAL, em seus aspectos éticos e metodológicos, para a utilização de 396 ratos neonatos heterogênicos Wistar, incluindo 198 machos, 198 fêmeas provenientes de 50 ratas Wistar mães adultas, advindos do Biotério Setorial do Departamento de Bioquímica da UFRGS. O projeto está de acordo com os preceitos das Diretrizes e Normas Nacionais e Internacionais, especialmente a Lei 11.794 de 08 de novembro de 2008, o Decreto 6899 de 15 de julho de 2009, e as normas editadas pelo Conselho Nacional de Controle da Experimentação Animal (CONCEA), que disciplinam a produção, manutenção e/ou utilização de animais do filo Chordata, subfilo Vertebrata (exceto o homem) em atividade de ensino ou pesquisa.

Porto Alegre, Quarta-Feira, 23 de Novembro de 2022

Maite de M. Vieira

MAITE DE MORAES VIEIRA
Coordenador da comissão de ética